

# Selective Catalytic Hydrogenation for Industrial 1-Hexene Purification

A thesis submitted to the University of Cape Town in partial fulfillment of the requirements for the degree of **Master of Science in Engineering**

Lynsey McEwan

June 2010

CENTRE OF CATALYSIS RESEARCH  
DEPARTMENT OF CHEMICAL ENGINEERING  
UNIVERSITY OF CAPE TOWN



## Synopsis

Linear alpha-olefins, including 1-hexene, are used mainly as co-monomers in the production of polymers. The very low tolerance of the polymerisation catalyst to highly unsaturated impurities makes removal of these impurities from the olefin feedstock crucial. In South Africa, linear alpha-olefins are a major product of Fischer-Tropsch synthesis. A complex extractive distillation process is used to separate impurities from the product stream. A final polishing step by adsorption results in a significant loss of valuable alpha-olefin.

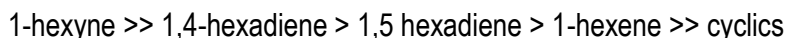
Selective catalytic hydrogenation has been successfully applied for the purification of C<sub>2</sub>-C<sub>5</sub> olefin streams; as such there is much interest in the process as a potential route for the purification of 1-hexene. The objective is to selectively hydrogenate impurities, but to inhibit the hydrogenation of the alpha-olefin to the alkane and double-bond isomerisation to internal olefins. Studies at the University of Cape Town have investigated its potential for purification of 1-hexene streams. Monometallic gold on titania catalysts have exhibited promising specificity and selectivity compared to commercial palladium based catalysts, however, further work employing a more realistic feed (multiple impurities at lower levels) was required.

The objective of this study was to further investigate the process for the purification of a more realistic 1-hexene stream under improved reaction conditions. This objective was addressed through the use of industrially relevant feedstocks containing multiple impurities, including hexyne, hexadienes and cyclo-olefins, at low levels (~ 2000 ppm). The study investigated the use of multiple reactors with the ability for interstage hydrogen replenishment, as well as the effects of H<sub>2</sub>/impurity ratio.

For this study, a new experimental test unit was designed and constructed with the aim of driving the conversion of impurities towards 100%. The unit consists of three downflow trickle-bed reactors in series, with a hydrogen dissolving vessel employed upstream of each reactor to ensure the absence of gas phase hydrogen. A single batch of Au/TiO<sub>2</sub> catalyst was tested to compare operation of 1, 2 and 3 reactors in series, as well as molar H<sub>2</sub>/impurity ratios of 1 and 2, at 30 bar<sub>g</sub> pressure and a weight hourly space velocity of 3 hr<sup>-1</sup> in the temperature range of 60 - 120°C. The selection of catalyst and operating conditions was based on experience gained from previous studies.

The study has successfully concluded that 1-hexyne conversions of greater than 90% can be maintained at low feed impurity levels (~2000 ppm), without significant loss of valuable 1-hexene. However, the removal

of diene and cyclic impurities remains much more difficult. The conversion of hexadiene impurities was low throughout and generally less than 10%, whilst no measurable conversion of cyclic impurities was observed. The relative reactivity of the impurities studied is described by the series:



The best conditions for the conversion of 1-hexyne were achieved using a single reactor, with no hydrogen replenishment, utilising a  $\text{H}_2$ /impurity ratio of two. This configuration attains greater than 90% conversion of the alkyne at  $120^\circ\text{C}$ , whilst achieving a small desirable 1-hexene gain. Diene conversion is low (~5%) for this setup and can be improved by the use of intersatge hydrogen replenishment via the multiple reactor configuration. However, this is accompanied by an increasing loss of valuable 1-hexene.

Contrary to expectations, operation with multiple reactors, where the hydrogen levels are kept low and replenished stepwise, did not minimise the loss of 1-hexene but rather resulted in an increased 1-hexene loss. This was mainly a result of 1-hexene hydrogenation to n-hexane.

The results of this study suggest that gold catalysed selective hydrogenation remains an industrially interesting opportunity for the purification of 1-hexene streams. To declare the process industrially viable there is still significant work required with respect to the removal of diene impurities. It is believed this may be improved by operating at a lower WHSV and by employing a catalyst containing smaller gold particles in order to increase the available gold surface area.

## Plagiarism declaration

I know the meaning of plagiarism and declare that all the work in the document, save for that which is properly acknowledged, is my own.

## Acknowledgements

Firstly I would like to thank MINTEK and project AUTEK for their financial support and for supplying the gold solution to prepare the catalysts used in this study, as well for doing ICP analysis on the prepared catalyst.

A special word of thanks is reserved for my supervisors, Prof. Jack Fletcher and Mr. Stephen Roberts, for their invaluable technical expertise, guidance and encouragement throughout the project. An extended thanks to Stephen for always making time and for all the much needed help – it is very much appreciated. Thanks are also extended to other academic staff in the Centre of Catalysis Research at the Department of Chemical Engineering, UCT, in particular Prof. Eric van Steen and Mr Walter Böhringer for their valuable teachings. In general, other support within the Department of Chemical Engineering must also be mentioned such as Helen Divey (Manager Main Laboratory), Marc Wüst (Technical Officer, Centre of Catalysis), Dirk Reyskens (Manager Catalysis Laboratory) and Joey (technical assistance).

Construction of the new test unit was possible thanks to the skilled work done by the workshop and the technical expertise of Waldo, Andile and Cobus in the Catalysis laboratory.

Previous studies were carried out at UCT by Mr. Jason McPherson (2003), Ms. Tiffany Brown (2004), Mr. Abinash Ramasary (2008) and Ms. Melissa Julius (2008); these provided the groundwork for this study. A special thanks to Melissa for her introduction to the experimental procedures and apparatus' as well as for sharing her experience and technical support.

Finally I would like to thank all members of the Centre of Catalysis Research, both students and support staff, for creating an engaging work environment. I would also like to thank my friends and family for their support during my studies.

# Table of contents

<b>SYNOPSIS</b>	<b>i</b>
<b>ACKNOWLEDGEMENTS</b>	<b>iii</b>
<b>TABLE OF CONTENTS</b>	<b>iv</b>
<b>LIST OF FIGURES</b>	<b>vii</b>
<b>LIST OF TABLES</b>	<b>x</b>
<b>LIST OF SYMBOLS</b>	<b>x</b>
<b>GLOSSARY</b>	<b>xi</b>
<b>1. INTRODUCTION</b>	<b>1</b>
<b>2. BACKGROUND</b>	<b>4</b>
<b>2.1. Production and industrial application of linear <math>\alpha</math>-olefins</b>	<b>4</b>
2.1.1. Production of linear $\alpha$ -olefins	4
2.1.2. Application of linear $\alpha$ -olefins	4
<b>2.2. Production and industrial application of 1-hexene</b>	<b>5</b>
2.2.1. Production of 1-hexene	5
2.2.1.1. Ethylene oligomerisation	5
2.2.1.2. Recovery from Fischer-Tropsch product	6
2.2.2. Industrial application of 1-hexene	7
<b>2.3. The necessity of purity in co-monomer feedstock</b>	<b>7</b>
<b>2.4. Purification of <math>\alpha</math>-olefins by selective hydrogenation</b>	<b>8</b>
2.4.1. Selective hydrogenation of C <sub>2</sub> -C <sub>5</sub> $\alpha$ -olefin streams	8
2.4.1.1. Typical catalysts and conditions	9
2.4.2. Selective hydrogenation of C <sub>6</sub> $\alpha$ -olefin streams	9
2.4.3. Selective hydrogenation catalysts	10
2.4.3.1. Palladium catalysts	10
2.4.3.2. Gold Catalysts	10
2.4.3.3. Support material	11
<b>2.5. Mechanism and kinetics</b>	<b>11</b>
2.5.1. Mechanism of hydrogenation	11
2.5.2. Hydrogenation of alkadienes and alkynes	12
2.5.3. Specificity and selectivity	14

---

<b>2.6.</b>	<b>The influence of excess and gaseous hydrogen</b>	<b>17</b>
2.6.1.	Hydrogen limitation	17
2.6.2.	Elimination of gas phase hydrogen	18
2.6.2.1.	Hydrogen solubility in 1-hexene	18
2.6.3.	Hydrogen/impurity ratio	19
<b>2.7.</b>	<b>The influence of space velocity</b>	<b>20</b>
<b>3.</b>	<b>PREVIOUS WORK</b>	<b>22</b>
<b>4.</b>	<b>OBJECTIVES</b>	<b>24</b>
<b>5.</b>	<b>EXPERIMENTAL</b>	<b>25</b>
<b>5.1.</b>	<b>Catalysts</b>	<b>25</b>
5.1.1.	Catalyst preparation	25
5.1.2.	Catalyst Characterisation	26
5.1.2.1.	Catalyst loading	26
5.1.2.2.	Metal particle size	26
<b>5.2.</b>	<b>Feedstocks</b>	<b>26</b>
<b>5.3.</b>	<b>Catalyst performance test unit</b>	<b>28</b>
5.3.1.	Design improvements to previous apparatus	31
5.3.1.1.	Reactor setup	31
5.3.1.2.	Temperature control	31
5.3.1.3.	Valve switching issue	31
5.3.2.	Feed system	32
5.3.3.	Dissolver/Reactor configuration	32
5.3.4.	Hydrogen dissolution vessel	33
5.3.5.	Reactor	33
5.3.6.	Sampling loop	34
5.3.7.	Pressure control	34
5.3.8.	Temperature control	35
<b>5.4.</b>	<b>Experimental operating procedures</b>	<b>35</b>
5.4.1.	Catalyst loading	35
5.4.2.	System pressure test	36
5.4.3.	Catalyst activation / reduction	36
5.4.4.	Start-up procedure	36
5.4.5.	Variation of reaction conditions	37
5.4.6.	Variation of reactor configuration	37
5.4.7.	Sampling	37
5.4.8.	Draining the product catch pots	37
5.4.9.	Shutdown procedure	37
<b>5.5.</b>	<b>Operating conditions</b>	<b>38</b>
<b>5.6.</b>	<b>Feed and product analysis</b>	<b>39</b>
5.6.1.	Gas chromatography	39

---

5.6.2.	Data work-up	40
5.6.2.1.	Conversion and catalyst performance parameters	42
<b>6.</b>	<b>RESULTS</b>	<b>46</b>
<b>6.1.</b>	<b>Experimental runs</b>	<b>46</b>
<b>6.2.</b>	<b>Preliminary Findings</b>	<b>47</b>
6.2.1.	Blank experiments	47
6.2.2.	Verification of new test unit performance	47
6.2.3.	Experimental reproducibility	49
6.2.4.	Catalyst stability	50
<b>6.3.</b>	<b>Catalyst characterization</b>	<b>51</b>
6.3.1.	Gold particle size	51
6.3.2.	Gold loading and loading efficiency	53
<b>6.4.</b>	<b>Catalyst performance</b>	<b>54</b>
6.4.1.	Feed 1; Variation of reactor configuration and overall H <sub>2</sub> /impurity ratio	54
6.4.1.1.	Overall H <sub>2</sub> /impurity = 1	54
6.4.1.2.	Overall H <sub>2</sub> /impurity = 2	58
6.4.2.	Feed 2; Variation of reactor configuration	62
<b>6.5.</b>	<b>Degree of hydrogen dissolution</b>	<b>65</b>
<b>7.</b>	<b>DISCUSSION</b>	<b>67</b>
<b>7.1.</b>	<b>Preliminary findings</b>	<b>67</b>
<b>7.2.</b>	<b>Overall findings</b>	<b>68</b>
7.2.1.	Impurity conversion	68
<b>7.3.</b>	<b>Effect of reactor configuration and limited hydrogen availability</b>	<b>70</b>
7.3.1.	Alkyne conversion	70
7.3.2.	Diene conversion	71
7.3.3.	1-hexene loss, n-hexane and hexene isomer ppm changes	72
<b>7.4.</b>	<b>Relative reactivity of impurities</b>	<b>74</b>
<b>8.</b>	<b>CONCLUSIONS</b>	<b>75</b>
	<b>APPENDIX I – CALIBRATION CURVES</b>	<b>82</b>
	<b>APPENDIX II - PREPARATION OF FEED MIXTURE BY MASS</b>	<b>86</b>
	<b>APPENDIX III – TABULATED HYDROGENATION DATA</b>	<b>88</b>
	<b>APPENDIX IV – FOLD OUT REFERENCE TABLE</b>	<b>99</b>

## List of figures

Figure 2.1: Uses of $\alpha$ -olefins (2002 estimate).....	5
Figure 2.2: Block flow diagram of Sasol extractive distillation process .....	6
Figure 2.3: Typical impurities present in a C <sub>6</sub> $\alpha$ -olefin stream and boiling points .....	7
Figure 2.4: Horiuti-Polanyi mechanism of hydrogenation illustrated for ethene hydrogenation.....	12
Figure 2.5: Idealised reaction scheme for the hydrogenation of a highly unsaturated impurity ( <i>Molnar et al., 2001</i> )...13	
Figure 2.6: Volcano plot illustrating the relative rate of alkene, alkadiene and alkyne hydrogenation as a function of their heat of adsorption for Pd catalysts ( <i>Julius, 2008</i> ) .....	14
Figure 2.7: Detailed Reaction scheme (with 1-hexyne and 1,5-hexadiene as example impurities) .....	15
Figure 2.8: Idealised specificity plot ( <i>Adapted from McPherson, 2003</i> ) .....	16
Figure 2.9: Effect of space time on hydrogen consumption rate ( <i>McPherson, 2003</i> ).....	18
Figure 2.10: Solubility of hydrogen in 1-hexene as a function of temperature at various pressures .....	19
Figure 2.11: Comparison of 1-hexyne conversion at stoichiometric and excess hydrogen ( <i>Julius, 2008</i> ) .....	20
Figure 3.1: Results of previous findings and desired range of operation .....	23
Figure 5.1: Picture of experimental test unit.....	29
Figure 5.2: Schematic illustration of experimental test unit .....	30
Figure 5.3: Schematic illustration of dissolver/reactor setup .....	32
Figure 5.4: View of top of reactor/dissolver block.....	33
Figure 5.5: Sampling loop .....	34
Figure 5.6: Schematic illustration of reactor packing.....	35
Figure 5.7: A typical sample chromatogram and analysis.....	40
Figure 5.8: Linearity of model impurities .....	41
Figure 6.1: 1-hexyne conversion for Au/TiO <sub>2</sub> at 60, 90 and 120°C .....	48
Figure 6.2: 1-hexene gain for Au/TiO <sub>2</sub> at 60, 90 and 120°C .....	48
Figure 6.3: Hexene isomer change for Au/TiO <sub>2</sub> at 60, 90 and 120°C .....	49



---

Figure 6.4: n-hexane change for Au/TiO <sub>2</sub> at 60, 90 and 120°C .....	49
Figure 6.5: Run 2a, 2b and 3 illustrating experimental reproducibility.....	49
Figure 6.6: Catalyst stability during run 4 .....	50
Figure 6.7: Sample TEM images of the gold impregnation catalyst.....	51
Figure 6.8: Overall particle size distribution for 1 wt% Au/TiO <sub>2</sub> .....	52
Figure 6.9: Particle size distribution for comparing particles at the centre and edges of the extrudate .....	53
Figure 6.10: Impurity conversion for 1 reactor.....	56
Figure 6.11: Impurity conversion for 2 reactors.....	56
Figure 6.12: Impurity conversion for 3 reactors.....	56
Figure 6.13: 1-hexene gain/loss, comparing 1,2 and 3 reactor setup at 60, 90 and 120°C .....	57
Figure 6.14: Hexene isomer net change, comparing 1,2 and 3 reactor setup at 60, 90 and 120°C .....	57
Figure 6.15: n-hexane net change, comparing 1,2 and 3 reactor setup at 60, 90 and 120°C .....	57
Figure 6.16: Impurity conversion for 1 reactor (excess H <sub>2</sub> ) .....	60
Figure 6.17: Impurity conversion for 2 reactors (excess H <sub>2</sub> ) .....	60
Figure 6.18: Impurity conversion for 3 reactors (excess H <sub>2</sub> ) .....	60
Figure 6.19: 1-hexene gain/loss, comparing 1, 2 and 3 reactor setup at 60, 90 and 120°C .....	61
Figure 6.20: Hexene isomer net change, comparing 1, 2 and 3 reactor setup at 60, 90 and 120°C .....	61
Figure 6.21: n-hexane net change, comparing 1, 2 and 3 reactor setup at 60, 90 and 120°C.....	61
Figure 6.22: Impurity conversion for 1 reactor (Feed 2).....	63
Figure 6.23: Impurity conversion for 2 reactors (Feed 2) .....	63
Figure 6.24: Impurity conversion for 3 reactors (Feed 2) .....	63
Figure 6.25: 1-hexene gain/loss for 1, 2 and 3 reactors at 60, 90 and 120°C.....	64
Figure 6.26: n-hexane net change for 1, 2 and 3 reactors at 60, 90 and 120°C.....	64
Figure 6.27: Hexene isomer net change for 1, 2 and 3 reactors at 60, 90 and 120°C.....	65
Figure 6.28: 1-hexyne conversion for dissolver 1 and dissolver 2 at 60, 90 and 120°C .....	66
Figure 6.29: 1-hexene gain for dissolver 1 and dissolver 2 at 60, 90 and 120°C.....	66

---

Figure 7.1: 1-hexyne conversion at 120°C for 1, 2 and 3 reactors under overall H <sub>2</sub> /impurity of 1 and 2.....	68
Figure 7.2: 1,5-hexadiene conversion at 120°C for 1, 2 and 3 reactors under overall H <sub>2</sub> /impurity of 1 and 2.....	68
Figure 7.3: 1,4-hexadiene conversion at 120°C for 1, 2 and 3 reactors under overall H <sub>2</sub> /impurity of 1 and 2.....	68
Figure 7.4: 1-hexene gain/loss at 120°C for 1,2 and 3 reactors under overall H <sub>2</sub> /impurity = 1 and 2.....	70
Figure 7.5: Comparing 1-hexyne conversion for different reactor configurations at 60, 90 and 120°C.....	70
Figure 7.6: Comparing 1,5-hexadiene conversion for different reactor configurations at 60, 90 and 120°C.....	71
Figure 7.7: Comparing 1,4-hexadiene conversion for different reactor configurations at 60, 90 and 120°C.....	71
Figure 7.8: Total impurity conversion by hydrogenation for different reactor configurations at 60, 90 and 120°C .....	72
Figure 7.9: Δ n-hexane at 120°C for 1,2 and 3 reactors under overall H <sub>2</sub> /impurity = 1 and 2 .....	73
Figure 7.10: Δ Hexene isomers at 120°C for 1,2 and 3 reactors under overall H <sub>2</sub> /impurity = 1 and 2 .....	73

## List of tables

Table 2.1: Illustration of initial and final impurity levels for C <sub>2</sub> -C <sub>5</sub> α-olefin streams.....	9
Table 5.1: Catalyst preparation parameters .....	25
Table 5.2: Approximate feed compositions .....	27
Table 5.3: Supplier and purity of compounds used as feeds and co-feeds .....	27
Table 5.4: Standard and experimental range of operating conditions.....	38
Table 5.5: Gas chromatographic conditions .....	39
Table 6.1: Summarised list of experimental runs .....	46
Table 6.2: Approximate feed compositions .....	47
Table 6.3: Average particle sizes .....	52
Table 6.4: Results of ICP analysis .....	53

## List of symbols

$F_i$	kmol/min	Molar flowrate of species i
$g_{cat}$	grams	Mass of catalyst
$K_{i,ads}$	-	Adsorption coefficient of species i
$k_i$	-	Reaction rate constant for species i
$r_i$	μmol/min.gcat	Rate of reaction of species i
$S$	-	Hydrogenation selectivity: hydrogenation vs. isomerisation
$Sp$	-	Specificity: impurity removal vs. 1-hexene loss
$X_i$	mol/mol	Molar conversion of species i
$x_i$	mol/mol	Molar fraction of species i

## Glossary

1,4-HD	1,4-hexadiene
1,5-HD	1,5-hexadiene
2,4-HD	2,4-hexadiene
FIC	Flow indicator/controller
FID	Flame ionisation detector
H <sub>2</sub> /oil	Molar hydrogen to hydrocarbon ratio
LAO	Linear alpha olefins
MCP	1-methyl-1-cyclopentene
MFC	Mass flow controller
PI	Pressure indicator
PIC	Pressure indicator/controller
ppm	parts per million
ppb	parts per billion
sccm	standard cubic centimetres per minute
TEM	Transmission Electron Microscopy
TI	Temperature indicator
TIC	Temperature indicator/controller
WHSV	Weight hourly space velocity ( $\text{g}_{\text{hydrocarbon}}/\text{g}_{\text{cat}}\cdot\text{hr}$ )

## 1. Introduction

---

Linear  $\alpha$ -olefins have an extensive range of applications as intermediates in the chemicals industry, but are primarily used as co-monomers in the production of polymers. 1-butene, 1-hexene or 1-octene is blended with a monomer to alter or enhance properties of the resulting polymer, such as flexibility, impact resistance and strength. Global growth of the polymer industry has resulted in a steady increase in the demand for linear  $\alpha$ -olefins over the past decade. This growth is expected to remain steady through 2010, averaging around 5% per annum ([www.colin-houston.com](http://www.colin-houston.com)).

Purification of the  $\alpha$ -olefin co-monomer feedstock is crucial, as impurities are known to poison the downstream polymerisation catalyst (*Molnar et al., 2001*). Moreover, advances in the polymer industry have resulted in the use of increasingly selective and sensitive polymerisation catalysts and as such the acceptable level of impurities has decreased, boosting the demand for very high purity linear  $\alpha$ -olefin feedstocks.

The production of linear  $\alpha$ -olefins is done either by ethylene oligomerisation or extraction from Fischer-Tropsch hydrocarbon streams. In South Africa, C<sub>5</sub>-C<sub>8</sub>  $\alpha$ -olefins are recovered from coal-derived Fischer-Tropsch product streams. Globally Sasol is the 4<sup>th</sup> largest producer of linear  $\alpha$ -olefins and the addition of a 3<sup>rd</sup> 1-hexene train in 2000 has increased its annual production of 1-hexene to 200 000 tons. Currently, a complex distillation and extractive-distillation process is used to purify the C<sub>6</sub>  $\alpha$ -olefin stream. Although this process is effective, there is a significant loss of valuable  $\alpha$ -olefin product. As such, there remains significant industrial interest in alternative processes to selectively remove impurities such as alkadienes, alkynes and substituted cyclo-alkenes from the linear  $\alpha$ -olefin product.

There is specific interest in selective catalytic hydrogenation as a potential route for the purification of 1-hexene as it has been successfully applied for the purification of C<sub>2</sub> – C<sub>5</sub>  $\alpha$ -olefin streams. The objective is to selectively hydrogenate impurities, but to inhibit the hydrogenation of the  $\alpha$ -olefin to the alkane and double-bond isomerisation to internal olefins. As a result, several previous studies have investigated this method as an alternative.

The industrial selective hydrogenation of C<sub>3+</sub> streams is typically performed in a trickle bed configuration at low temperature (< 150°C) and high pressure (> 15 bar) (*Arnold et al., 1997*). Alumina supported palladium or bimetallic palladium-silver catalysts are generally used. The use of the acidic alumina support has been linked to an increase in double-bond isomerisation in higher olefins, and thus to a loss of valuable  $\alpha$ -olefin (*McPherson et al., 2000*). This is not a concern in the purification of C<sub>2</sub> and C<sub>3</sub> olefins for which no double-bond isomers exist, but in the C<sub>6</sub> case the use of a non-acidic support is deemed necessary.

Initial studies into the selective hydrogenation of C<sub>6</sub>  $\alpha$ -olefin streams employed the typical commercial selective hydrogenation catalysts, Pd-Ag/Al<sub>2</sub>O<sub>3</sub> and Pd/Al<sub>2</sub>O<sub>3</sub>, as well as Au/TiO<sub>2</sub> (*McPherson, 2003*). The Au/TiO<sub>2</sub> catalysts showed the highest conversion of impurity relative to the conversion of 1-hexene, but yielded very poor activity overall. Pd-based catalysts showed higher activity but this was accompanied by an unacceptable loss of 1-hexene (*McPherson, 2003*). Further studies (*Brown, 2004; Ramasary, 2008*) achieved much more favourable results by lowering the hydrogen/oil ratio and through the inclusion of a pre-dissolver to dissolve gaseous hydrogen into the reaction mixture.

Gold catalysis is a relatively new field and there is a growing excitement around the potential gold may hold as an industrial catalyst. The potential to use gold catalysts for an application such as selective hydrogenation is especially exciting in the South African context due to the countries rich gold reserves, which make it home to some of the world's largest gold mining houses. Project AuTEK is a research initiative between Mintek and three of these (AngloGold Ashanti, GoldFields and Harmony Gold), the aim of which is to research and develop novel applications for gold – of which catalysis is a promising prospect.

The latest study (*Julius, 2008*) has indicated that Au/TiO<sub>2</sub> achieves excellent specificity and selectivity for this process under the improved reaction conditions. However, all previous studies have employed a pure 1-hexene feed doped with impurities, typically using 1-hexyne as a model impurity. High conversions were obtained, but, if this method of selective hydrogenation is to be industrially applied, it is essential that the catalyst must be able to purify the actual industrial feedstock with a conversion of above 95%. Also, since higher unsaturated impurities (such as 1-hexyne) are more reactive than less unsaturated impurities (such as hexadienes), the process of selective hydrogenation cannot simply be transferred to the industrial range.

Thus, the obvious extension of the research, and objective of this project, is the use of Au/TiO<sub>2</sub> catalysts with industrially relevant feedstocks containing multiple impurities, including hexynes, hexadienes and cyclic-olefins, in order to confirm that the process can be applied industrially.

## 2. Background

---

This chapter provides an introduction to the production and industrial importance of linear  $\alpha$ -olefins, in particular 1-hexene, as well as consideration of selective hydrogenation as a method for the purification of  $\alpha$ -olefin feedstocks.

### 2.1. Production and industrial application of linear $\alpha$ -olefins

Olefins are aliphatic hydrocarbons with at least one carbon-carbon double bond. Linear  $\alpha$ -olefins (LAOs) are straight-chain molecules which have a single double bond located at the alpha (or primary) position. They are also known as 1-olefins or 1-alkenes.

#### 2.1.1. Production of linear $\alpha$ -olefins

Industrially, linear  $\alpha$ -olefins are produced either by ethylene oligomerisation or recovered from Fischer-Tropsch product streams. Three companies dominate the global  $\alpha$ -olefin market; Chevron-Philips, Ineos (formerly BP) and Shell, all of which produce a wide range of even-numbered  $\alpha$ -olefins via ethylene oligomerisation ([www.colin-houston.com](http://www.colin-houston.com)). The annual global demand for linear  $\alpha$ -olefins in the range C<sub>4</sub>-C<sub>20</sub> amounts to well over 3 million tons ([nexant.ecnext.com](http://nexant.ecnext.com)).

The only commercial process to isolate linear  $\alpha$ -olefins from synthetic crude is practiced by Sasol in South Africa. Sasol uses synthesis gas, derived from coal gasification, to produce fuels and other chemicals via Fischer-Tropsch synthesis. A wide range of olefins are produced and recovered by extractive distillation, the major commercial products being 1-hexene and 1-octene. In 2007, Sasol doubled its 1-octene capacity by the addition of a 100 000 ton/year plant ([www.engineeringnews.co.za](http://www.engineeringnews.co.za)).

#### 2.1.2. Application of linear $\alpha$ -olefins

Linear  $\alpha$ -olefins are of major industrial importance and have a wide range of applications. Short-to-medium linear  $\alpha$ -olefins (C<sub>4</sub>-C<sub>8</sub>) are used mainly as co-monomers in polymer production. Medium chains (C<sub>8</sub>-C<sub>12</sub>) find use as raw materials in the production of synthetic lubricants, whilst higher linear  $\alpha$ -olefins in the range C<sub>12</sub>-C<sub>16</sub> are used as detergent intermediates. Longer linear  $\alpha$ -olefins (C<sub>18</sub>+) find use as lubricant additives



and oilfield chemicals ([www.the-innovation-group.com](http://www.the-innovation-group.com)). The wide range of applications for  $\alpha$ -olefins is illustrated in figure 2.1 below.

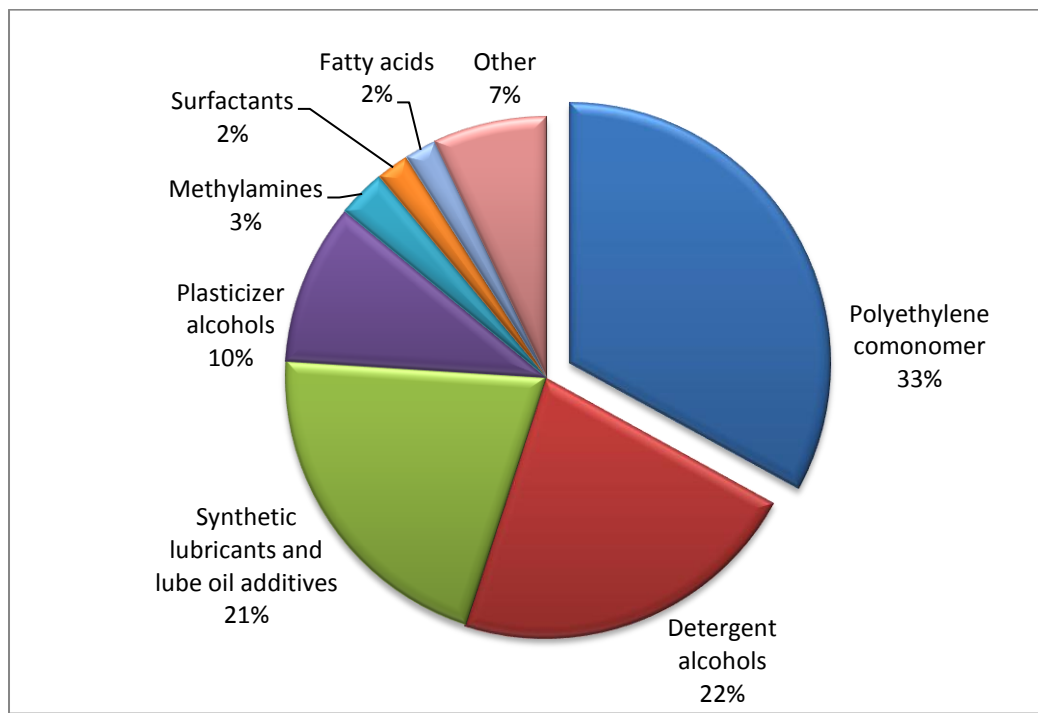


Figure 2.1: Uses of  $\alpha$ -olefins (2002 estimate)  
([www.the-innovation-group.com](http://www.the-innovation-group.com))

## 2.2. Production and industrial application of 1-hexene

### 2.2.1. Production of 1-hexene

Industrially 1-hexene is produced by ethylene oligomerisation or recovered from Fischer-Tropsch product streams. Approximately 600 000 tons of 1-hexene is produced annually ([www.cpchem.com](http://www.cpchem.com)).

#### 2.2.1.1. Ethylene oligomerisation

There are several commercial processes which oligomerise ethylene to linear  $\alpha$ -olefins. Most of these are based on a 1 or 2-step Ziegler process, and produce wide distributions of even-numbered linear  $\alpha$ -olefins (Böhringer, 2008). Recently Chevron Philips Chemicals has successfully introduced a selective ethylene

trimerisation process which is the first and only commercial process to selectively produce co-monomer grade 1-hexene from ethylene ([www.cpchem.com](http://www.cpchem.com)).

### 2.2.1.2. Recovery from Fischer-Tropsch product

LAOs, including 1-hexene, are a major product of high temperature Fischer-Tropsch synthesis over iron-based catalysts. In South Africa, over 200 000 tons of 1-hexene is produced per annum by Sasol and recovered via a complex extractive distillation process.

The C<sub>6</sub> broadcut is distilled from the Fischer-Tropsch product. This stream consists mainly of 1-hexene, along with small quantities of other hydrocarbons and oxygenates. The close boiling points of tertiary olefins and branched paraffins to 1-hexene make separation by distillation difficult. Thus, a complex four-stage process is employed, as illustrated in figure 2.2.

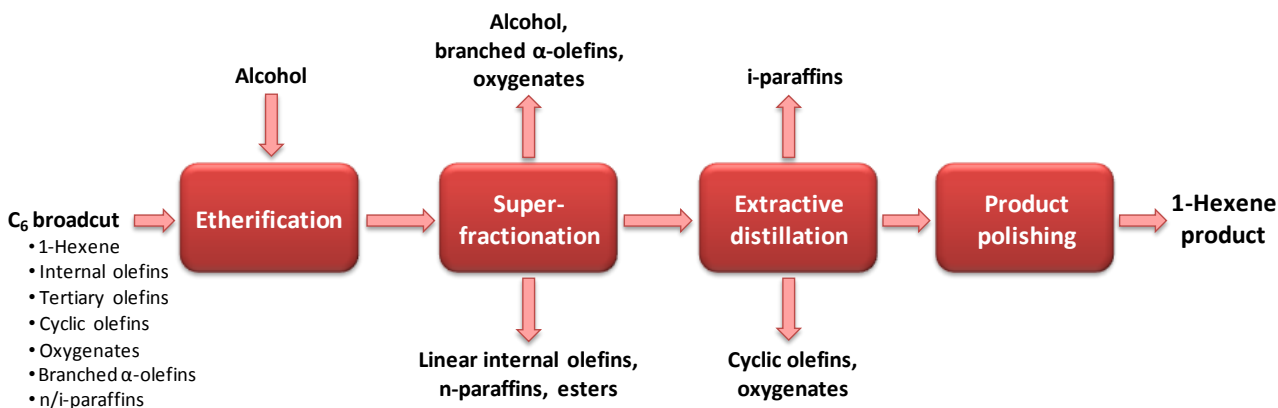


Figure 2.2: Block flow diagram of Sasol extractive distillation process

(Julius, 2008)

In the etherification step, the addition of alcohol produces ethers from the tertiary olefins. The difference in boiling points between the resulting ethers and 1-hexene is now large enough to allow branched olefins and ethers to be removed by distillation downstream. Next, the super-fractionation stage separates more volatile branched  $\alpha$ -olefins, unconverted alcohol and oxygenates as well as the less volatile internal olefins, n-paraffins and ethers from the 1-hexene stream. The product stream from the super-fractionation stage still contains cyclic olefins, iso-paraffins, dienes and hexynes. The extractive distillation step is a two-stage distillation which removes iso-paraffins, cyclics and oxygenates from the 1-hexene by the addition of a polar

solvent. The product generally exceeds 98.5 wt% 1-hexene; this is further improved by downstream polishing via adsorption, which aims to remove the last traces of impurities from the product. Although the extractive distillation process successfully reduces impurity levels, it is accompanied by a significant loss of valuable  $\alpha$ -olefin product during the final polishing step. Another costly disadvantage is the need for frequent regeneration of the guard beds.

### 2.2.2. Industrial application of 1-hexene

The major use of 1-hexene is as a co-monomer in the production of polyethylene. It also finds use as an intermediate in the production of synthetic fatty acids, oxo-alcohols, hexyl mercaptans and organic aluminium compounds. ([www.innovene.com](http://www.innovene.com))

### 2.3. The necessity of purity in co-monomer feedstock

Industrial  $\alpha$ -olefin feedstocks are often contaminated with traces of impurities such as dienes and alkynes, which are known to poison the downstream polymerisation catalyst. Examples of the impurities common in a  $C_6$   $\alpha$ -olefin stream are illustrated in Figure 2.3. New processes require increasingly pure feed stocks, and current polymerisation catalysts can tolerate a maximum of 10 ppm diolefin and acetylenic impurities (*Hugon et al., 2007*). The catalyst can tolerate saturated hydrocarbons such as alkanes, but the inclusion of alkanes in the feed will limit the monomer partial pressure and thus reduce the rate of polymerisation.

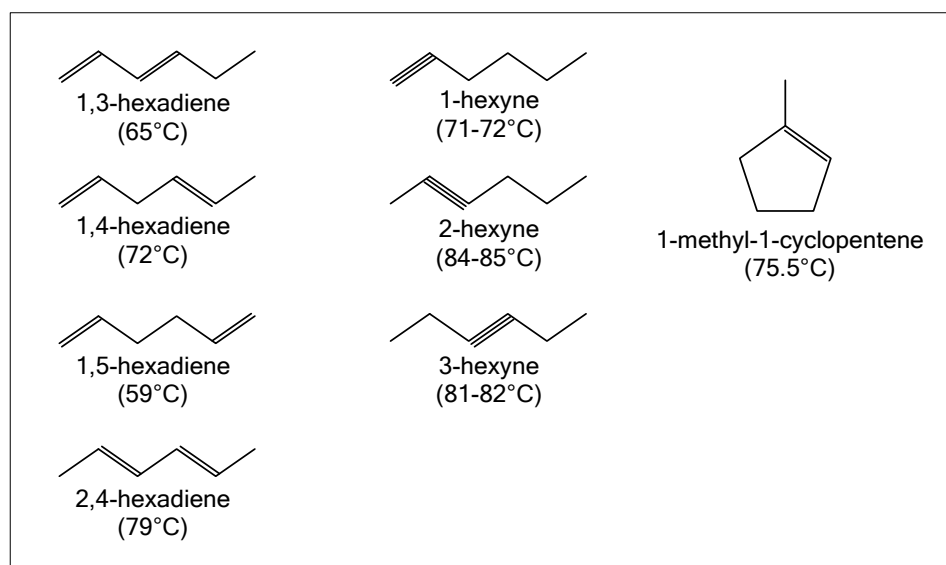


Figure 2.3: Typical impurities present in a  $C_6$   $\alpha$ -olefin stream and boiling points

Currently, the Sasol purification process includes a product polishing step following the extractive distillation. The polishing is a 2-stage adsorption using guard beds, which removes the final traces of impurities from the product. Whilst impurity levels are successfully reduced, the process may be considered to be complex and expensive.

## **2.4. Purification of $\alpha$ -olefins by selective hydrogenation**

Purification by distillation and other conventional methods are not practical due to the similar boiling points of impurities and  $\alpha$ -olefin. The objective of selective hydrogenation is to selectively hydrogenate the impurities to the desired  $\alpha$ -olefin, but to inhibit the hydrogenation of the  $\alpha$ -olefin to the alkane and double-bond isomerisation to internal olefins. The principal aim is to minimise the loss of  $\alpha$ -olefin product.

An advantage of using a catalytic process over a typical separation process is that the catalytic process aims to transform the impurities into the desired olefin as opposed to simply removing them (*Molnar et al., 2001*), as such there is potential for a net gain in desired olefin product.

### **2.4.1. Selective hydrogenation of C<sub>2</sub>-C<sub>5</sub> $\alpha$ -olefin streams**

Industrially, catalytic selective hydrogenation is applied to the C<sub>2</sub> to C<sub>5</sub> olefin streams from the steam cracker (*Molnar et al., 2001*). The removal of alkyne and diene impurities from C<sub>2</sub>-C<sub>4</sub>  $\alpha$ -olefin streams is necessary to avoid the poisoning of the downstream polymerisation catalysts. For example, ethyne content in ethylene should be reduced to 5-10 ppm to prevent poisoning (*Deganello et al., 1996*).

A typical C<sub>5+</sub> pyrolysis gasoline may contain as much as 18-22 wt% diolefins, cyclo-diolefins, and alkenyl aromatics (*Debuisschert et al., 2003*). These compounds polymerize to form gums and must be removed prior to use in fuel blending, without the loss of octane number. Nickel or palladium based catalysts can be used for the selective hydrogenation of these multiple-unsaturated compounds to olefins, cyclo-olefins, and corresponding alkyl aromatics ([www.jmcatalysts.com](http://www.jmcatalysts.com)).

Table 2.1: Illustration of initial and final impurity levels for C<sub>2</sub>-C<sub>5</sub>  $\alpha$ -olefin streams

Olefin stream	Impurities	Initial	→	Final
C <sub>2</sub>	Ethyne	2 vol%	→	5 ppm
C <sub>3</sub>	Propyne, propadiene	4 vol%	→	10 ppm
C <sub>4</sub>	1,3-butadiene	3 vol%	→	10 ppm
C <sub>5</sub>	Dienes, cyclic dienes	15-20 vol%	→	< 100 ppm

#### 2.4.1.1. Typical catalysts and conditions

Typically Pd and Pd-Ag catalysts are employed for the selective hydrogenation of alkadienes and alkynes in the C<sub>2</sub>-C<sub>5</sub> range, and the improved specificity of the bimetallic Pd-Ag catalyst is well documented (*Poniec & Bond, 1995; Sales et al., 2000 a&b*). Various studies have focussed on improving the performance for hydrogenation through the addition of an alternative second metal, such as Cu (*Guczi et al., 1999*), Ag (*Zhang and Li, 2000*) or Au (*Bond and Rawle, 1996*); or by controlling the acidity of support material and varying the metal dispersion.

#### 2.4.2. Selective hydrogenation of C<sub>6</sub> $\alpha$ -olefin streams

While selective hydrogenation is successfully applied for the purification of C<sub>2</sub>-C<sub>5</sub> olefin streams, its potential for C<sub>6</sub> purification is complicated by the issue of double bond isomerisation. The migration of the double bond is undesired in 1-hexene, as it results in a loss of the valuable product.

For C<sub>2</sub> and C<sub>3</sub> streams, double bond isomerisation is not a problem, and in the case of a C<sub>5</sub> stream it is desired as it results in a gain in octane number (*Le Page et al., 1987*). Double bond isomerisation is undesired in the C<sub>4</sub> case and is minimised by the addition of CO to the feed and the use of a selective catalyst to hinder readsorption and subsequent isomerisation or hydrogenation of 1-butene (*Arnold et al., 1997*).

*McPherson (2000)* noted that extent of double bond isomerisation may be minimised by the choice of support. In a study employing a commercial 1-octene stream it was observed that the acidity of the support may play a major role; over alumina supported catalysts considerable amounts of internal olefins were

formed, whereas almost none were produced when using the titania supported catalysts at the same conditions. It is believed that acidic sites present on the alumina carrier facilitate the formation of internal olefins via a carbenium ion mechanism. As expected the extent of double bond isomerisation is also increased by operation at higher reaction temperatures (*McPherson et al., 2000*).

Thus, whilst effectively used to purify C<sub>2</sub> – C<sub>5</sub> streams, selective catalytic hydrogenation cannot be simply transferred to the purification of C<sub>6</sub> streams. For that reason, typical Pd and bimetallic Pd catalysts, which are industrially employed for C<sub>2</sub> – C<sub>5</sub> streams, may not be the best choice for higher  $\alpha$ -olefin purification.

### 2.4.3. Selective hydrogenation catalysts

#### 2.4.3.1. Palladium catalysts

Palladium and metal promoted (bimetallic) palladium catalysts are used industrially for the purification of C<sub>2</sub>-C<sub>5</sub>  $\alpha$ -olefin streams. The addition of a co-metal, typically Ag, is generally recognised to increase the selectivity of the process (*Sales et al., 2000a*).

#### 2.4.3.2. Gold Catalysts

Gold was considered as a catalyst for the hydrogenation of alkenes as early as 1973 (*Bond and Sermon, 1973*), however the results were poor when compared to typical palladium-based catalysts. More recent studies have shown that gold catalysts are effective for various hydrogenation reactions involving linear alkenes, alkynes, cyclohexene and acetone (*Zanella et al., 2004*). However, gold is not currently applied industrially as a selective hydrogenation catalyst.

The performance of gold catalysts is highly dependent on particle size, support selection and dispersion (*Hutchings and Haruta, 2005*). Careful selection of the preparation method is vital to achieve optimum dispersion and particle size distribution.

In terms of selective hydrogenation, monometallic gold catalysts have exhibited high selectivity in C<sub>2</sub>, C<sub>3</sub> and C<sub>4</sub> streams:

- *Jia et al. (2000)* obtained 100% selectivity for the hydrogenation of ethyne to ethene in the temperature range 313-523 K using Au/Al<sub>2</sub>O<sub>3</sub>

- *Lopez-Sanchez et al. (2005)* described the 100% selectivity of Au/TiO<sub>2</sub> and Au/Fe<sub>2</sub>O<sub>3</sub> catalysts for the selective hydrogenation of propyne to propene
- *Hugon et al. (2007)* investigated the selective hydrogenation of butadiene in an excess of propene, and reported that the poor activity of gold when compared to palladium is largely compensated by the fact that gold catalysts are much more selective.

Furthermore, *Julius (2008)* has indicated that Au/TiO<sub>2</sub> achieves excellent specificity and selectivity for selective hydrogenation of 1-hexyne in 1-hexene.

#### 2.4.3.3. Support material

Hydrogenation catalysts typically use alumina, silica or carbon as a support. As the cheapest support material, alumina is commonly used for both mono- and bi-metallic hydrogenation catalysts. However, alumina is not favoured for the hydrogenation of higher LAO streams, as it is mildly acidic. It is thought that acidic sites facilitate the formation of internal olefins via a carbenium ion mechanism. This double bond isomerisation of the desired product decreases the selectivity of the catalyst. As such, a non-acidic support such as titania is preferred (*McPherson, 2000*).

## 2.5. Mechanism and kinetics

The selective hydrogenation process consists of a complex series of parallel reactions. Insight into the mechanism and kinetics of selective hydrogenation is made difficult by a combination of factors all playing a major role, these include choice of catalyst, catalyst particle size and operating conditions.

### 2.5.1. Mechanism of hydrogenation

The Horiuti and Polanyi mechanism of hydrogenation, illustrated in figure 2.4, has been widely used for over 70 years (*Ponec and Bond, 1995*). The mechanism proposes that hydrogen is first dissociated and then added to an adsorbed ethyl radical (the 'half-hydrogenated' intermediate).

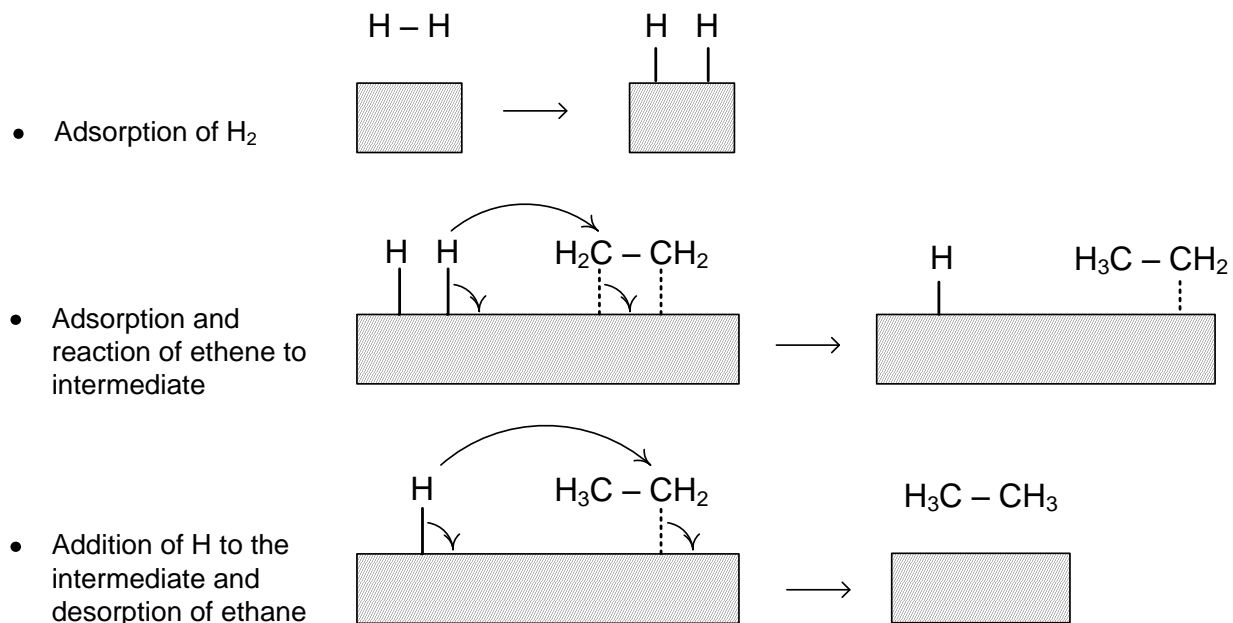


Figure 2.4: Horiuti-Polanyi mechanism of hydrogenation illustrated for ethene hydrogenation

Whilst double bond isomerisation, cis-trans isomerisation and skeletal isomerisation may also occur, this path is still considered to describe the underlying mechanism. The basic mechanism and assumption illustrated here also applies to both alkyne and alkadiene hydrogenation.

### 2.5.2. Hydrogenation of alkadienes and alkynes

The hydrogenation of multiple-unsaturated impurities occurs in such a way that intermediate products may be selectively produced. Two types of selectivity are defined, thermodynamic selectivity and mechanistic selectivity (Molnar *et al.*, 2001). Figure 2.5 presents the idealised mechanism for the hydrogenation of a highly unsaturated impurity. The impurity can be either partially or completely hydrogenated to the olefin or paraffin.



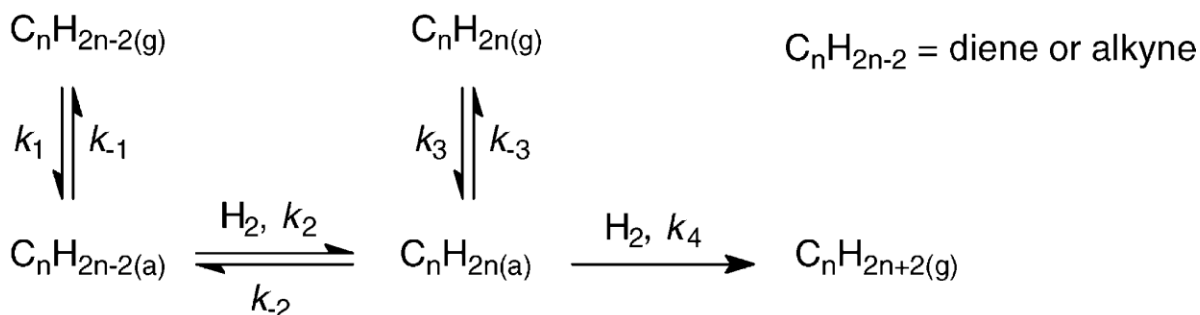


Figure 2.5: Idealised reaction scheme for the hydrogenation of a highly unsaturated impurity (Molnar et al., 2001)

It is suggested that ‘mechanistic’ selectivity occurs as a result of  $k_2 \gg k_4$ , which will result formation of the olefin, and that ‘thermodynamic’ selectivity occurs due to strength of adsorption,  $k_1/k_{-1} \gg k_3/k_{-3}$ . The stronger adsorption of the highly unsaturated molecule (such as alkyne) inhibits the readsorption of the alkene and thus further hydrogenation to the alkane is inhibited. Thermodynamics would favour complete hydrogenation over partial hydrogenation, and the high selectivity observed for palladium and gold catalysts may be regarded as a result of the stronger adsorption of the alkyne over the alkene (Molnar et al., 2001, Segura et al., 2007).

It is accepted that adsorption on the surface of a metal catalyst is a function of the level of unsaturation of a molecule. By this, alkynes are more strongly adsorbed than alkenes, and alkenes are more strongly adsorbed than the corresponding alkanes (Ponec and Bond, 1995). A volcano plot, as illustrated in figure 2.6, is used to illustrate the ‘thermodynamic’ selectivity, and describes the relative reactivity of impurities based on the difference in adsorption strength. If a species is too strongly adsorbed on the catalyst surface it may not react. As such, there is a range of preferred adsorption strengths which result in higher overall reactivities. Outside this range, the species are either adsorbed too weakly or too strongly and as a result their reactivity decreases.

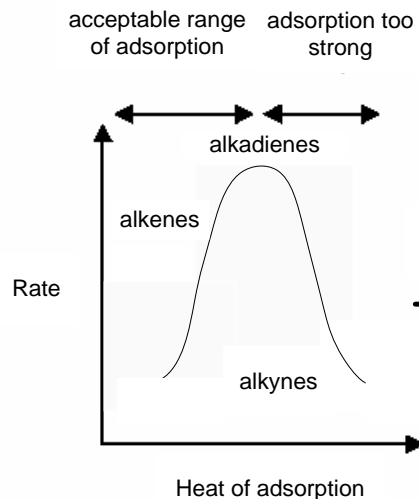
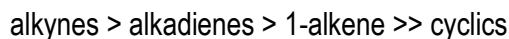


Figure 2.6: Volcano plot illustrating the relative rate of alkene, alkadiene and alkyne hydrogenation as a function of their heat of adsorption for Pd catalysts (Julius, 2008)

In terms of mechanistic selectivity, the hydrogenation of the alkene is faster than that of the alkyne. However, due to the higher adsorption strength of the alkyne, the alkyne will be preferred until its concentration is low enough to allow adsorption of the alkene (Molnar *et al.*, 2001).

McPherson (2003) concluded that the relative reactivity of impurities could be described by the following series:



In addition, it is thought that the hydrogenation activity of non-conjugated dienes (1,5- and 1,4-hexadiene) is very similar to that of the 1-alkene, and slightly greater than that of the conjugated 2,4-hexadiene (Sales *et al.*, 2000(a) and McPherson, 2003)

### 2.5.3. Specificity and selectivity

The simplistic reaction scheme in figure 2.5 neglects the possible isomerisation of olefin and impurity. Figure 2.7 presents a more detailed reaction scheme, with 1-hexyne and 1,5-hexadiene used as example impurities. It has also been shown that there exists a direct route to the alkane from the impurity (Nijhuis *et al.*, 2003). Only the hydrogenation of impurities is desired for olefin purification, since conversion by

isomerisation results in no net impurity removal. The objective is to minimise reaction of the  $\alpha$ -olefin, as both isomerisation and hydrogenation will result in a loss of valuable product.

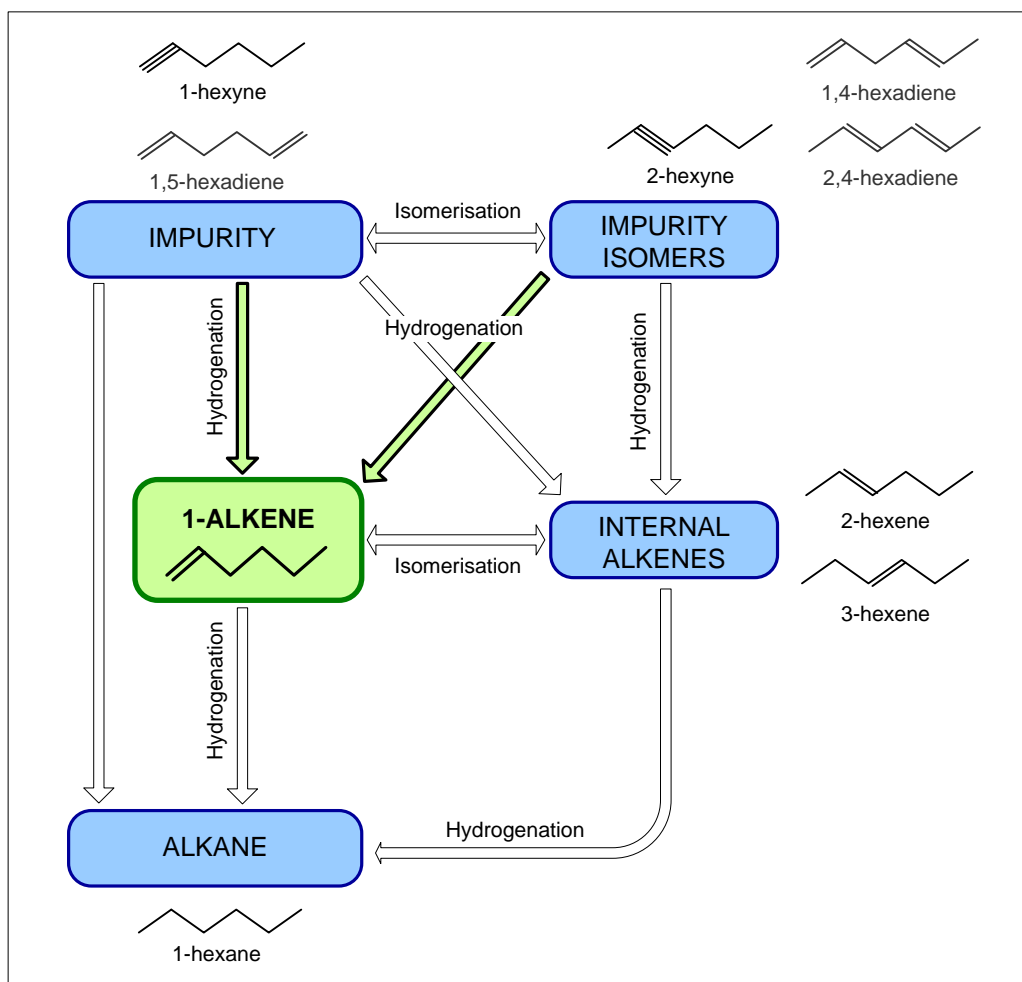


Figure 2.7: Detailed Reaction scheme (with 1-hexyne and 1,5-hexadiene as example impurities)

This can be simplified into two pseudo-parallel reactions describing the desired reactions and the undesired reactions. Both pseudo-parallel reactions are assumed to be first order with respect to hydrocarbon concentration:

- **Desired:** Hydrogenation of impurities and impurity isomers
- **Undesired:** Loss of the  $\alpha$ -olefin via hydrogenation or isomerisation

Criteria were developed to provide a measure of the quality of the catalysts. 'Specificity' was defined as the ratio of the desired to undesired reactions:

$$S_p = \frac{X_{\text{impurity}}}{X_{1\text{-hexene}}}$$

A specificity of one indicates that the rate of removal of the impurity is equal to the rate of removal of 1-hexene. A large positive value for specificity suggests that the desired conversion of impurities is high compared to the hydrogenation and isomerisation of 1-hexene. A negative value for specificity indicates that 1-hexene is being produced by the hydrogenation of impurities. Figure 2.8 below illustrates the idealised specificity curves developed by *McPherson*. A reasonable fit to the experimental results was observed at low conversion of impurity (< 25%).

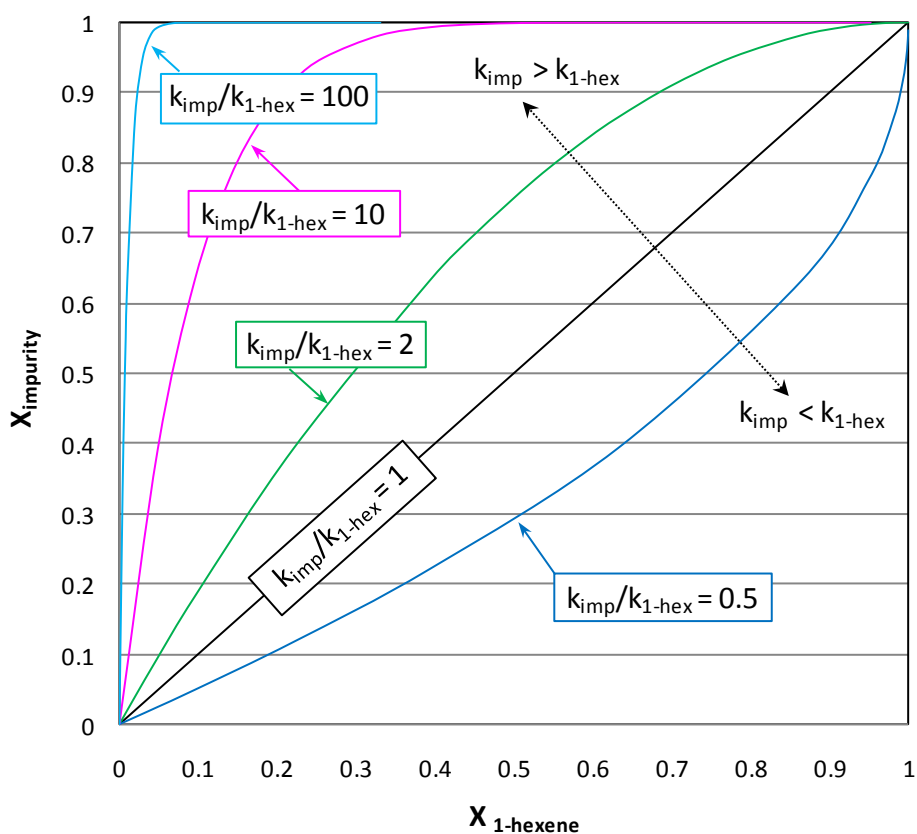


Figure 2.8: Idealised specificity plot (Adapted from McPherson, 2003)

'Selectivity' was defined as the ratio of 1-hexene hydrogenation to total 1-hexene conversion.

$$S = \frac{X_{\text{hydrogenation}}}{X_{\text{hydrogenation+isomerisation}}}$$

This measure quantifies the extent to which conversion happens via hydrogenation. High values are favoured as it is more desirable to obtain an olefin (hydrogenation product) than an internal alkene (double bond isomerisation product).

## 2.6. The influence of excess and gaseous hydrogen

### 2.6.1. Hydrogen limitation

A study conducted by *Ardiaca et al. (2001)* investigated the hydrogenation of butynes and butadienes using a Pd egg-shell catalyst. The study revealed that the dominant cause of mass transfer effects is the existence of a hydrogen limitation.

*McPherson (2003)* tested the selectivity of various catalysts for the hydrogenation of particular impurities in 1-hexene. A comparison of the hydrogenation activity of a given catalyst for the selective hydrogenation of 1,5-hexadiene in 1-hexene at different space times and various temperatures is illustrated in figure 2.9. A hydrogen mass transfer limitation was observed from gas to liquid phase at temperatures above 60°C. With increasing space-time, the rate of hydrogen consumption was seen to decrease at both temperatures for the more active catalyst. The observed hydrogen mass transfer limitation was attributed to a decreased gas-liquid interfacial area, due to reduced turbulence in the reactor. This limited the transfer of hydrogen into the liquid phase and to the catalyst surface.

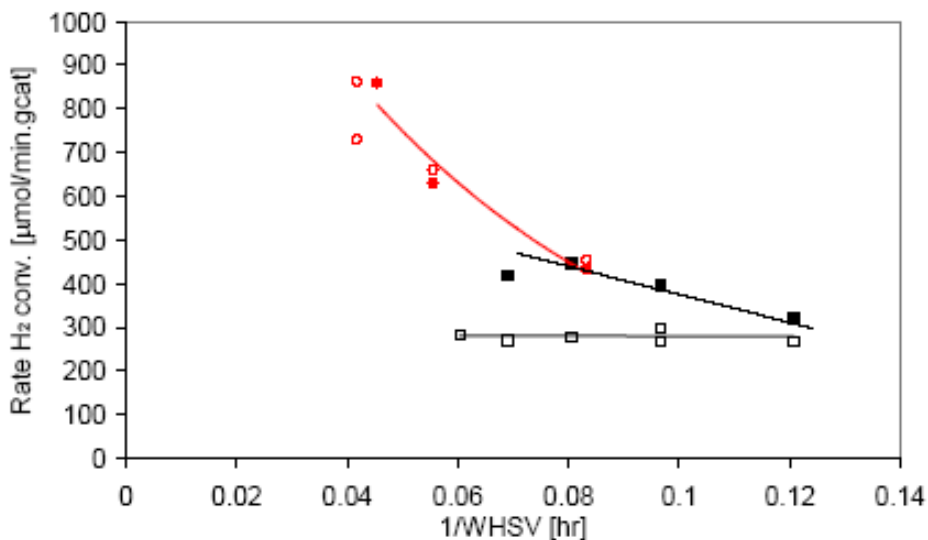


Figure 2.9: Effect of space time on hydrogen consumption rate (McPherson, 2003)

[■ less active catalyst, ○ more active catalyst, P = 15 bar, H<sub>2</sub>/oil = 0.2 (molar), WHSV g<sub>total hydrocarbons</sub>/g<sub>catalyst</sub>·hr]

## 2.6.2. Elimination of gas phase hydrogen

The effect of gas phase hydrogen on the selective hydrogenation of butadiene and butyne in 1-butene was investigated by *Nierlich and Obenhaus, (1986)*. The absence of gaseous hydrogen resulted in higher impurity conversion and a 1-butene gain.

In a similar investigation *Brown (2005)* continued the work of *McPherson (2003)*. Gaseous hydrogen was eliminated from the reactor by the addition of a hydrogen pre-dissolver vessel upstream, and by limiting hydrogen supply to the amount soluble in 1-hexene. A hundred-fold increase in specificity was observed, with values of approximately 100 obtained in some cases. It was concluded that the absence of gaseous hydrogen eliminates hydrogen mass transfer limitations from the gas to the liquid phase and therefore results in an improved impurity conversion, as well as improved specificity (*Brown, 2005*).

### 2.6.2.1. Hydrogen solubility in 1-hexene

As noted above, the work of *Nierlich and Obenhaus (1986)* and *Brown (2005)* has shown that the elimination of gaseous hydrogen in the reactor is necessary to achieve high specificity. Therefore, it is necessary to ensure that all hydrogen feed is dissolved in the liquid phase.

To determine the solubility of hydrogen in the feed, *Ramasary (2008)* designed a simulation in ASPEN, a chemical engineering simulation program. Calculations were based on a pure 1-hexene liquid feed, since the industrial feed will consist of approximately 99 mol% 1-hexene, and impurities can be ignored since they are also olefinic C<sub>6</sub> compounds. Figure 2.10 presents the results of the simulation, illustrating the solubility of hydrogen as a function of temperature at various pressures. The solubility of hydrogen is negligible at atmospheric pressure, but increases with both pressure and temperature.

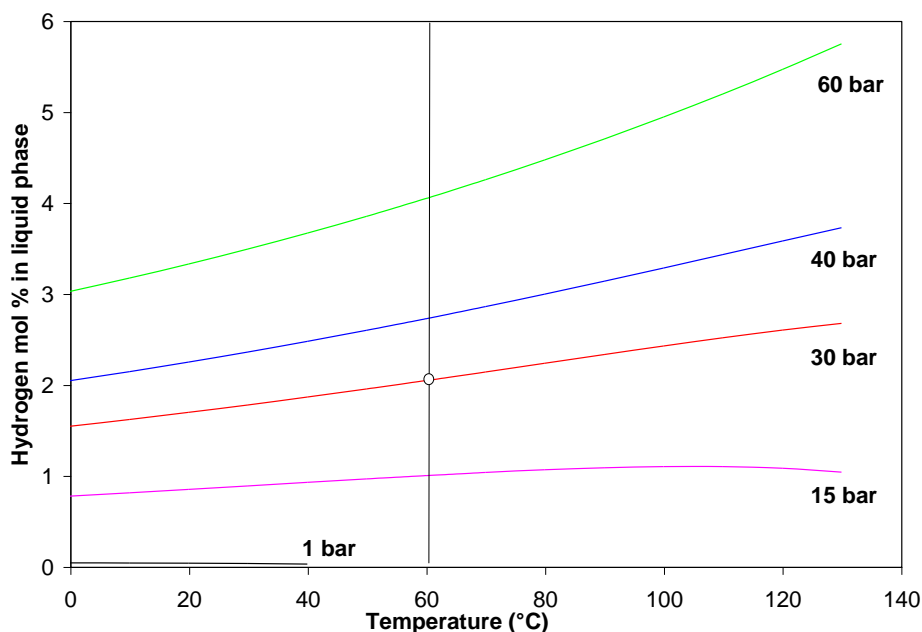


Figure 2.10: Solubility of hydrogen in 1-hexene as a function of temperature at various pressures (ASPEN simulation). (*Ramasary, 2008*).

### 2.6.3. Hydrogen/impurity ratio

It is considered necessary to operate at low, approximately stoichiometric hydrogen/impurity ratio; as hydrogen in excess of the amount required to hydrogenate the impurities will likely result in the undesired hydrogenation of the 1-olefin (*Ardiaca et al., 2001*). However, in the industrial purification of C<sub>2</sub> olefin streams by hydrogenation, the stoichiometric ratio of hydrogen/ethyne (1/1) is not applied. The catalyst is not 100% selective to ethene; therefore an excess of hydrogen is required to obtain complete conversion of ethyne. An increase in hydrogen content accelerates the conversion of the alkyne, but results in a decrease in selectivity due to complete hydrogenation to the alkane (*Duca et al., 1996*).

However work by *Julius (2008)* saw evidence of a hydrogen limitation when operating at stoichiometric levels. As figure 2.11 illustrates, a hexyne conversion of approximately 70% was achieved at stoichiometric hydrogen, this conversion was improved to ~95% under excess hydrogen.

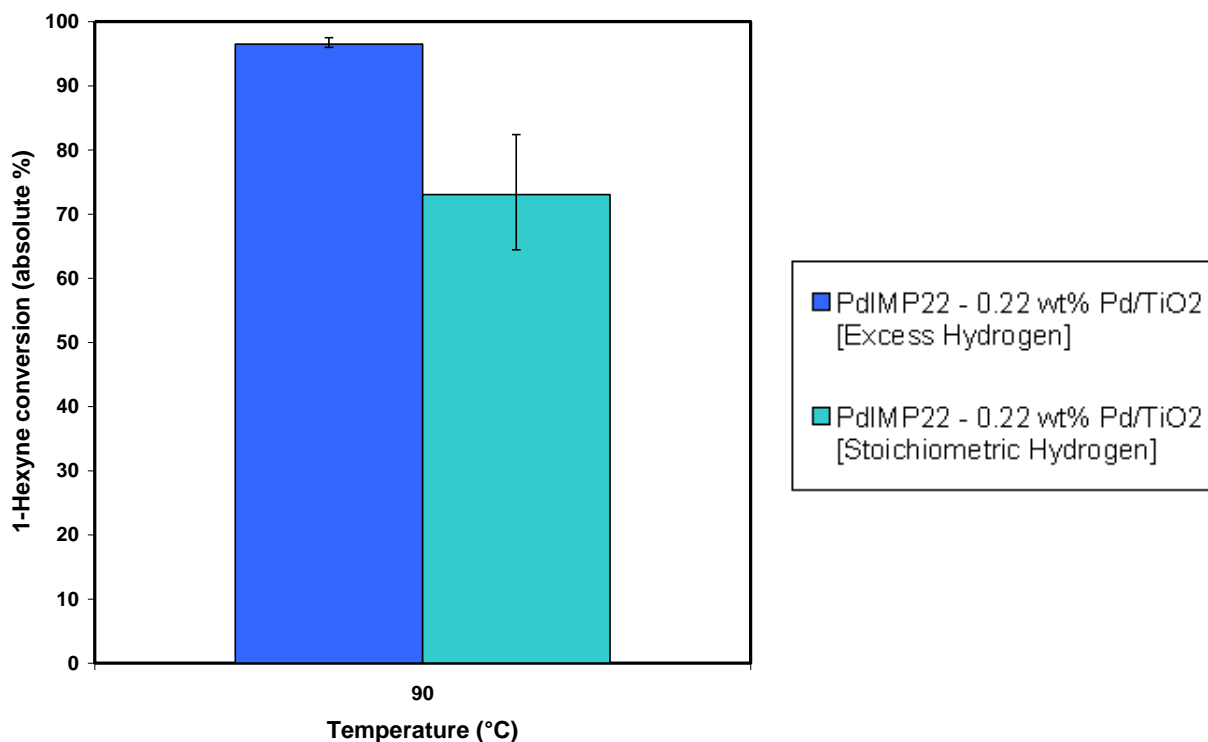


Figure 2.11: Comparison of 1-hexyne conversion at stoichiometric and excess hydrogen (*Julius, 2008*)

## 2.7. The influence of space velocity

In a 2002 patent work referring to the removal of alkadiene impurities from long chain (C<sub>12</sub>-C<sub>18</sub>) alkene fractions over palladium catalysts, *Himelfarb and Bolinger (2002)* point out that operation at low space velocity, allowing a long exposure time between the feedstock and the catalyst, resulted in reduced alkadiene content without a significant increase in the alkane content, particularly when the hydrogen levels in the reaction gas are limited. It is surprising that this long exposure time did not result in the undesired hydrogenation of the alkene to the alkane, as would be expected.



The work does not specifically refer to an  $\alpha$ -olefin feed but rather to an “olefin feedstock” and a “predominantly linear olefin feed”. However it is stated that the olefin stream is to be used downstream in a hydroformylation process to form an alcohol with a high percentage of linear primary alcohols. This indicates that the olefin feed probably consists of mostly 1-alkenes, and signifies that this effect of space velocity could be relevant to this study.

### 3. Previous work

---

Since 2001, several investigations on the selective hydrogenation of 1-hexene have been undertaken at the University of Cape Town. These have provided a basis for the work carried out for this project.

Initial work by *McPherson (2003)* employed Pd-Ag/Al<sub>2</sub>O<sub>3</sub> and Pd/Al<sub>2</sub>O<sub>3</sub>, typical commercial catalysts for selective hydrogenation of C<sub>2</sub> – C<sub>5</sub> streams, as well as a semi-commercial, developmental Au/TiO<sub>2</sub> catalyst. Liquid phase hydrogenation was conducted using a trickle bed arrangement. It was noted that Au/TiO<sub>2</sub> catalysts showed the highest specificity but yielded overall poor activity. The performance of all catalysts was rather disappointing in comparison to that of commercial catalysts for the C<sub>2</sub>-C<sub>5</sub> range. It was concluded relative impurity reactivities may be described by the general rule:

alkynes > alkadienes > 1-alkene > cyclics (*McPherson, 2003*).

It was thought that the presence of gas-phase hydrogen in this liquid-phase process may have reduced the selectivity of the catalyst, as noted by *Nierlich and Obenhaus (1986)*. As such, further studies (*Brown, 2004; Ramasary, 2008*) attempted to improve the reaction conditions through the inclusion of a pre-saturator to dissolve gaseous hydrogen in the reaction mixture. *Brown* also operated at low (close to stoichiometric) hydrogen/impurity ratios. These measures led to much more favourable results, and a fifty-fold increase in specificity to approximately 100 was recorded. *Brown* also investigated the effect of co-adsorbents (CO and ethanol); however there was no observed effect on catalyst selectivity and specificity.

The latest study (*Julius, 2008*) observed an overall improvement in catalyst performance, and has confirmed that Au/TiO<sub>2</sub> achieves excellent selectivity for this process under the improved reaction conditions. In terms of specificity, the previously adopted 'performance' measure, negative numbers were generally observed, with monometallic gold catalysts yielding a 1-hexene gain.

Figure 3.1 illustrates the results of each previous project as points on an idealised specificity plot, it can be seen that as the work has progressed the loss of 1-hexene has been almost eliminated, whilst the conversion of model impurity, 1-hexyne, has increased to up to 70%.

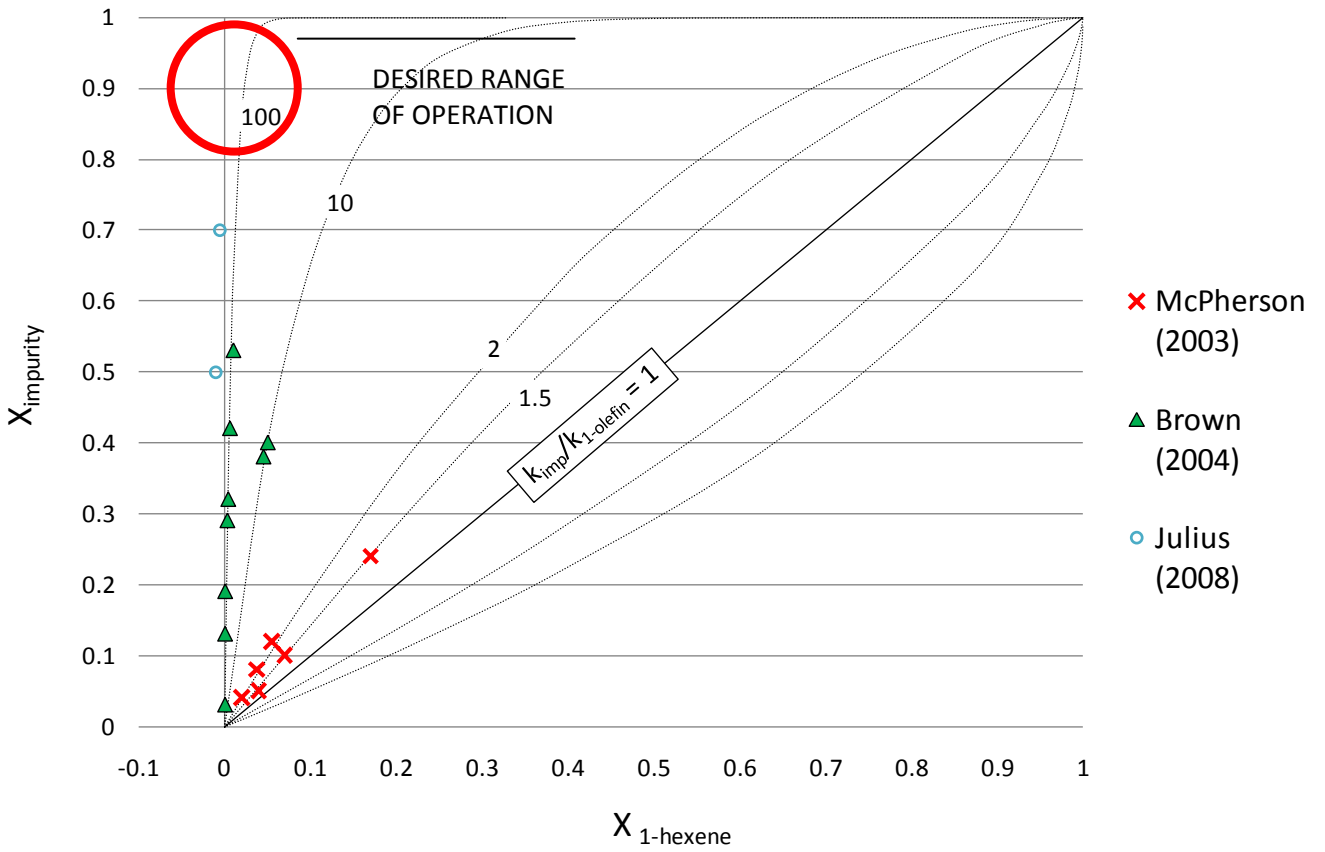


Figure 3.1: Results of previous findings and desired range of operation

## 4. Objectives

---

The overall objective of the project is to evaluate the industrial potential of selective catalytic hydrogenation as a method for the purification of a 1-hexene stream. More specifically, the aim is to extend the previous work into the industrial range, where product impurity levels of less than 100 ppm are generally required. The gold-based catalyst which exhibited promising results in the work of *Julius (2009)* will be employed.

In order to confirm that the process is industrially applicable, this study seeks to investigate impurity removal at the industrial range through:

- Construction of a new experimental apparatus designed to drive the conversion of impurities towards 100%. The apparatus is to make use of an effective pre-dissolver and a multiple reactor configuration with hydrogen replenishment system.
- Development of a method to identify and quantify impurity levels in the industrial range, allowing for the identification of individual impurity species at levels less than 100 ppm.
- Testing with industrially relevant feedstocks. A 'model' industrial C<sub>6</sub>  $\alpha$ -olefin stream will be employed; impurities will include a blend of alkynes, dienes and cycloalkenes.
- Evaluating the performance of the catalyst for the 1-hexene purification, in terms of activity, selectivity and specificity.

The study aims to answer the following key questions:

- Will the gold catalyst (Au/TiO<sub>2</sub>) retain high/negative specificity and high selectivity for the hydrogenation of impurities down to approximately 100 ppm impurities?
- What influence will hydrogen/impurity ratio have on impurity removal and 1-hexene loss at low impurity levels?
- How will operation with multiple reactors and hydrogen replenishment influence the hydrogenation of impurities and loss of 1-hexene?
- How will the series describing relative reactivity of impurities (alkynes > alkadienes > 1-alkene >> cyclics) be affected by operation at very high impurity removal and with multiple reactors?

## 5. Experimental

---

The only catalyst employed in this study was gold on titania prepared by incipient wetness impregnation. This catalyst was selected based on its performance in previous studies (*Julius, 2008*), with the objective of studying the effects of hydrogen availability and replenishment on the process.

### 5.1. Catalysts

A single batch of catalyst was prepared for use in this study. This catalyst was prepared via impregnation of TiO<sub>2</sub> with 1 wt % gold using chloroauric acid solution (HAuCl<sub>4</sub>).

#### 5.1.1. Catalyst preparation

Titania (TiO<sub>2</sub> extrudates, Degussa P25) was used as the support material. The pore volume of the TiO<sub>2</sub> extrudates was determined to be approximately 0.45 cm<sup>3</sup>/g, by a visual inspection of liquid uptake. Chloroauric acid solution (HAuCl<sub>4</sub>, 250 g<sub>Au</sub>/l, supplied by Mintek) was used as the gold precursor. Deionised water was used at all times.

The Au/TiO<sub>2</sub> catalyst was prepared via incipient wetness impregnation. The gold solution was diluted with deionised water to a desired volume and concentration such that the liquid would just fill the pore volume of the support material and the resulting catalyst would contain 1 wt% Au. The diluted solution was added dropwise to the extrudates. This was followed by agitated drying using a rotary evaporator (Buchi Rotavapour, with bath temperature 60°C) to remove all excess water. The catalyst was then dried overnight at 120°C and calcined in air for 3 hours at 400°C. The details of the preparation are described in table 5.1.

Table 5.1: Catalyst preparation parameters

Catalyst	TiO <sub>2</sub> (g)	Pore volume of TiO <sub>2</sub> (ml)	Volume HAuCl <sub>4</sub> (ml)	Volume H <sub>2</sub> O (ml)
Au IMP 1	50.0	22.5	2.0	20.5

### **5.1.2. Catalyst Characterisation**

#### **5.1.2.1. Catalyst loading**

The catalyst loading, specifically the Au content, is provided in table 6.2 in the results section, and was determined using Inductively Coupled Plasma – Atomic Emission Spectroscopy (ICP-AES).

#### **5.1.2.2. Metal particle size**

Transmission Electron Microscopy (TEM) was employed to examine the catalyst surface, and to thus determine the size and distribution of gold particles on the carrier support. The TEM instrument employed was the LEO 912 (Leo, now Zeiss, Germany).

Both fine powder and extrudate samples of the catalyst, as well as the titania support, were analysed. The extrudate samples had to be prepared using the “resin” method, where the samples are cut into very fine slices for better visibility under the microscope. Pill sized sample holders containing one catalyst pellet each were filled with resin. After solidification at 60°C overnight, the hard resin was cut in an Ultramicrotome LEICA Ultracut S (Leica, Austria) cutting machine to 0.1µm thick sample slices. These were placed on fine copper-grids. Digital photos of the catalyst and titania support were taken, and particles sizes were determined by measurement using IMAGE J software.

## **5.2. Feedstocks**

The 1-hexene base feedstock used for this study was supplied at > 99% purity, whilst the balance consisted of various unsaturated C<sub>6</sub> isomer compounds and hexane. Model impurity compounds were used to spike the 1-hexene feedstock to a desired level of impurities. The chosen model impurities were 1-hexyne, 1,5-hexadiene, 1,4-hexadiene, 2,4-hexadiene and 1-methyl-cyclopentene. Three different feed conditions were studied using one, or a combination, of these model impurities. The approximate feed compositions are detailed in table 5.2. Further details of the feed preparation method are provided in appendix II.

Table 5.2: Feed compositions

<b>Feed 1:</b>		<b>Feed 2:</b>		<b>Feed 3:</b>	
1-hexene	98.7%	1-hexene	99.1%	1-hexene	98.7%
1-hexyne	0.2%			1-hexyne	1%
1,5-hexadiene	0.2%	1,5-hexadiene	0.2%		
1,4-hexadiene	0.2%	1,4-hexadiene	0.2%		
1-methyl-1-cyclopentene	0.2%	1-methyl-1-cyclopentene	0.2%		
2,4-hexadiene	0.2%				
Other*	0.3%	Other*	0.3%	Other*	0.3%

\*Other refers to n-hexane and branched C<sub>6</sub> alkanes that were introduced with the 1-hexene

Liquid and gaseous compounds employed as feed or co-feeds are listed in table 5.3. The gaseous H<sub>2</sub> and N<sub>2</sub> feedstocks were provided via the reticulated laboratory supply lines, fed respectively from gas cylinders supplied by Air Liquide.

Table 5.3: Supplier and purity of compounds used as feeds and co-feeds

<b>Compound</b>	<b>Supplier</b>	<b>Purity</b>
1-Hexene	Sigma Aldrich	99.3%
1,5-hexadiene	Sigma Aldrich	97%
1-methyl-1-cyclopentene	Sigma Aldrich	98%
1-Hexyne	Sigma Aldrich	97%
1,4-hexadiene	Sigma Aldrich	99%, mix of cis and trans isomers
2,4-hexadiene	Sigma Aldrich	90%, mix of isomers
Hydrogen	Air Liquide	99.999%.
Nitrogen	Air Liquide	99.999%.

### 5.3. Catalyst performance test unit

Figure 5.1 is a picture of the test unit; the apparatus is also illustrated schematically in figure 5.2.

The reaction zone consists of three downflow trickle-bed reactors in series, mounted inside a brass block for isothermal operation. A dissolver is employed upstream of each reactor (within the reactor block) to ensure the complete dissolution of the gaseous H<sub>2</sub> in the 1-hexene.

The liquid hydrocarbon feed is supplied via a metering pump and the gaseous feed components via mass flow controllers. A sampling loop is provided downstream of the reactor. The reactor effluent proceeds via the sampling loop and is collected in one of two product catch pots, with gaseous effluent venting to atmosphere via a needle valve. The major components of the experimental test apparatus are described in sections 5.3.1 to 5.3.5, all referring to figure 5.1. Valves, fittings, tubing etc. where no specific manufacturer is mentioned, were obtained from Swagelok<sup>®</sup>. All equipment in contact with the feed or product was made from stainless steel (SS-316).



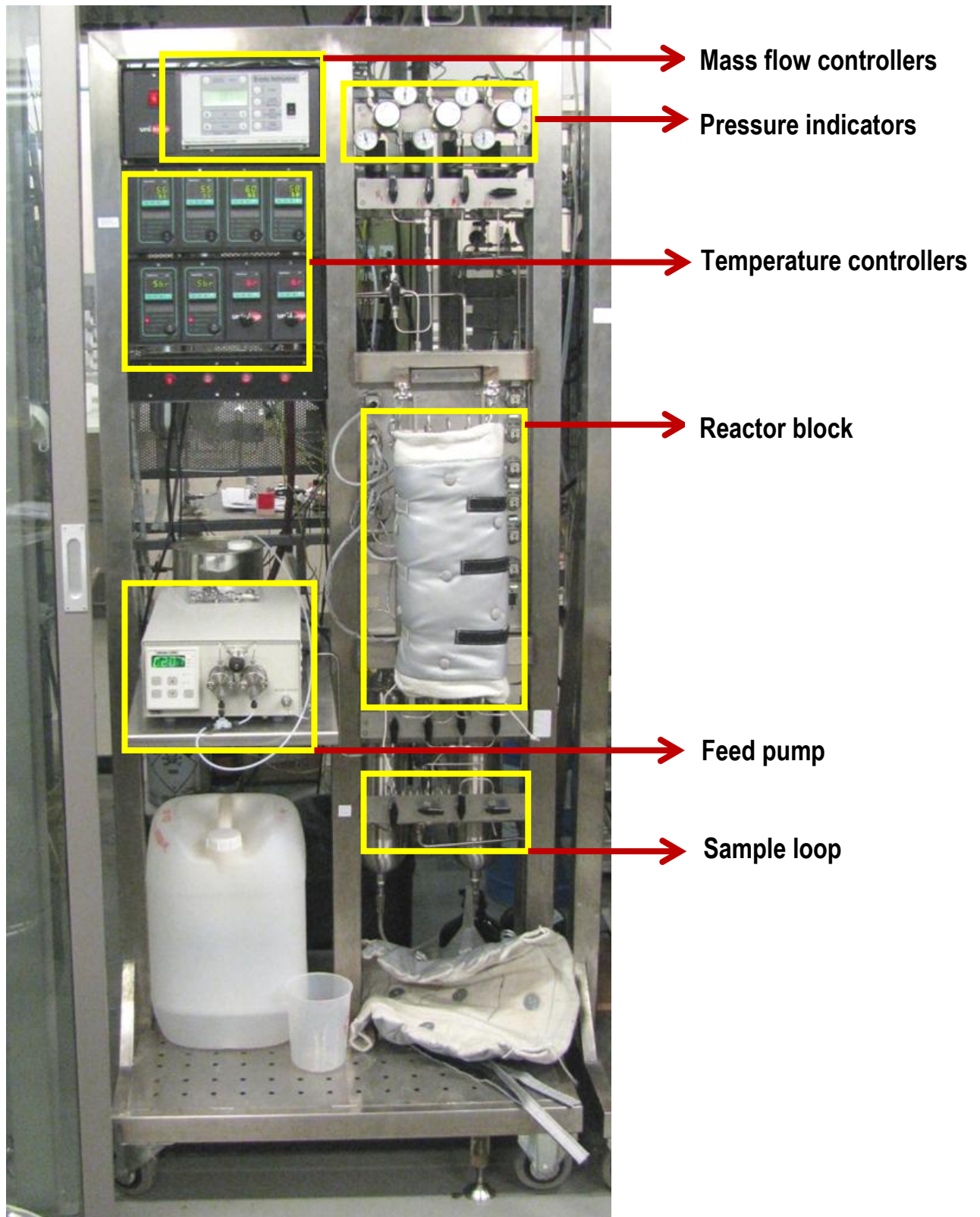


Figure 5.1: Picture of experimental test unit

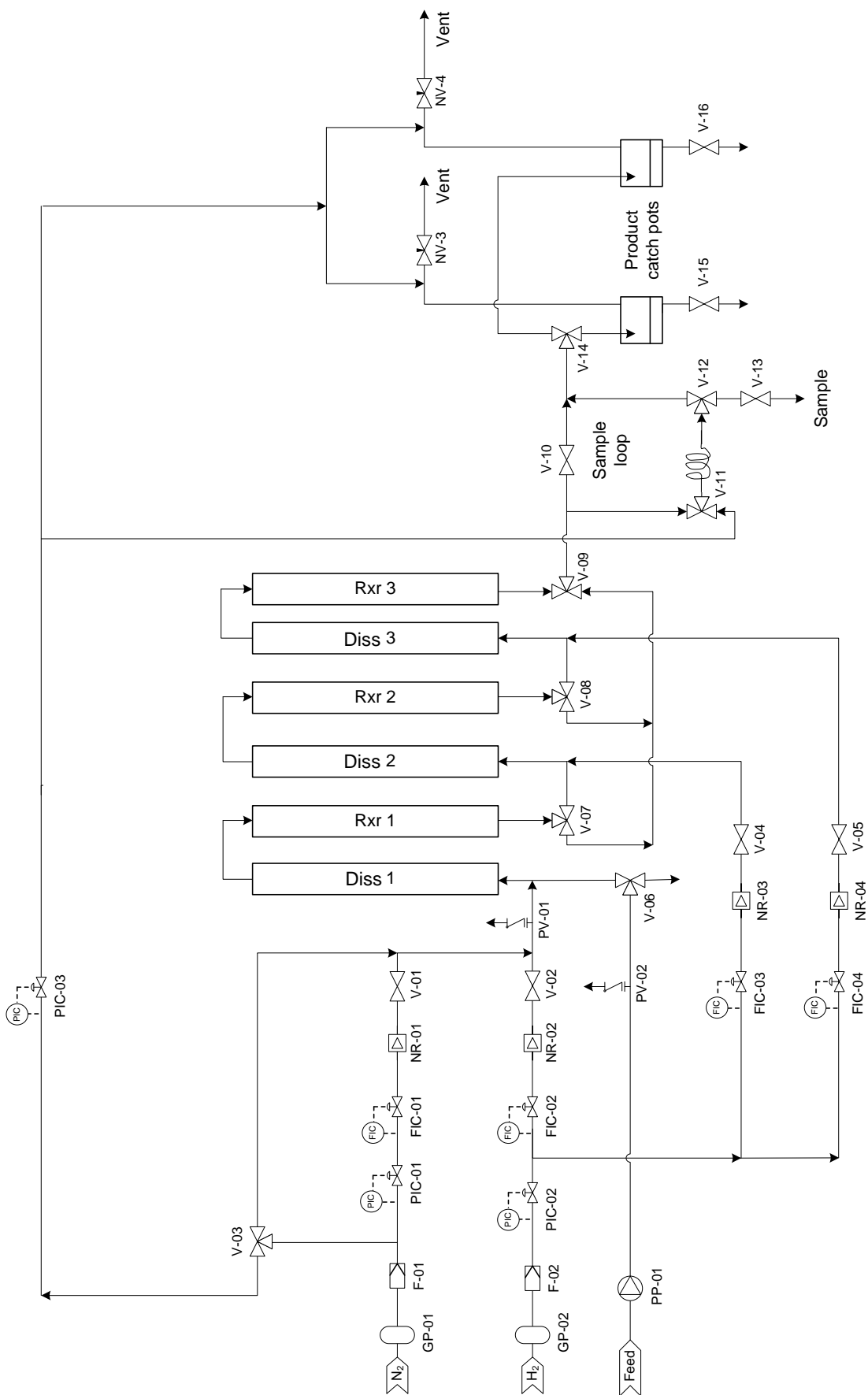


Figure 5.2: Schematic illustration of experimental test unit

### **5.3.1. Design improvements to previous apparatus**

#### **5.3.1.1. Reactor setup**

The old experimental apparatus made use of a single reactor, the reactor body consisted of an 11 cm long stainless steel tube with an internal diameter of 1.6 cm and the total internal volume was approximately 22 cm<sup>3</sup>. In designing the new test unit, allowance for operation as a single reactor as well as two, or three reactors in series was provided, as well as the option of inter-stage hydrogen replenishment when using multiple reactors; this is described further in section 5.3.3. The new reactor tubes are longer and thinner (¼ inch tube of length 35 cm), allowing for easier loading and improved radial temperature distribution. Each unpacked reactor has a volume of approximately 4.4 cm<sup>3</sup>.

#### **5.3.1.2. Temperature control**

In the previous test unit the temperature within the reactor and dissolver was controlled by placing both vessels in a thermostated bath filled with silicon oil, and heat was provided by a heating coil submerged in the bath. This was improved in the new test unit by placing the entire reactor/dissolver setup within a machined brass housing, the temperature of which is controlled by three individually controlled heater bands to ensure isothermal operation consistent with the original apparatus. The new design is more practically functional and allows for easier and cleaner loading and unloading of the reactors. The block is insulated with a heating jacket.

During commissioning of the apparatus a blank test was performed to confirm the isothermal operation of the block. A thermocouple was inserted into each reactor and the tubes packed with silicon carbide. Standard reaction conditions were applied in terms of olefin flow and the system was left to equilibrate overnight, following which the thermocouple readings were noted. The thermocouples were then pulled axially 5 cm up the reactor, and after an hour the temperature readings noted. This was repeated along the length of the reactor for 60, 90 and 120°C. The thermocouple readings did not vary more than 2°C from the set-point and as such operation was considered isothermal.

#### **5.3.1.3. Valve switching issue**

In the old test unit, relatively large fluctuations in impurity conversion were observed due to valve switching during sampling, as well as due to pressure fluctuations caused by emptying of the waste vessel during operation. This has been improved in the new test unit by improvements in the design of the sample loop

and by the inclusion of 2 large waste vessels GP-03 and GP-04. Product flow can be switched between these 2 vessels and eliminates the problem of emptying the waste vessel during operation.

### 5.3.2. Feed system

Hydrogen gas is supplied via the house gas line via valves (V-02, V-04 and V-05), and regulated by inline pressure controller (PIC-02) (manufactured by Tescom) and mass flow controllers (FIC-02, FIC-03 and FIC-04) (manufactured by Brooks). Nitrogen is supplied via valve (V-01) and regulated by inline pressure controller (PIC-01) and mass flow controller (FIC-01). Non-return valves (NR-01, NR-02, NR-03 and NR-04) are located downstream of the flow controllers and guard catch pots (GP-01 and GP-02) are located upstream. This configuration provides protection for the house gas lines against possible backflow of liquid in the event of a downstream line or reactor blockage. Liquid feed is supplied by pump (PP-01) (Series 1, Scientific Systems) to the dissolver/reactor combination. The feed mixture bottle was placed on a balance (GX4000, A & D), this enabled the confirmation of the accuracy of the feed flow rate to 2 decimal places.

### 5.3.3. Dissolver/Reactor configuration

The reactor configuration is illustrated schematically in figure 5.3; the system consists of three downflow trickle-bed reactors in series, mounted inside a brass block for isothermal operation. A dissolver is employed upstream of each reactor (within the single reactor block). Figure 5.4 shows the top of the reactor/dissolver block, with the flow of feed illustrated.

The system has been designed to allow operation as a single reactor as well as two, or three reactors in series and provides the option of inter-stage hydrogen replenishment when using multiple reactors.

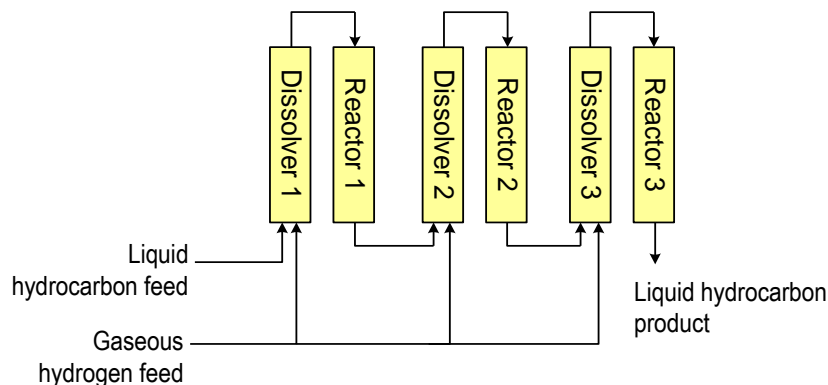


Figure 5.3: Schematic illustration of dissolver/reactor configuration.

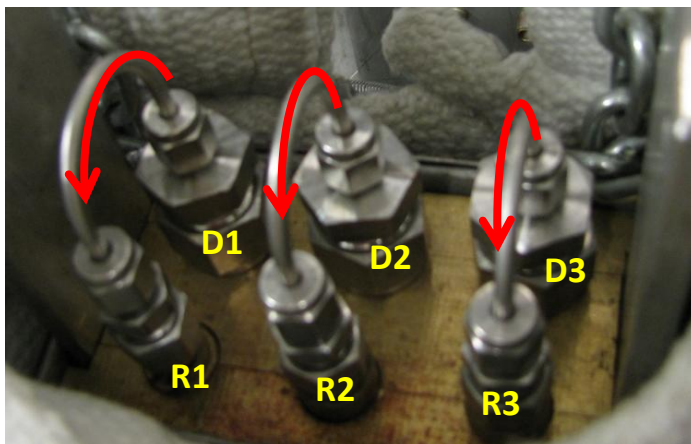


Figure 5.4: View of top of reactor/dissolver block.

'R' denotes Reactors and 'D' denotes Dissolvers. Red lines illustrate the flow of hydrocarbon feed

#### 5.3.4. Hydrogen dissolution vessel

Each dissolver tube is filled with inert silicon carbide (1340 -1660  $\mu\text{m}$ ) to facilitate the dissolution of the gaseous hydrogen in the 1-hexene feed. The silicon carbide particles serve to break the gaseous hydrogen into small bubbles, thus increasing the gas/liquid inter-facial area, the radial distribution of the bubbles and the residence time of the hydrogen and as such enabling complete dissolution. The dissolver tubes are all  $\frac{1}{2}$  inch Swagelok<sup>®</sup> tubes of length 35 cm with internal diameter approximately 10 mm. The bottom of the dissolver consists of an entrance point for the gas and liquid feeds ( $\frac{1}{2}$  inch Swagelok<sup>®</sup>) whilst the top of the dissolver ( $\frac{1}{2}$  inch Swagelok<sup>®</sup>) is connected to the reactor. The equivalent available contacting volume is approximately 11 cm<sup>3</sup>.

#### 5.3.5. Reactor

The reactor body consists of a  $\frac{1}{4}$  inch Swagelok<sup>®</sup> tube of length 35 cm with internal diameter approximately 4 mm. The unpacked reactor has a volume of approximately 4.4 cm<sup>3</sup>. The top of the reactor consists of an entrance point for the feed from the dissolver ( $\frac{1}{4}$  inch Swagelok<sup>®</sup>) whilst the bottom of the reactor ( $\frac{1}{4}$  inch Swagelok<sup>®</sup>) is connected to either the next dissolver, or the sampling loop, via a 3 way valve.

### 5.3.6. Sampling loop

The sampling loop downstream of the reactor provides for the collection of a liquid product sample without depressurization of the system. The loop is bypassed via valve V-10. Whilst an experiment is running valve V-10 is closed and the sample loop is constantly flushed with product, liquid flows through the loop to the product catch pots via valves V-11 and V-12. During sample collection the loop is bypassed by opening valve V-10, whilst the isolated loop between V-11 and V-12 is expelled under nitrogen pressure by opening valve V-13. In this way, the sample may be collected under pressure such that there is no pressure drop when switching back to the sampling loop. Liquid product samples are collected from the test unit and analysed in an off-line gas chromatograph. The sampling loop is illustrated in figure 5.5.

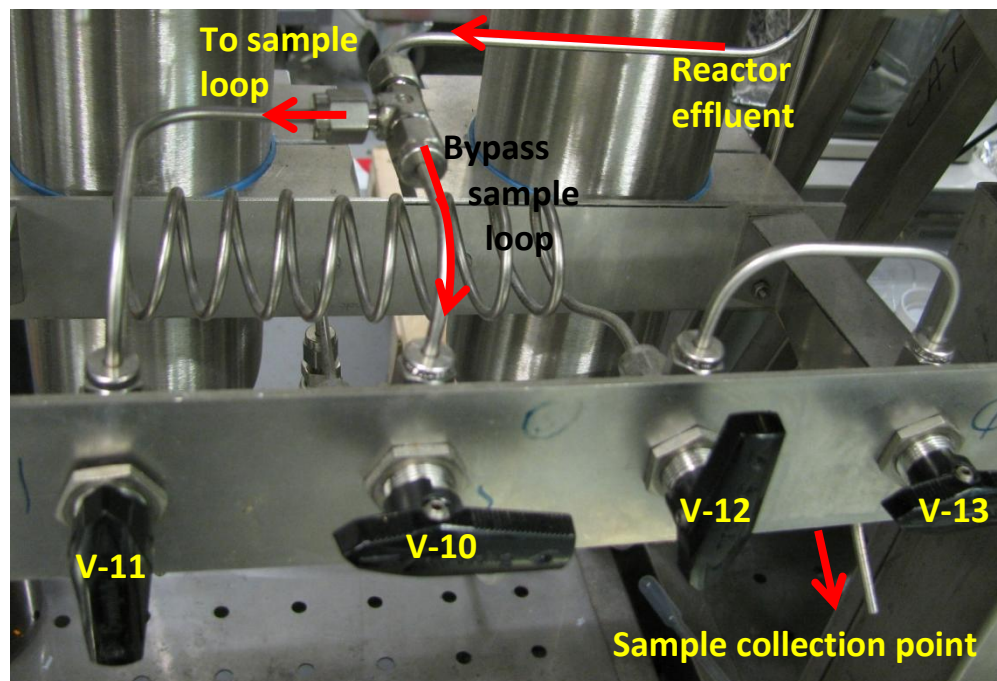


Figure 5.5: Sampling loop

### 5.3.7. Pressure control

The pressure in the system is maintained through the use of nitrogen as a pressure regulating gas. The nitrogen gas pressure is regulated by an in-line pressure controller (PIC-03). The nitrogen is added to the gas stream from the reactor downstream of the product catch pot. The combined gas stream is throttled at approximately 20 ml/min (at STP) from each regulating needle valve (NV-03 and NV-04) before being

vented. In this way, the pressure in the reactor is set and maintained constant by the pressure of the added nitrogen stream.

**5.3.8. Temperature control**

The reactor/saturator block is heated to the desired temperature (60, 90 or 120°C) via three heating bands. The block is insulated with a heating jacket. The flow of liquid within the reactor/dissolver tubes is slow enough to ensure that the feed reaches the desired temperature quickly, and hence no external pre-heating of the feed is required.

**5.4. Experimental operating procedures**

**5.4.1. Catalyst loading**

A small piece of silane treated glass wool is used to plug the bottom of the reactor, in order to prevent any loss of catalyst from the bed during loading. Inert silicon carbide granules are packed above and below the catalyst bed, and serve as a flow distributor and bed support. The total volume of the unpacked reactor is approximately 4.4 cm<sup>3</sup>. Another piece of glass wool is used to plug the top of the reactor tube.

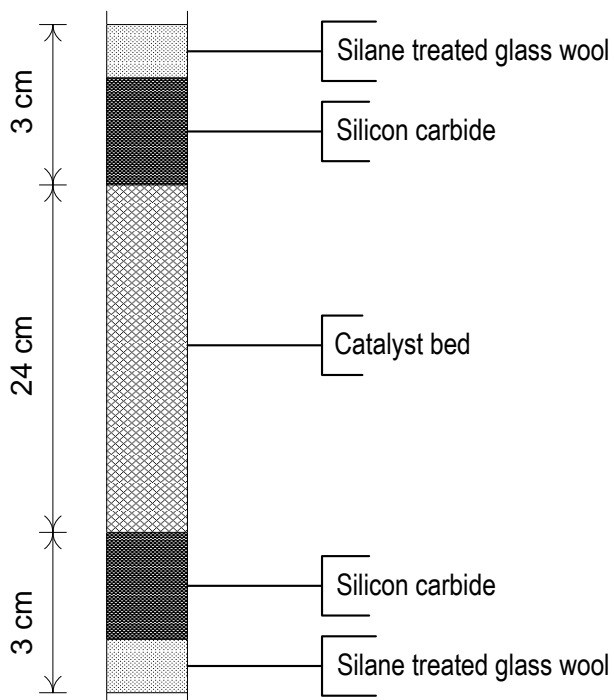


Figure 5.6: Schematic illustration of reactor packing

#### **5.4.2. System pressure test**

Following catalyst loading, a system pressure test is performed to ensure that all fittings are leak tight. The unit is pressurized to 30 bar<sub>g</sub> using via the nitrogen line. The unit is judged leak tight when no pressure drop occurs overnight.

#### **5.4.3. Catalyst activation / reduction**

The catalyst activation/reduction procedure described below is as performed according to all previous studies (*McPherson, 2003; Brown, 2005; Ramasary, 2008; and Julius, 2008*).

A mixture of 5 mol % hydrogen and 95 mol % nitrogen (2 sccm hydrogen and 38 sccm nitrogen) is set to flow over the catalyst via valves V-01 and V-02 (V-04 and V-05 also used depending on number of reactors being used) and mass flow controllers FIC-01 and FIC-02 (FIC-03 and FIC-04 likewise). The reactor block is heated to a temperature of 90°C and the reactor is maintained at this temperature for 3 hours. Thereafter, valve V-01 is closed and the flow changed to hydrogen only via valve V-02 (V-04 and V-05) and FIC-02 (FIC-03 and FIC-04) at 100 sccm. The reactor is maintained at these conditions for a further hour. The temperature is then set to the desired reaction temperature.

#### **5.4.4. Start-up procedure**

Following activation/reduction, when the temperature of reactor block has reached the desired reaction temperature, the mass flow controllers FIC-01 and FIC-02 (FIC-03 and FIC-04) are set to the desired gas flows and the rig is pressurised to 30 bar<sub>g</sub> by introducing the regulating gas. The hydrogen inlet gas pressure is adjusted via pressure regulator PIC-02 to 35 bar<sub>g</sub>. The hydrogen pressure is set 5 bar above the reaction pressure to provide the necessary pressure difference for hydrogen flow to occur.

Sample loop valves V-11 and V-12 are set in position to allow flow from the reactor through the sample loop to the product catch pot, while the sample loop bypass valve V-08 is closed. Thus, the sample loop is constantly flushed with product.

When the temperature and pressure of operation have stabilised, the pump (PP-01) is purged with the feed mixture at 1 ml/min to ensure removal of any air-bubbles trapped in the line or pump head. This is achieved by opening valve V-06, setting the pump flow rate to 1 ml/min and switching the pump on. Following this,



the desired liquid flow can be set on the pump and the balance is monitored until steady state is reached (typically 1 hour).

### 5.4.5. Variation of reaction conditions

Following alteration of reaction variables, such as temperature, hydrogen:oil ratio or pump flow rate, the system is left overnight to stabilise (approximately 12 hours).

### 5.4.6. Variation of reactor configuration

When changing operation between 1, 2 or 3 reactors in series, the catalyst charges are reloaded and the necessary valves opened or closed to allow flow through 1, 2 or 3 reactors. When using 2 or 3 reactors the catalyst mass used in each individual reactor is the same as for the single reactor case (i.e. the **total** mass is twice or three times that used for operation as a single reactor), and the reactant flow increased to keep the same weight hourly space velocity.

### 5.4.7. Sampling

Collection of samples is performed as described in section 5.3.3. Four samples are taken daily and are analysed immediately by gas chromatography. Following analysis sample vials are stored in the refrigerator to prevent evaporation of volatile compounds.

### 5.4.8. Draining the product catch pots

Product catch pots GP-03 and GP-04 are 2.2 litre Swagelok<sup>®</sup> vessels. The pots must be drained every few days during an experimental run. Valve V-14 is used to direct product to one or other catch pot. To drain a pot the flow is directed to the other pot and the drainage valve (V-15 or V-16) opened.

### 5.4.9. Shutdown procedure

Once an experimental run has been completed, the feed pump is switched off. The gas flow is changed from hydrogen to nitrogen at the maximum flow rate of 100 sccm (FIC-01) by opening valve V-01 and closing valves V-02, V-03 and V-04. The temperature is set to 60°C in order to strip residual hydrocarbons from the system. After approximately 3 hours the nitrogen flow rate is reduced and the test unit is left to flush overnight.

The heating bands are then turned off, the pressure regulating gas is switched off and the system is left to depressurise. All remaining liquid is collected from the product catch pots (GP-03 and GP-04).

Once the reactor block has cooled, the reactor tubes are removed and opened. The spent catalyst, silicon carbide and glass wool are removed. Thereafter the reactor is washed with acetone and dried with compressed air. The reactor is reloaded according to section 5.4.1 and the next experimental run is started.

### 5.5. Operating conditions

The performance of the catalyst is evaluated at the operating conditions listed in table 5.4. For the purpose of evaluating the influence of operating variables on the catalyst performance, pressure, space velocity (WHSV) and hydrogen/oil ratio were varied as presented. Conditions are routinely reset to the 'standard value' in order to determine whether catalyst deactivation has occurred over the course of an experiment.

Table 5.4: Standard and experimental range of operating conditions

<b>Condition</b>	<b>Standard value</b>	<b>Range</b>
<b>WHSV</b> ( $\text{g}_{\text{feed}} / \text{g}_{\text{cat}} \cdot \text{hr}$ )	3	3, 11
<b>H<sub>2</sub> / oil ratio</b> ( $\text{mol}_{\text{H}_2} / \text{mol}_{\text{hydrocarbon}(\text{total})}$ )	0.01	0.01, 0.02
<b>Pressure</b> (Bar <sub>g</sub> )	30	-
<b>Temperature</b> (°C)	60	60, 90, 120

## 5.6. Feed and product analysis

### 5.6.1. Gas chromatography

The analysis of the liquid samples is done by gas chromatography and flame ionisation detection (FID) with automated sample injection (0.1 µl sample volume). Chromatographic conditions are detailed in table 5.5.

Table 5.5: Gas chromatographic conditions

<b>Gas chromatograph</b>	Varian model 3900
<b>Autosampler</b>	Varian model 8400
<b>Detector</b>	Flame ionisation detector
<b>Carrier gas</b>	Helium
<b>Make-up gas</b>	Nitrogen
<b>Carrier gas linear velocity</b>	42.2 cm/min
<b>Split ratio</b>	50 : 1
<b>Liquid sample volume</b>	0.1 µl
<b>Column head pressure</b>	1.430 bar
<b>Detector temperature</b>	250 °C
<b>Injector temperature</b>	180 °C
<b>Column type</b>	PLOT fused silica column
<b>Stationary phase</b>	Al <sub>2</sub> O <sub>3</sub> /Na <sub>2</sub> SO <sub>4</sub>
<b>Column manufacturer</b>	Varian - CP7568
<b>Column length</b>	50 m
<b>Column internal diameter</b>	0.53 mm
<b>Film thickness</b>	10 µm
<b>Column temperature program</b>	60-110 °C (Rate 5°C/min) 110-160 °C (Rate 12°C/min) 160-200°C (Rate 15°C/min) 200°C (20 minutes)

Peaks observed in the chromatogram were identified by the injection of known components and compared on the basis of retention time. Figure 5.7 illustrates a typical chromatogram, the peaks are labelled to indicate the identity of each compound.

No peaks were observed in the region expected for cracked products (<C<sub>6</sub>) or dimers (in the C<sub>12</sub> range).

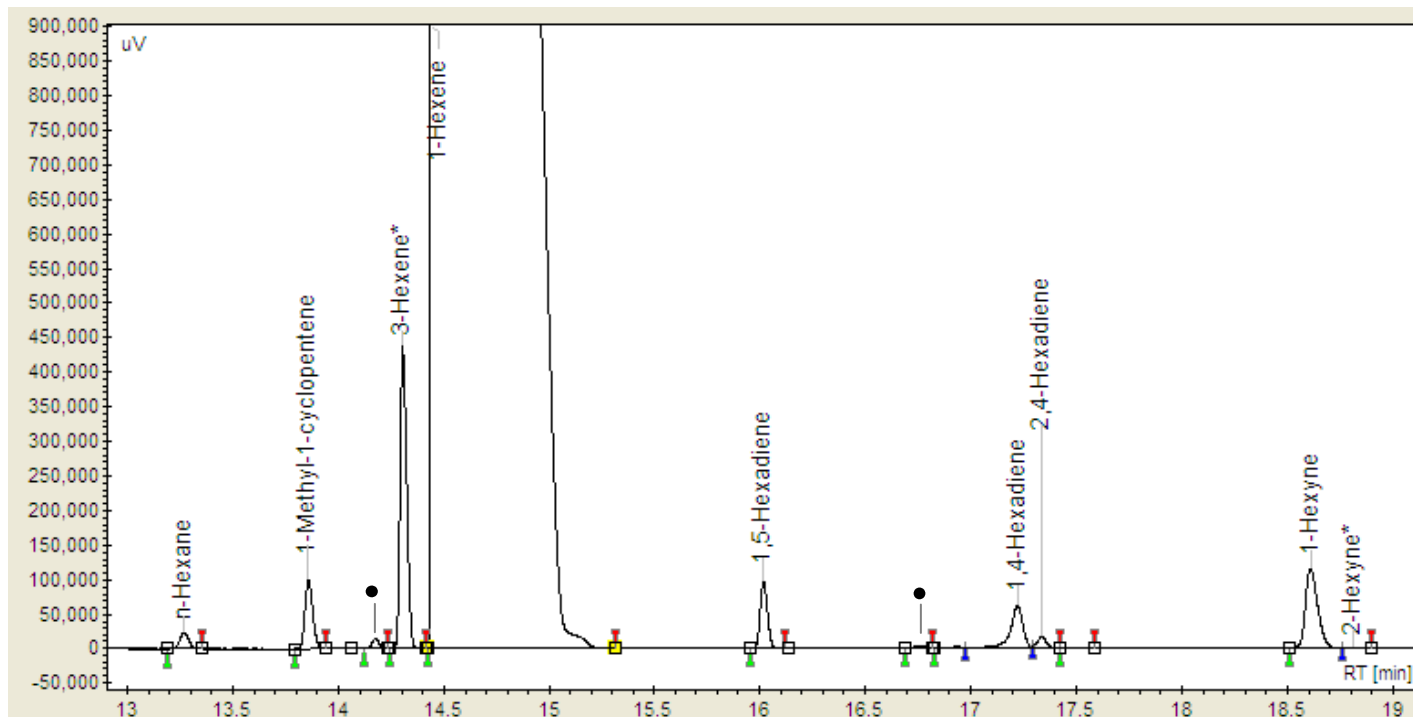


Figure 5.7: A typical sample chromatogram and analysis (\* indicates high likelihood of that compound or isomer thereof; • indicates unknown component)

### 5.6.2. Data work-up

The FID response factors for all components were considered to be unity with respect to carbon mass. This was justified on the basis of the signal of hydrocarbons in the FID being proportional to the amount of carbon. A carbon mass balance of 100 % is assumed as the basis for all calculations and since no peaks of other carbon number hydrocarbons (cracked or polymeric products) were observed, peak areas were considered proportional to moles, and peak area percentage was identical with molar percentage.

A calibration curve was prepared for each model impurity plotting the GC response against the known ppm of standard mixture in the range between 62 and 2000 ppm. The relationship between the known

component ppm from the standard mixture and the calculated ppm from the GC peak area response were very close to linear for all impurities down to less than 60 ppm. Figure 5.8 (and inset) illustrates the linearity of selected model impurities (those not illustrated here are provided in appendix I).

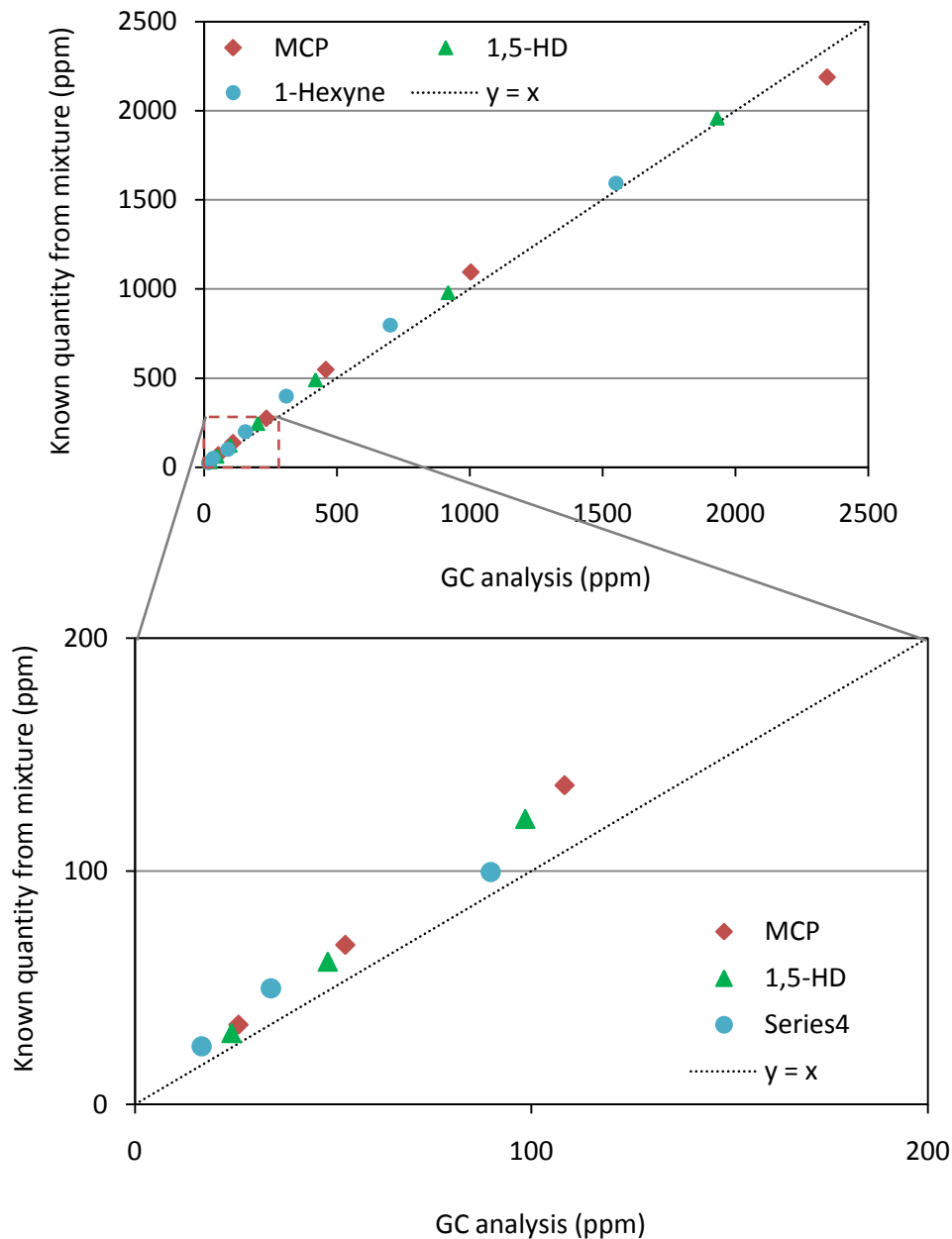


Figure 5.8: Linearity of model impurities

**5.6.2.1. Conversion and catalyst performance parameters**

The conversions of the five model impurities (as detailed in section 5.2) and 1-hexene were monitored, as well as the gain in n-hexane and hexane isomers. Selectivity and specificity were employed as measures of catalyst performance.

- **1-hexene conversion**

The calculation of the conversion of 1-hexene is simply the difference between the 1-hexene fraction in the feed and product streams over the fraction in the feed.

$$X_{1 \text{ Hexene}} = \frac{X_{1 \text{ Hexene, feed}} - X_{1 \text{ Hexene, product}}}{X_{1 \text{ Hexene, feed}}}$$

Eq. 1

Any loss of 1-hexene, by hydrogenation (to n-hexane) or isomerisation (to hexene isomers), is taken into account in this equation.

The partial hydrogenation of impurities (1-hexyne or diene impurities) to 1-hexene may potentially result in negative values for 1-hexene conversion. A negative 1-hexene conversion value indicates a net gain in 1-hexene, whilst a positive value for 1-hexene conversion indicates a net loss in 1-hexene.

- **Total impurity conversion**

In the calculation of total impurity conversion, only the hydrogenation of impurity is taken into account as the impurity isomerisation is not a net impurity removal. The feed total impurity is therefore defined as the total pure impurity and any of its isomers and, thus, only the hydrogenation of these species is taken into account as total impurity removal.

$$X_{\text{Total impurity}} = \frac{\left( X_{\text{Total impurity, feed}} - X_{\text{Total impurity, product}} \right) + \left( X_{\text{impurity isomers, feed}} - X_{\text{impurity isomers, product}} \right)}{X_{\text{Total impurity, feed}} + X_{\text{impurity isomers, feed}}}$$

Eq. 2

- **Individual impurity conversion**

The conversion of each separate model impurity is also determined to ascertain which impurity species are being converted.

$$X_{\text{impurity}} = \frac{X_{\text{impurity, feed}} - X_{\text{impurity, product}}}{X_{\text{impurity, feed}}}$$

Eq. 3

- **Hydrogen conversion**

Hydrogen is consumed in all hydrogenation reactions: 1-hexene and impurity hydrogenation, as well as hydrogenation of impurity isomers. Impurities with multiple unsaturation (hexadienes and hexynes) may be hydrogenated twice, first to a mono-ene and subsequently to n-hexane. Thus, the net hydrogen usage may be calculated by considering the hydrogenation of impurities and impurity isomers, as well as n-hexane formation. Hence, hydrogen usage is defined according to equations 4 and 5 below.

$$X_{\text{H}_2} = \frac{H_2 \text{ feed} - H_2 \text{ product}}{H_2 \text{ product}}$$

Eq. 4

$$X_{\text{H}_2} = \frac{\left( X_{\text{impurity + impurity isomers, feed}} - X_{\text{impurity + impurity isomers, product}} \right) + \left( X_{\text{hexane, product}} - X_{\text{hexane, feed}} \right)}{\frac{H_2}{\text{Oil ratio}}}$$

Eq. 5

- **Hydrogenation activity**

The rate of hydrogen consumption per gram of catalyst is calculated from the hydrogen conversion (equation 5) and the hydrogen feed flowrate.

$$r_{\text{H}_2} = \frac{F_{\text{H}_2} \cdot X_{\text{H}_2}}{g_{\text{cat}}}$$

Eq. 6

The rate of hydrogen consumption is expressed as  $\mu\text{mol}/\text{min}\cdot\text{g}_{\text{cat}}$ ,  $\mu\text{mol}/\text{min}\cdot\text{g}_{\text{metal}}$  and  $\mu\text{mol}/\text{min}\cdot\text{g}_{\text{Au}}$ .

- Selectivity**

Unsaturated feed components can be hydrogenated, isomerised or both of these. Selectivity is therefore defined to quantify the extent to which conversion proceeds via hydrogenation, according to equation 7:

$$S = \frac{X_{\text{Hydrogenation}}}{X_{\text{Hydrogenation}} + X_{\text{Isomerisation}}}$$

Eq. 7

Where conversion via hydrogenation  $X_{\text{Hydrogenation}}$  is defined as:

$$X_{\text{Hydrogenation}} = \left( x_{\text{hexane, product}} - x_{\text{hexane, feed}} \right) + \left( x_{\text{impurity + impurity isomers, feed}} - x_{\text{impurity + impurity isomers, product}} \right)$$

Eq. 8

And conversion via isomerisation  $X_{\text{Isomerisation}}$  is defined as:

$$X_{\text{Isomerisation}} = \left( x_{\text{impurity isomers, product}} - x_{\text{impurity isomers, feed}} \right) + \left( x_{\text{hexene isomers, product}} - x_{\text{hexene isomers, feed}} \right)$$

Eq. 9

A selectivity of unity indicates that all conversion occurs via hydrogenation, while a value of zero indicates all conversion occurs via isomerisation.

- Specificity**

The reaction scheme can be simplified to two pseudo-parallel reactions describing the desired reactions, viz. the hydrogenation of impurities and their isomers, and the undesired reactions, viz. the hydrogenation and isomerisation of 1-hexene. Assuming that both reactions are first order with respect to hydrocarbon concentration, the specificity parameter (Sp) which describes the overall reaction 'selectivity' with respect to the desired and undesired reactions may be defined as:

$$Sp = \frac{\text{Impurity removal}}{1 \text{ hexene loss}} = \frac{X_{\text{impurity}}}{X_{1 \text{ hexene}}}$$

Eq. 10

Where X is the conversion of the relevant components.



A large specificity value indicates that the desired removal of impurity is much higher than the undesired loss of 1-hexene. A negative specificity value indicates a removal of impurity accompanied by a net gain in 1-hexene. Therefore, large positive values as well as negative values are desirable for the specificity term.

- **Δ 1-hexene (1-hexene net gain/loss)**

The absolute gain or loss in 1-hexene is calculated by equation 11 below:

$$\Delta \text{ 1-hexene} = \text{ppm}_{\text{1 hexene, product}} - \text{ppm}_{\text{1 hexene, feed}}$$

Eq. 11

A positive value will therefore indicate a net gain in 1-hexene while a negative value will indicate a 1-hexene loss.

- **Δ Hexene isomers (Hexene isomer net change)**

The net change in isomers of 1-hexene is calculated using equation 12 below:

$$\Delta \text{ Hexene isomers} = \text{ppm}_{\text{hexene isomers, product}} - \text{ppm}_{\text{hexene isomers, feed}}$$

Eq. 12

- **Δ n-hexane (n-hexane net change)**

Likewise the net change in n-hexane is calculated using equation 13 below:

$$\Delta \text{ n-hexane} = \text{ppm}_{\text{n hexane, product}} - \text{ppm}_{\text{n hexane, feed}}$$

Eq. 13

- **Error**

The error associated with each conversion, gain/loss and net change is calculated as the average deviation of the results from the 4 samples taken daily. The associated errors are illustrated as positive and negative error bars.

## 6. Results

### 6.1. Experimental runs

The titania supported gold catalyst was studied using a 1-hexene feedstock spiked with model impurities (as detailed in section 5.2). A summary of the experimental work carried out is given in table 6.1. All experiments were carried out at a pressure of 30 bar<sub>g</sub>. Temperatures of 60, 90 and 120°C were tested at a weight hourly space velocity (WHSV) of 3 hr<sup>-1</sup>. Three different feed conditions were also tested; these feed compositions are given in table 6.2. Hydrogen to total impurity ratios (mol : mol) of 1 and 2 were tested, with the reactor configurations of 1, 2 or 3 reactors in series. These conditions were selected based on previous results using the same catalyst (*Julius, 2008*). The data obtained from the hydrogenation runs is compiled in appendix III.

For convenience tables 6.1 and 6.2 are included as a fold out reference table in appendix IV. It is suggested that this appendix be used simultaneously with chapters 6 and 7 to provide the reader with a simple reference to experimental conditions associated with the results presented in these chapters.

Table 6.1: Summarised list of experimental runs

<i>Run</i>	<i>Number of reactors</i>	<i>Reactor packing</i>	<i>Feed</i>	<i>WHSV</i> ( <i>g<sub>feed</sub>/g<sub>cat</sub>.hr</i> )	<i>H<sub>2</sub>/impurity ratios</i> ( <i>mol/mol</i> )	<i>Temperatures</i> (°C)
0 (blank)	1	SiC	Feed 1	3	1	60, 90, 120
1	1	Au/TiO <sub>2</sub>	Feed 3	11	1	60, 90, 120
2a, 2b	1	Au/TiO <sub>2</sub>	Feed 1	3	1	60, 90, 120
3	1, 2, 3	Au/TiO <sub>2</sub>	Feed 1	3	1	60, 90, 120
4	1, 2, 3	Au/TiO <sub>2</sub>	Feed 1	3	2	60, 90, 120
5	1, 2, 3	Au/TiO <sub>2</sub>	Feed 2	3	1	60, 90, 120

Table 6.2: Feed compositions

<b>Feed 1:</b>		<b>Feed 2:</b>		<b>Feed 3:</b>	
1-hexene	98.7%	1-hexene	99.1%	1-hexene	98.7%
1-hexyne	0.2%			1-hexyne	1%
1,5-hexadiene	0.2%	1,5-hexadiene	0.2%		
1,4-hexadiene	0.2%	1,4-hexadiene	0.2%		
1-methyl-1-cyclopentene	0.2%	1-methyl-1-cyclopentene	0.2%		
2,4-hexadiene	0.2%				
Other*	0.3%	Other*	0.3%	Other*	0.3%

\*Other refers to n-hexane and branched C<sub>6</sub> alkanes that were introduced with the 1-hexene

## 6.2. Preliminary Findings

### 6.2.1. Blank experiments

A blank experiment (experiment 0 in table 6.1) was conducted using the inert catalyst diluent (SiC) in order to confirm that any observed reaction could be attributed to the catalyst. No isomerisation or hydrogenation of the feed occurred at the standard reaction conditions ( $T = 120^{\circ}\text{C}$ ,  $P = 30$  bar, 1 reactor, molar  $\text{H}_2/\text{impurity} = 1$ ,  $\text{WHSV} = 3 \text{ hr}^{-1}$ ). As such, the catalyst diluent and the experimental test unit were considered to be inert with respect to hexene isomerisation and hydrogenation, and all observed activity could be attributed to the catalyst.

### 6.2.2. Verification of new test unit performance

In order to confirm that the newly designed and constructed test unit was performing comparably with the previous apparatus (i.e. that used by *Julius, 2008*), a test was conducted (run 1 in table 6.1) using the same type of catalyst at identical conditions, under the same feed (feed 3 in table 6.2) and the results compared. Figure 6.1 to 6.4 compare the results for the new and old test units. Figure 6.1 illustrates the conversion of 1-hexyne which was the single model impurity for this run; similar results for both units were observed at 60, 90 and  $120^{\circ}\text{C}$ , when considering differences in equipment and catalyst batches. Figures 6.2 – 6.4

compare the results in terms of net ppm change in 1-hexene, hexene isomer and n-hexane. Note that the net changes are calculated as the differences in ppm of that component between the feed and product.

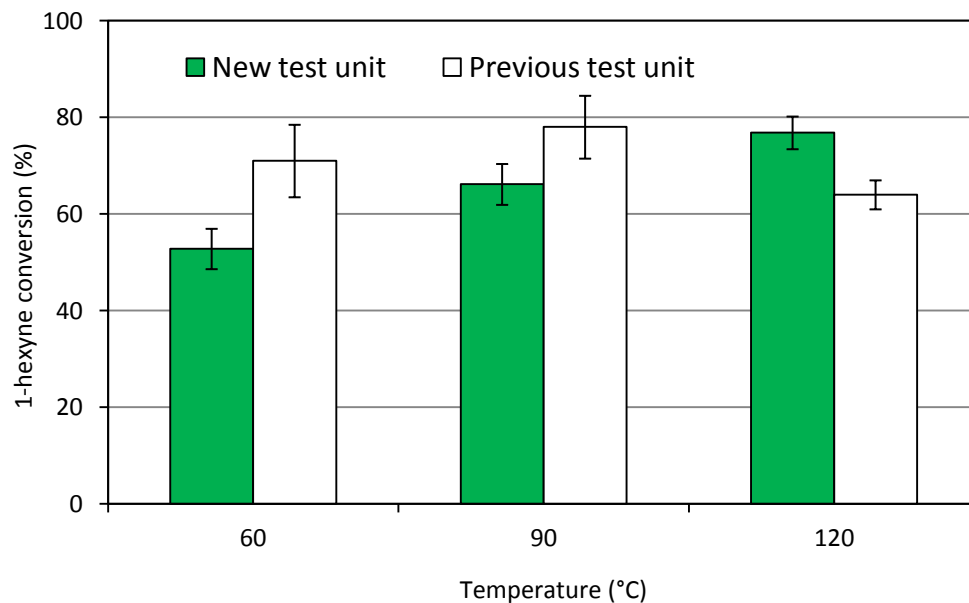


Figure 6.1: 1-hexyne conversion for Au/TiO<sub>2</sub> at 60, 90 and 120°C

(Run 1: Single reactor, Feed 3, WHSV = 11hr<sup>-1</sup>, H<sub>2</sub>/impurity ratio = 1; previous results: Julius, 2008)

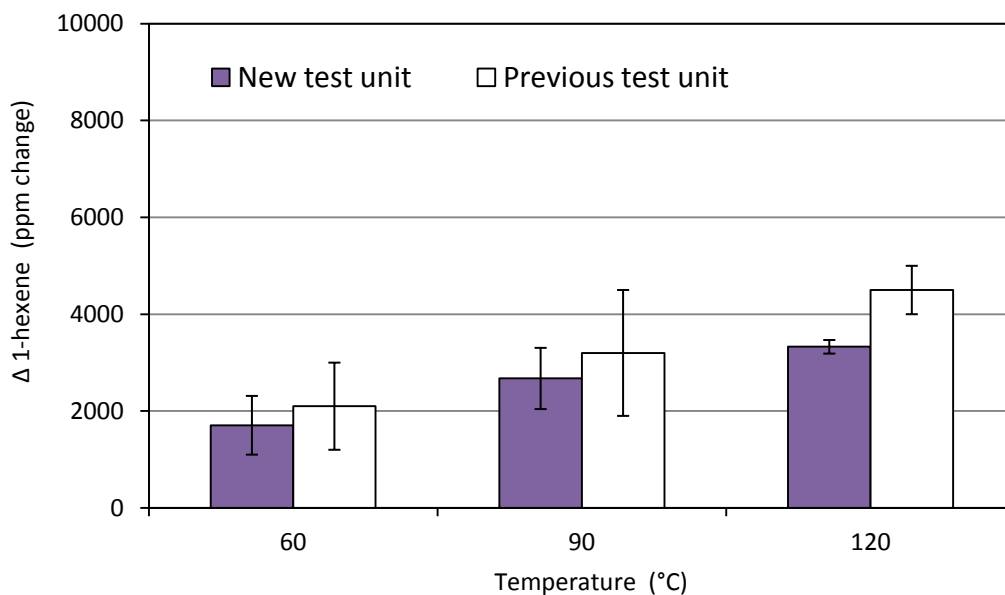


Figure 6.2: 1-hexene gain for Au/TiO<sub>2</sub> at 60, 90 and 120°C

(Run 1: Single reactor, Feed 3, WHSV = 11hr<sup>-1</sup>, H<sub>2</sub>/impurity ratio = 1; previous results: Julius, 2008)

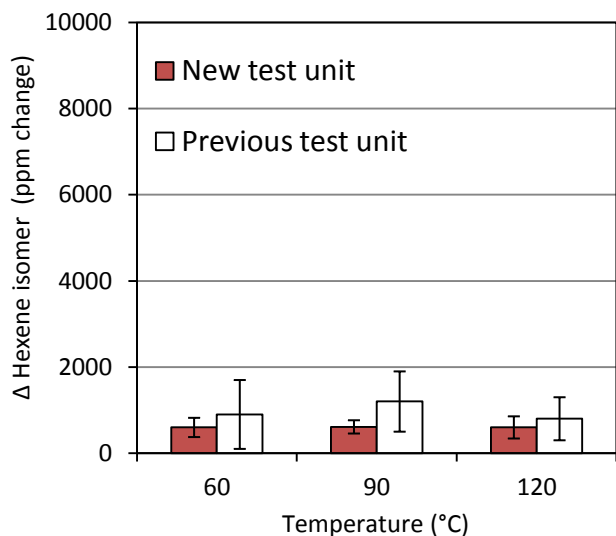


Figure 6.3: Hexene isomer change for Au/TiO<sub>2</sub> at 60, 90 and 120°C  
(Run 1: Single reactor, Feed 3, WHSV = 11hr<sup>-1</sup>, H<sub>2</sub>/impurity ratio = 1; Previous results: *Julius*, 2008)

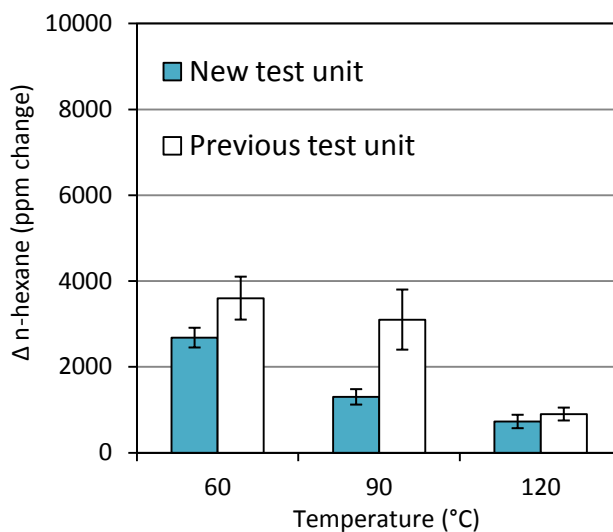


Figure 6.4: n-hexane change for Au/TiO<sub>2</sub> at 60, 90 and 120°C  
(Run 1: Single reactor, Feed 3, WHSV = 11hr<sup>-1</sup>, H<sub>2</sub>/impurity ratio = 1; Previous results: *Julius*, 2008)

### 6.2.3. Experimental reproducibility

Three separate tests (2a, 2b and 3 in table 6.1) were conducted at the same conditions with different catalyst charges to confirm the reproducibility of experimental results. Figure 6.5 illustrates the reproducibility for these tests; the total impurity conversion is shown as a function of temperature.

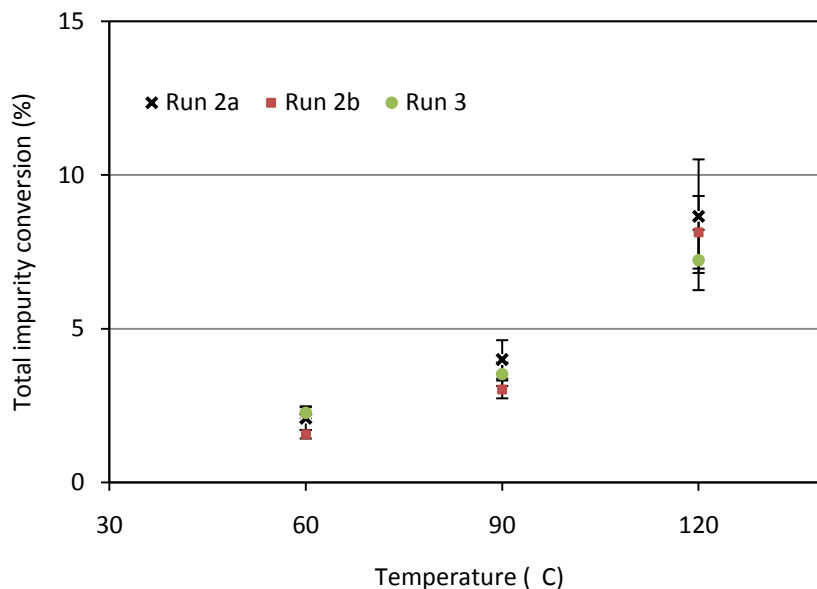


Figure 6.5: Runs 2a, 2b and 3 illustrating experimental reproducibility  
(3.0 g Au/TiO<sub>2</sub> catalyst, 1 reactor, 30 bar<sub>g</sub>, H<sub>2</sub>/oil = 0.01, WHSV = 3 hr<sup>-1</sup>)

#### 6.2.4. Catalyst stability

Catalyst performance was consistently monitored by returning to standard conditions after each variation of reaction conditions. In all cases, no significant change in catalyst performance was observed.

Figure 6.6 illustrates the catalyst stability as observed during run 4 (table 6.1). Initially, the catalyst was studied for the 2 reactor configuration at the standard conditions ( $T = 120^{\circ}\text{C}$ ,  $P = 30$  bar, molar  $\text{H}_2/\text{impurity} = 2$ ,  $\text{WHSV} = 3 \text{ hr}^{-1}$ ) and left to achieve steady state operation. Thereafter, the temperature was varied. After more than 80 hours on stream, the test was returned to the standard conditions. It was observed that conversion was unchanged compared to the initial results at these conditions.

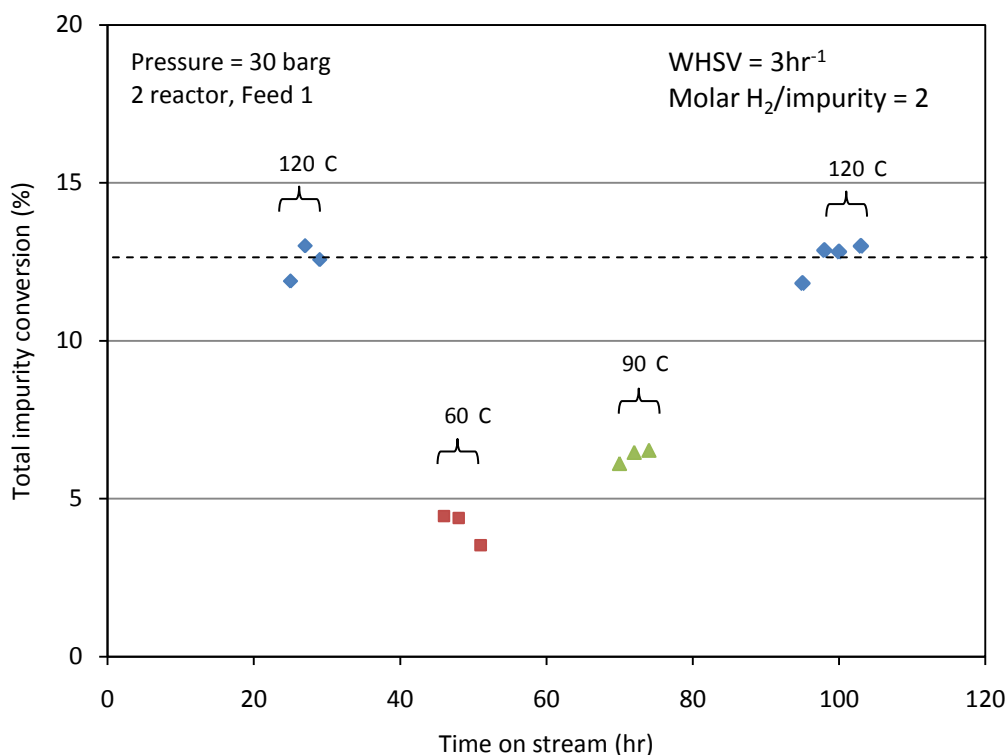


Figure 6.6: Catalyst stability during run 4

(Standard conditions:  $T = 120^{\circ}\text{C}$ ,  $P = 30$  bar, 2 reactor, molar  $\text{H}_2/\text{impurity} = 2$ ,  $\text{WHSV} = 3 \text{ hr}^{-1}$ )

### 6.3. Catalyst characterization

#### 6.3.1. Gold particle size

The gold metal particle sizes were determined using Transmission Electron Microscopy (TEM); method detailed in section 5.1.2.2. Images were taken of the catalyst surface and the gold particle sizes were determined by measurement using IMAGE J software. Figure 6.7 shows sample TEM images of the catalyst surface. TEM analysis of a crushed sample of the catalyst as well as of a cross-section of the catalyst extrudate was performed. Analysis of the cross-section of the extrudate enabled a comparison of the size of gold particles at the centre and edges of the extrudate. Table 6.3 details these results as well as the overall average particle size.

In general, TEM images of the gold impregnation catalyst revealed that many of the gold particles were large (in excess of 50 nm), this is in agreement with results for other gold impregnation catalysts (*Julius, 2008*) and literature (*Haruta, 1997*). The gold particles are clearly visible as large dark spots as illustrated in figure 6.7. Due to the large particle sizes, only a limited number of particles could be counted from the TEM images.

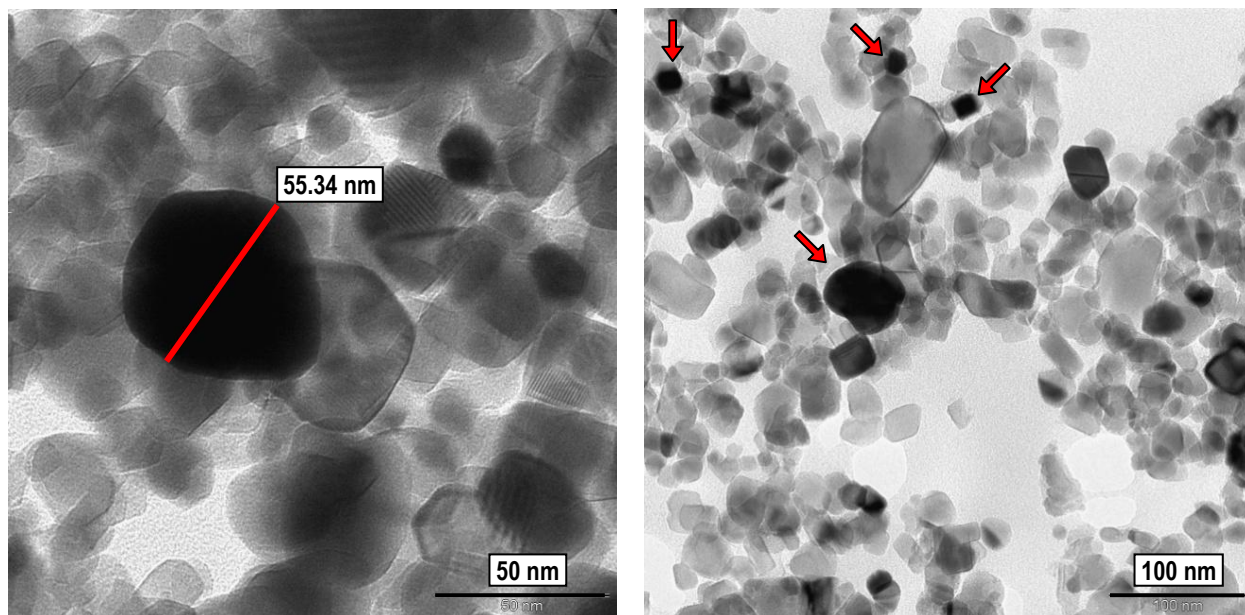
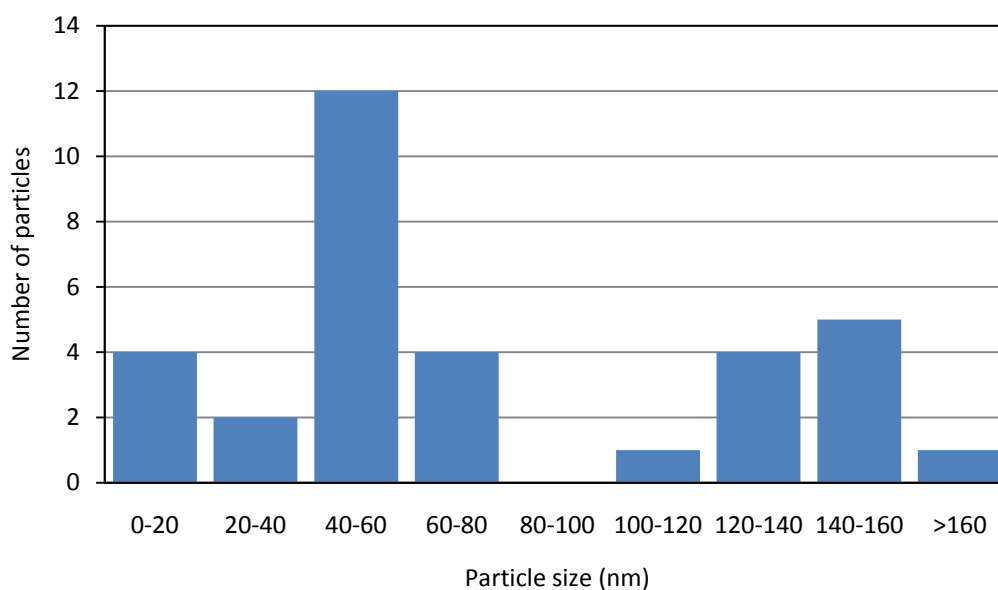


Figure 6.7: Sample TEM images of the gold impregnation catalyst

Table 6.3: Average particle sizes

	<b>Overall</b>	<b>Centre of extrudate</b>	<b>Edge of extrudate</b>
<b>Number particles measured</b>	33	13	12
<b>Average particle size (nm)</b>	77.4 ± 43.1	56.4 ± 12.8	134.0 ± 21.6

Figures 6.8 and 6.9 illustrate the gold particle size distribution; figure 6.8 includes all of the particles measured (crushed, centre and edge of extrudate) and illustrates the overall size distribution, while figure 6.9 compares the size distribution of particles found at the centre or at the edges of the extrudate. Figure 6.8 shows a bimodal distribution, with many particles within the ranges of 40-80 nm and 120-160 nm, and almost none between 80-120 nm. This bimodal distribution is clarified by figure 6.9 which illustrates the size distribution taking into account the position of the particles (at the centre or at the outer edges of the extrudate pellet). The first mode corresponds to the smaller particles in the centre, and the second mode corresponds to the larger particles at the edges. This is in agreement with the average particle sizes as reported in table 6.3.

Figure 6.8: Overall particle size distribution for 1 wt% Au/TiO<sub>2</sub>



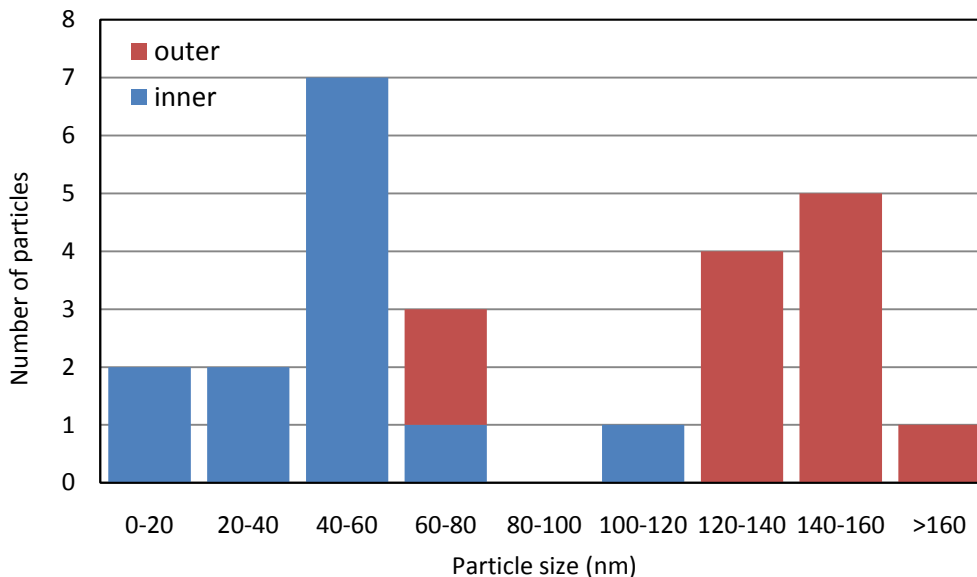


Figure 6.9: Particle size distribution comparing particles at the centre and edges of the extrudate (1 wt% Au/TiO<sub>2</sub>).

### 6.3.2. Gold loading and loading efficiency

Table 6.4 details the gold loading and efficiency. According to the gold analysis, by ICP, a loading of 0.99 wt % was achieved with a loading efficiency of 99%.

Table 6.4: Results of ICP analysis

<b>Target Au loading</b> (wt%)	<b>Achieved Au loading</b> (wt %)	<b>Loading efficiency</b>
1	0.99	99%

## 6.4. Catalyst performance

Note that in the case of operation with multiple reactors in series, the hydrogen feed was split equally and fed as illustrated in the reactor schematics. Also note that the ppm change measure for 1-hexene, hexene isomers and n-hexane is calculated as the ppm difference of the component between the feed and product (as described in equations 11, 12 and 13, section 5.6.2.1).

### 6.4.1. Feed 1; Variation of reactor configuration and overall H<sub>2</sub>/impurity ratio

- Figures 6.10 – 6.15 refer to run 3, where the H<sub>2</sub>/impurity ratio was equal to one (i.e. the stoichiometric amount of hydrogen required to hydrogenate the impurities was fed)
- Figures 6.16 – 6.21 refer to run 4, where the H<sub>2</sub>/impurity ratio was equal to two (i.e. twice the stoichiometric amount of hydrogen required to hydrogenate the impurities was fed).

Feed 1 contained 5 model impurities, namely, 1-hexyne; 1,5-hexadiene (1,5-HD); 2,4-hexadiene (2,4-HD); 1,4-hexadiene (1,4-HD) and 1-methyl-cyclopentene (MCP). The approximate feed composition is detailed in table 6.2.

#### 6.4.1.1. Overall H<sub>2</sub>/impurity = 1

Figures 6.10 – 6.12 show the removal of each separate impurity (MCP and 2,4-HD are excluded as no net removal was observed), as well as the total impurity conversion by hydrogenation as function of reaction temperature for 1, 2 and 3 reactors in series.

- **Alkyne conversion**

For the single reactor configuration (figure 6.10), 1-hexyne was the only impurity converted. An increase in conversion from ~10% to over 30% was seen as the temperature increased from 60 to 120°C. This is reflected in the values for total impurity hydrogenation which concomitantly increased from around 2% to approximately 8%.

For 2 and 3 reactors in series (figures 6.11 and 6.12) the 1-hexyne removals at 60°C are between 2-3%. At both 90 and 120°C, for the 2 and 3 reactor configurations, the 1-hexyne conversions were similar to those observed for the single reactor configuration, approximately ~15% at 90°C and between 30 and 35% at 120°C.

- **Diene conversion**

No conversion of 1,5- and 1,4-hexadiene was observed for the single reactor, this changed however when the 2 and 3 reactor configurations were used. For both 2 and 3 reactors the 1,5-HD conversion remained relatively constant at around 3% as the temperature increased from 60 to 120°C. 1,4-HD exhibited different behaviour; for 2 reactors the conversion increased from around 3% to approximately 5% with the temperature increase, while for 3 reactors the conversion increased from around 3% to almost 10%.

- **Total impurity hydrogenation**

The values for the total impurity conversion by hydrogenation were very similar regardless of reactor configuration, increasing from around 2% to approximately 8% as the temperature increased from 60 to 120°C.

- **1-hexene loss, hexene isomer and n-hexane gain**

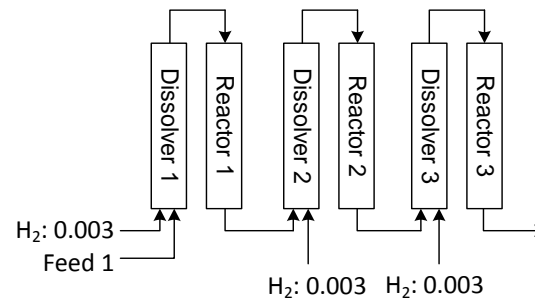
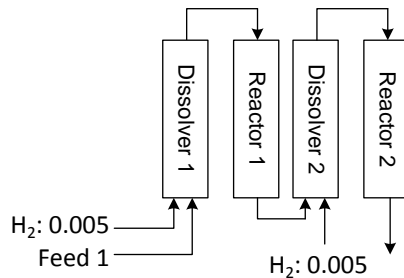
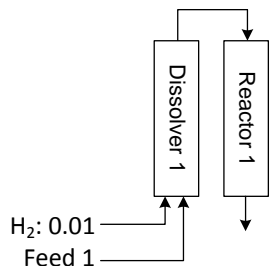
Figures 6.13 to 6.15 illustrate the net ppm change in 1-hexene, hexene isomer and n-hexane content for the 1, 2 or 3 reactor configurations. In terms of 1-hexene gain/loss, a slight loss was observed for the single reactor case, this increased from almost zero at 60°C to a loss of 250 ppm at 120°C. For the 2 reactor configuration virtually no change was seen at 60 and 90°C while a loss of approximately 250 ppm was observed at 120°C. A very slight gain in 1-hexene was observed for the 3 reactor configuration at 60 and 90°C; as the temperature was increased to 120°C this became a small loss. Overall these changes in 1-hexene content are very small and cannot be considered particularly significant; typically the error bars are within the range of standard experimental error.

Figure 6.15 illustrates the ppm change in n-hexane content observed for the different reactor setups at 60, 90 and 120°C. Overall the change in n-hexane was too low to be considered significant and reached a maximum of 200 ppm at 120°C.

In terms of the net change in hexene isomer content (figure 6.14) there was virtually no increase at 60°C for any of the reactor configurations. As the temperature was increased to 90°C a small increase was observed for the single reactor and for the 2 reactor configuration. At 120°C these changes were further increased. At each temperature the maximum net change was observed for the single reactor, this decreased as more reactors were used. Overall all of these changes remain relatively small (equating less than 750 ppm), and the error bars are well within the range of standard experimental error.

# Results

Run 3: Feed 1, Overall  $H_2$ /impurity = 1,  $WHSV = 3hr^{-1}$



## IMPURITY CONVERSIONS

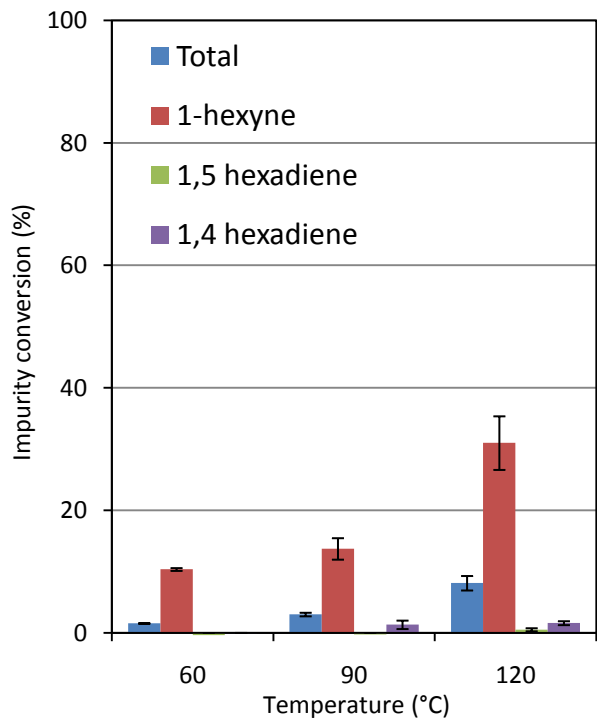


Figure 6.10: Impurity conversion for 1 reactor (Feed 1,  $WHSV = 3hr^{-1}$ ,  $H_2$ /impurity = 1,  $P = 30$  bar)

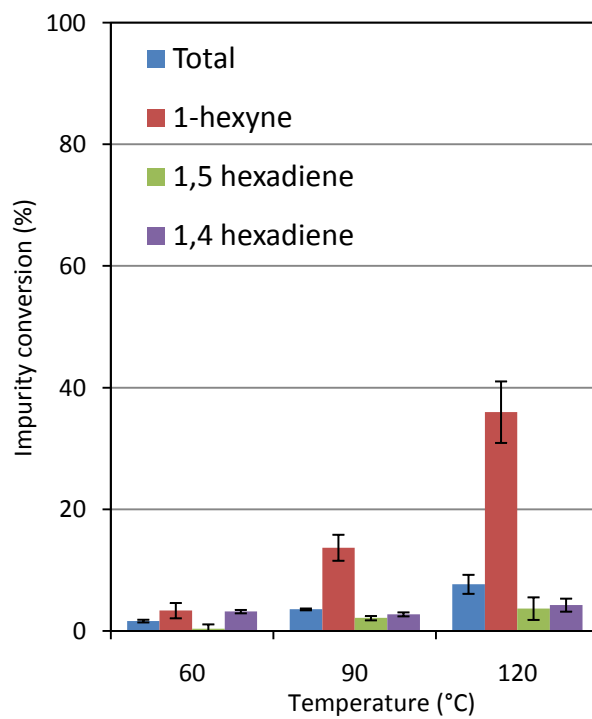


Figure 6.11: Impurity conversion for 2 reactors (Feed 1,  $WHSV = 3hr^{-1}$ ,  $H_2$ /impurity = 1,  $P = 30$  bar)

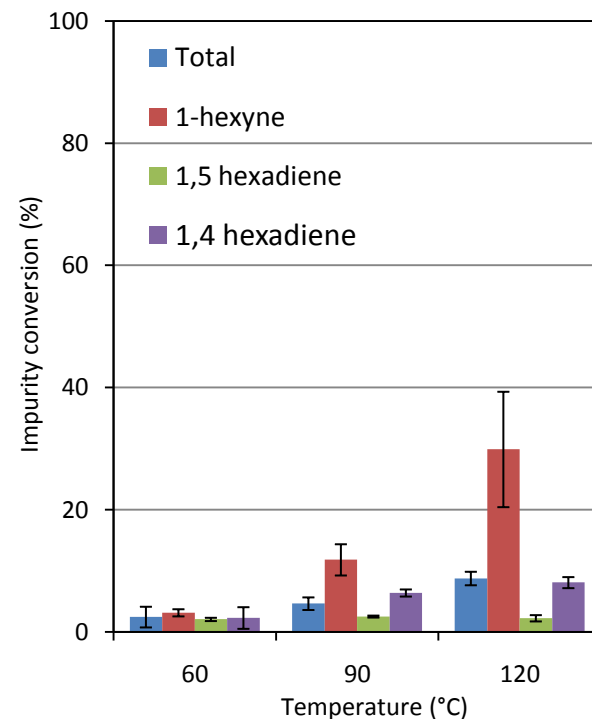


Figure 6.12: Impurity conversion for 3 reactors (Feed 1,  $WHSV = 3hr^{-1}$ ,  $H_2$ /impurity = 1,  $P = 30$  bar)

# Results

## RUN 3: 1-HEXENE, HEXENE ISOMER AND n-HEXANE PPM CHANGE PLOTS

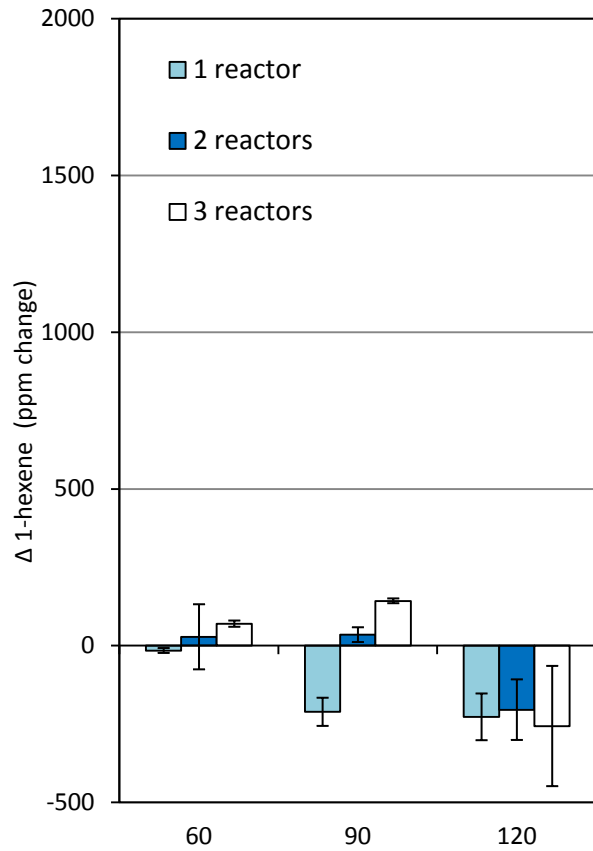


Figure 6.13: 1-hexene gain/loss, comparing 1, 2 and 3 reactor configuration at 60, 90 and 120°C  
(Feed 1, WHSV = 3hr<sup>-1</sup>, H<sub>2</sub>/impurity = 1, P = 30 bar)

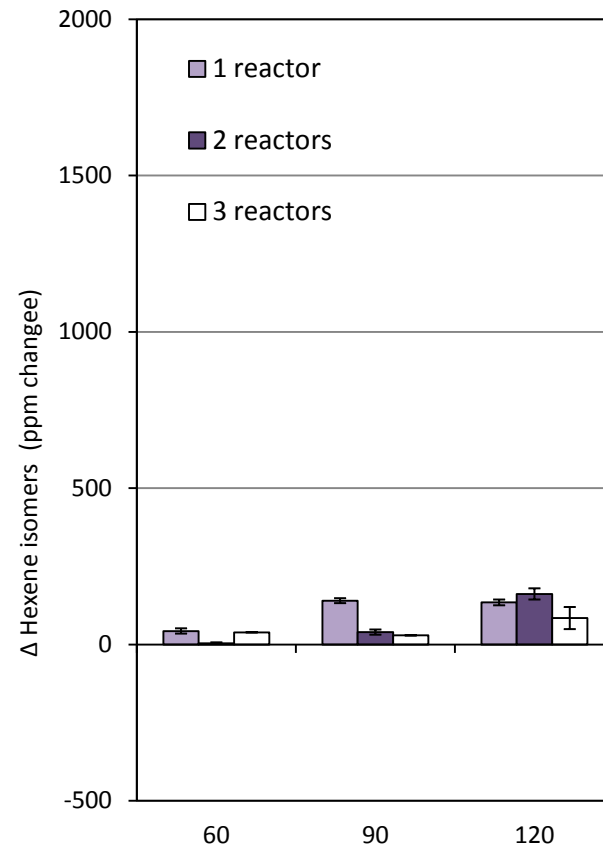


Figure 6.14: Hexene isomer net change, comparing 1, 2 and 3 reactor configuration at 60, 90 and 120°C  
(Feed 1, WHSV = 3hr<sup>-1</sup>, H<sub>2</sub>/impurity = 1, P = 30 bar)

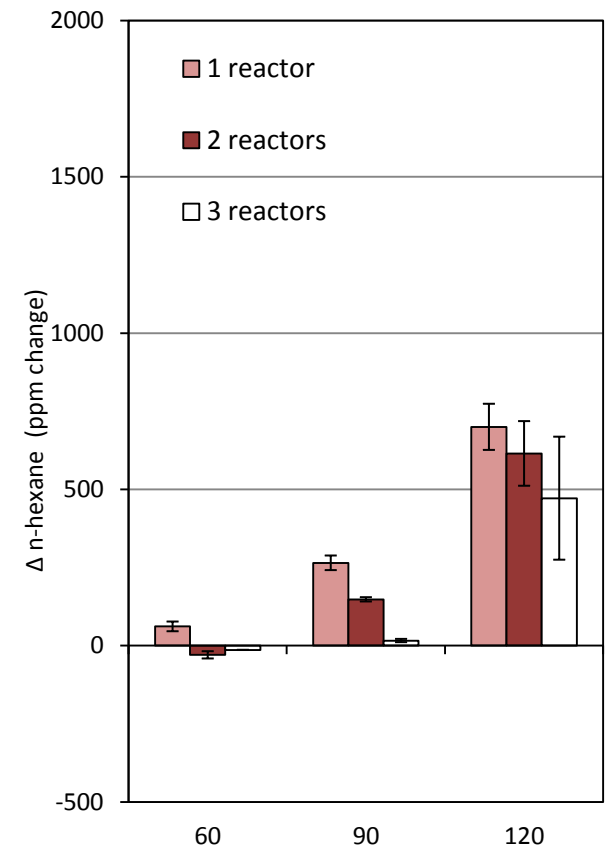


Figure 6.15: n-hexane net change, comparing 1, 2 and 3 reactor configuration at 60, 90 and 120°C  
(Feed 1, WHSV = 3hr<sup>-1</sup>, H<sub>2</sub>/impurity = 1, P = 30 bar)

#### 6.4.1.2. Overall H<sub>2</sub>/impurity = 2

An overview of the impurity removal results for the tests under excess hydrogen is shown in figures 6.16 – 6.18. The removal of each separate impurity, as well as the total impurity conversion by hydrogenation is shown as function of reaction temperature for 1, 2 and 3 reactors in series as illustrated. Again MCP and 2,4-HD are excluded as no net removal was observed.

- **Alkyne conversion**

Of the model impurities present in feed 1, 1-hexyne is clearly the most reactive, and was the only impurity to see a significant removal. Figure 6.16 illustrates the impurity conversions for the single reactor set up where the 1-hexyne conversion increased from ~15% to upwards of 80% as the temperature was increased from 60 to 120°C. Similar values for alkyne conversion were observed for the 2 and 3 reactor configurations (figures 6.17 and 6.18).

- **Diene conversion**

Overall the conversions of 1,5- and 1,4-hexadiene were higher than those observed when the H<sub>2</sub>/impurity ratio was equal to 1, however in general the values remained low at less than 10%.

- **Total impurity hydrogenation**

The values for the total impurity hydrogenation are similar regardless of reactor configuration, increasing from around 5% to approximately 12% as the temperature is increased from 60 to 120°C.

- **1-hexene loss, hexene isomer and n-hexane gain**

Figures 6.19 to 6.21 illustrate the net ppm change in 1-hexene, hexene isomer and n-hexane content for the 1, 2 or 3 reactor configurations.

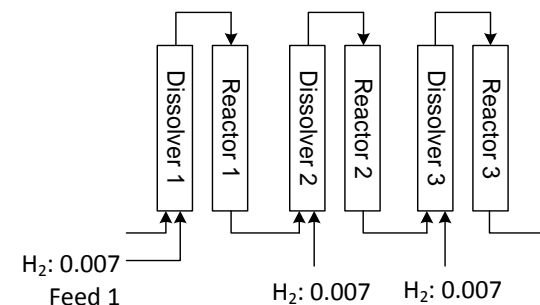
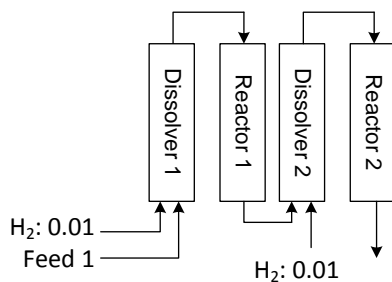
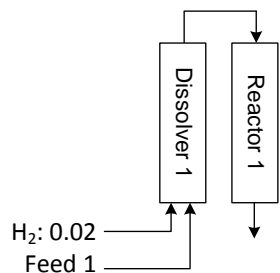
In terms of 1-hexene gain/loss (figure 6.19), a slight gain was observed for the single reactor case, this was constant at around 250 ppm for 60, 90 and 120°C. This was observed again for the 2 reactor configuration at 60 and 90°C, however at 120°C a large loss of 2500 ppm was observed. For the 3 reactor configuration virtually no change in 1-hexene content was observed at 60 and 90°C, but again as the temperature was increased to 120°C this became a significant loss of approximately 6000 ppm.

Figure 6.21 illustrates the net change in n-hexane content observed for the different reactor configurations at 60, 90 and 120°C. Overall the ppm increase in n-hexane content was low, and can be considered insignificant at 60 and 90°C for all reactor setups. At 120°C, however, the increase became significant and further increased as more reactors are used.

In terms of the net change in hexene isomer content (figure 6.20) there was virtually no change at 60°C for any of the reactor configurations. As the temperature was increased to 90°C a small increase was observed for each of the reactor configurations. At 120°C these were further increased. Similarly to the trend observed for n-hexane, the ppm change increased as more reactors were used.

# Results

**Run 4: Feed 1, Overall H<sub>2</sub>/impurity = 2, WHSV = 3hr<sup>-1</sup>**



## IMPURITY CONVERSIONS

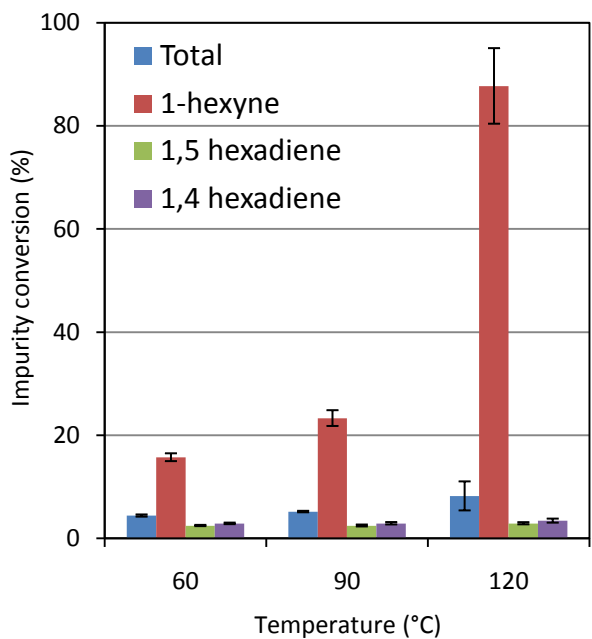


Figure 6.16: Impurity conversion for 1 reactor (Feed 1, WHSV = 3hr<sup>-1</sup>, H<sub>2</sub>/impurity = 2, P = 30 bar)

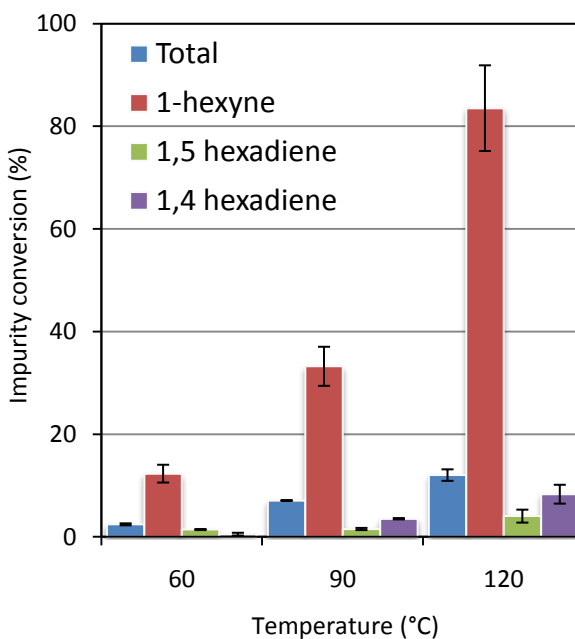


Figure 6.17: Impurity conversion for 2 reactors (Feed 1, WHSV = 3hr<sup>-1</sup>, H<sub>2</sub>/impurity = 2, P = 30 bar)

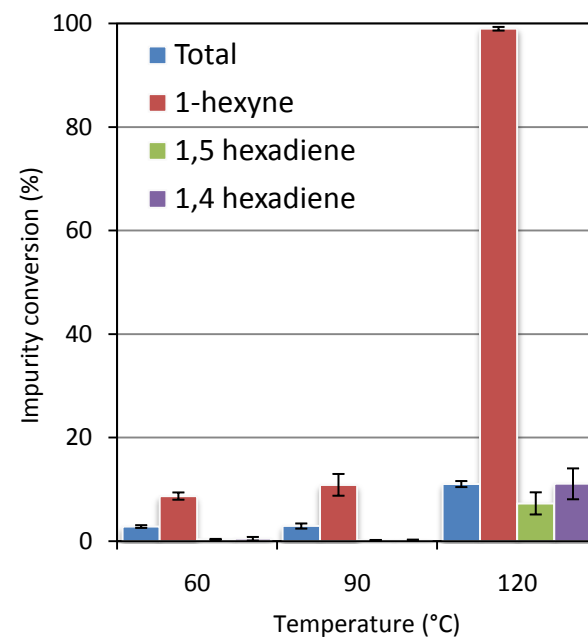


Figure 6.18: Impurity conversion for 3 reactors (Feed 1, WHSV = 3hr<sup>-1</sup>, H<sub>2</sub>/impurity = 2, P = 30 bar)



# Results

## RUN 4: 1-HEXENE, HEXENE ISOMER AND n-HEXANE PPM CHANGE PLOTS

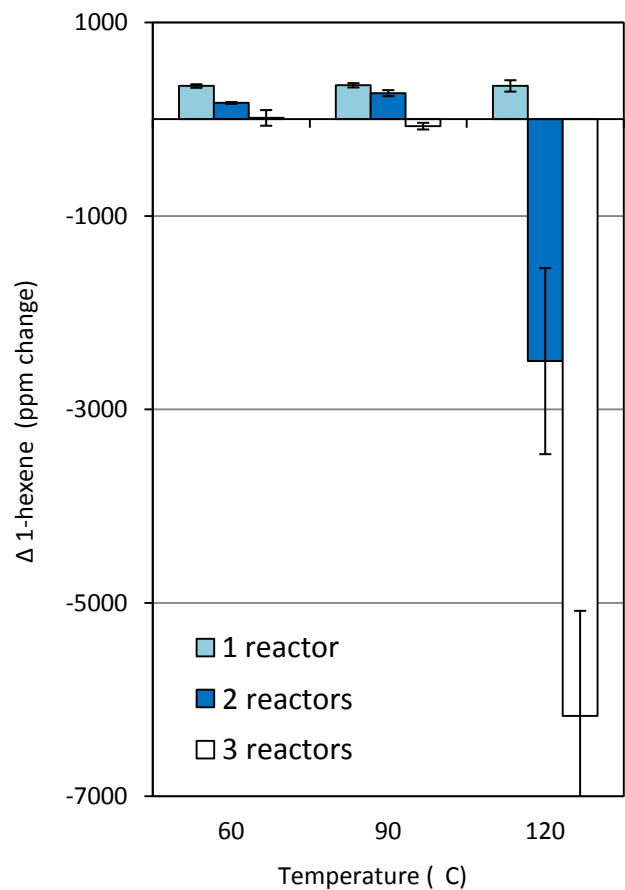


Figure 6.19: 1-hexene gain/loss, comparing 1, 2 and 3 reactor configuration at 60, 90 and 120°C  
(Feed 1, WHSV = 3hr<sup>-1</sup>, H<sub>2</sub>/impurity = 2, P = 30 bar)

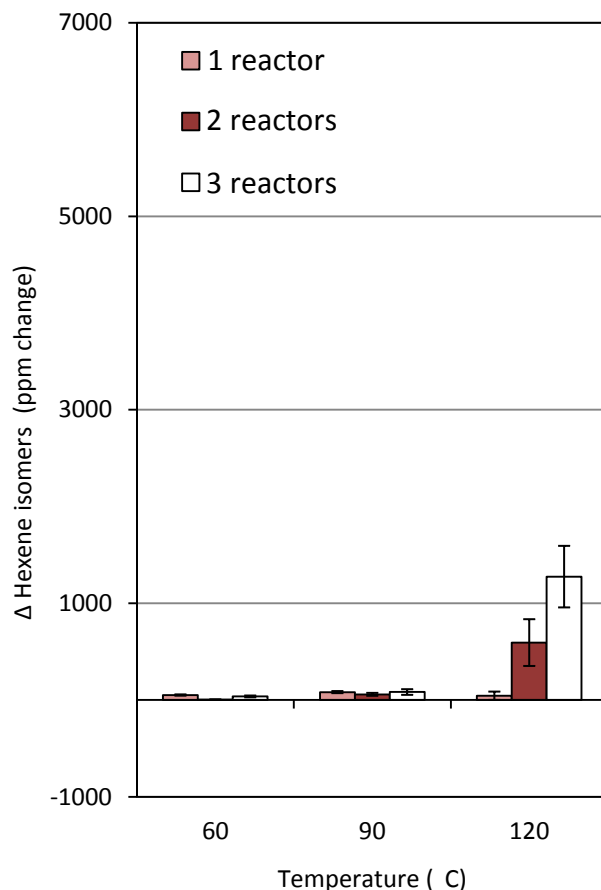


Figure 6.20: Hexene isomer net change, comparing 1, 2 and 3 reactor configuration at 60, 90 and 120°C  
(Feed 1, WHSV = 3hr<sup>-1</sup>, H<sub>2</sub>/impurity = 2, P = 30 bar)

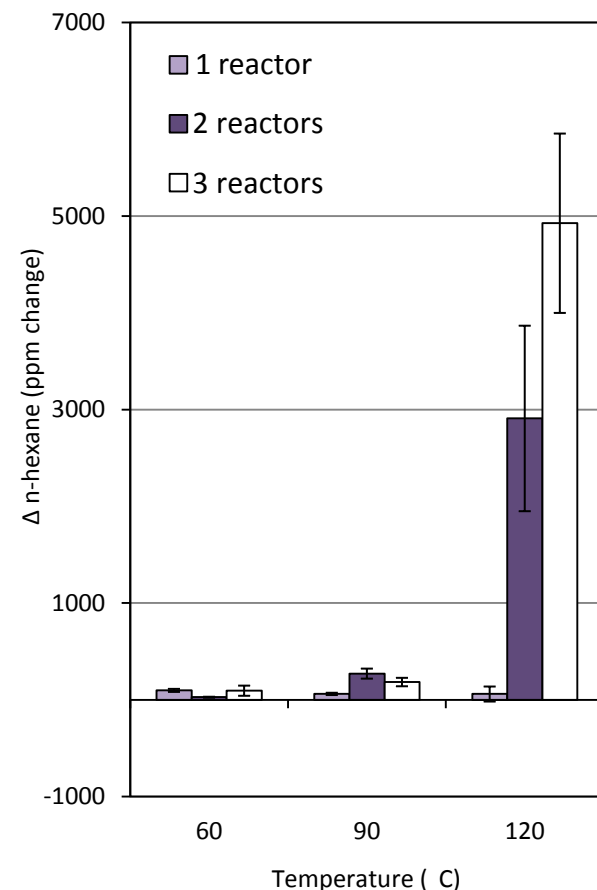


Figure 6.21: n-hexane net change, comparing 1, 2 and 3 reactor configuration at 60, 90 and 120°C  
(Feed 1, WHSV = 3hr<sup>-1</sup>, H<sub>2</sub>/impurity = 2, P = 30 bar)

### 6.4.2. Feed 2; Variation of reactor configuration

The results for the experiments employing feed 2 (Run 5 in table 6.1) are shown in figures 6.22 – 6.27. The aim of this experiment was to observe the reactivity of the diene and cyclic impurity compounds in the absence of 1-hexyne. Note that overall the hydrogen/total impurity ratio is unity in all cases.

- **Impurity removals**

The removal of each separate impurity, as well as the total impurity conversion by hydrogenation is shown as function of reaction temperature for 1, 2 and 3 reactors in series (figures 6.22 - 6.24).

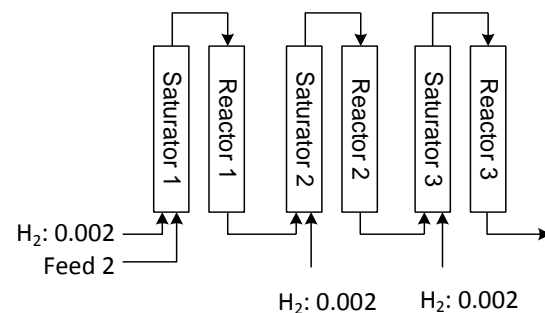
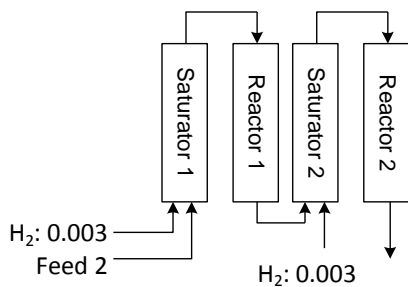
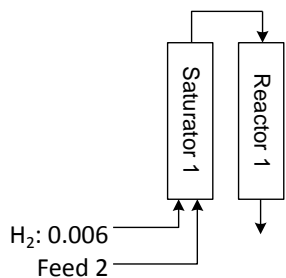
In the case of the single reactor configuration (figure 6.22), 1,4-HD shows a steady increase in conversion from approximately 3% to around 11% as the temperature is increased from 60 to 120°C. This is reflected in the values for total impurity hydrogenation which subsequently increase from around 1% to approximately 3%. Very similar results were observed in the case of the 2 and 3 reactor configurations (figures 6.23 and 6.24). Virtually no conversion of 1,5-HD was observed at 60 and 90°C for all reactor configurations. At 120°C low conversions were observed, however, these were too small to be considered significant (only ~1-2%).

- **1-Hexene, hexene isomer and n-hexane gain/loss**

Figures 6.25 to 6.27 illustrate the net ppm change in 1-hexene, n-hexane and hexene isomers for the 1, 2 or 3 reactor configurations at 60, 90 and 120°C. In terms of 1-hexene gain/loss (figure 6.25), no significant change is observed at 60°C for all reactor configurations. This becomes a loss as the temperature is increased. For each temperature the greatest loss is seen for the 3 reactor configuration.

# Results

**Run 5: Feed 2, Overall  $H_2$ /impurity = 1, WHSV =  $3\text{hr}^{-1}$**



## IMPURITY CONVERSIONS

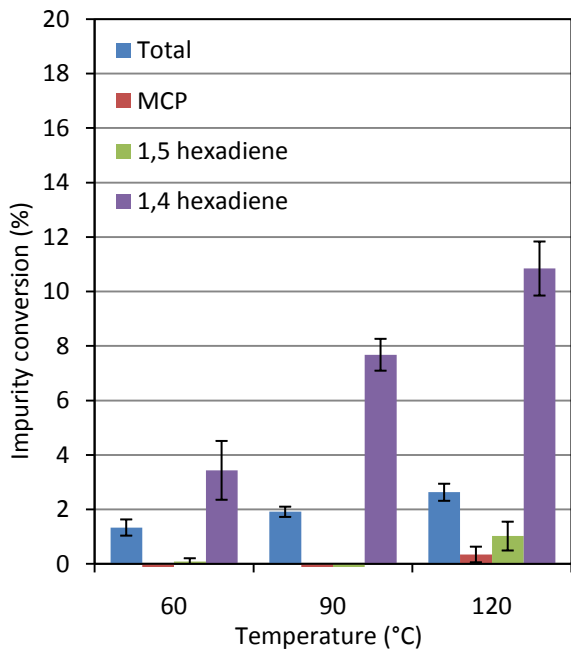


Figure 6.22: Impurity conversion for 1 reactor (Feed 2, WHSV =  $3\text{hr}^{-1}$ ,  $H_2$ /impurity = 1, P = 30 bar)

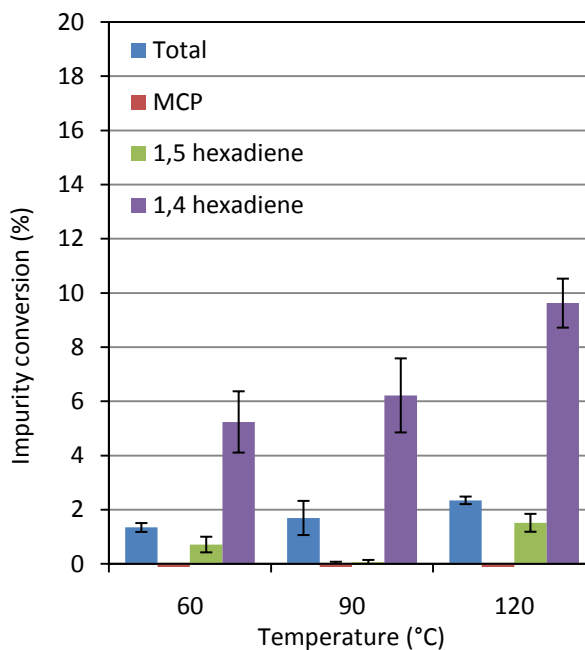


Figure 6.23: Impurity conversion for 2 reactors (Feed 2, WHSV =  $3\text{hr}^{-1}$ ,  $H_2$ /impurity = 1, P = 30 bar)

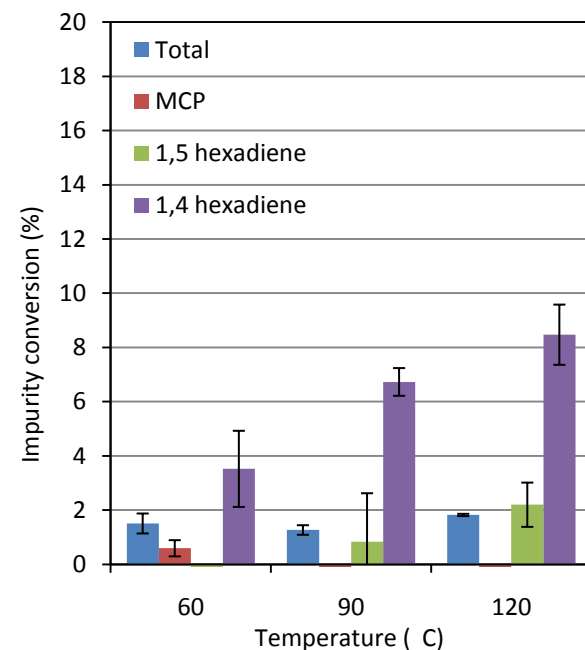


Figure 6.24: Impurity conversion for 3 reactors (Feed 2, WHSV =  $3\text{hr}^{-1}$ ,  $H_2$ /impurity = 1, P = 30 bar)

**RUN5: 1-HEXENE, n-HEXANE AND HEXENE ISOMER PPM CHANGE PLOTS**

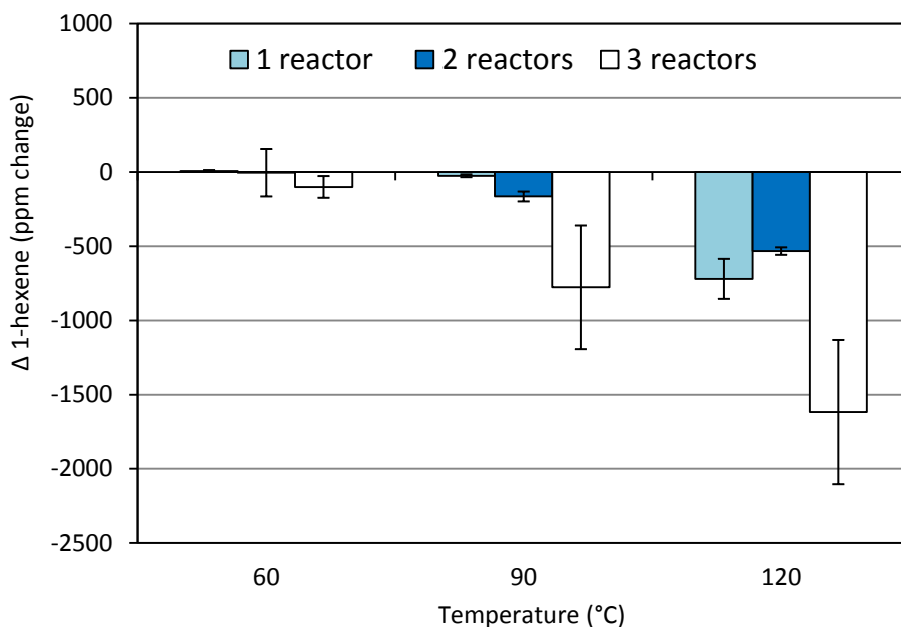


Figure 6.25: 1-hexene gain/loss for 1, 2 and 3 reactors at 60, 90 and 120°C  
(Feed 2, WHSV = 3hr<sup>-1</sup>, H<sub>2</sub>/impurity ratio = 1, P = 30 bar)

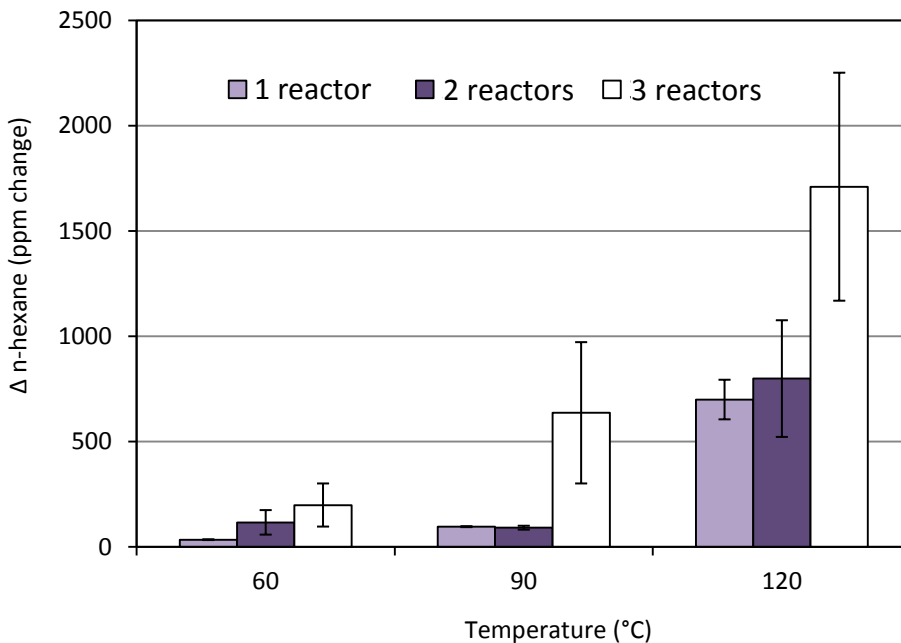


Figure 6.26: n-hexane net change for 1, 2 and 3 reactors at 60, 90 and 120°C  
(Feed 2, WHSV = 3hr<sup>-1</sup>, H<sub>2</sub>/impurity ratio = 1, P = 30 bar)

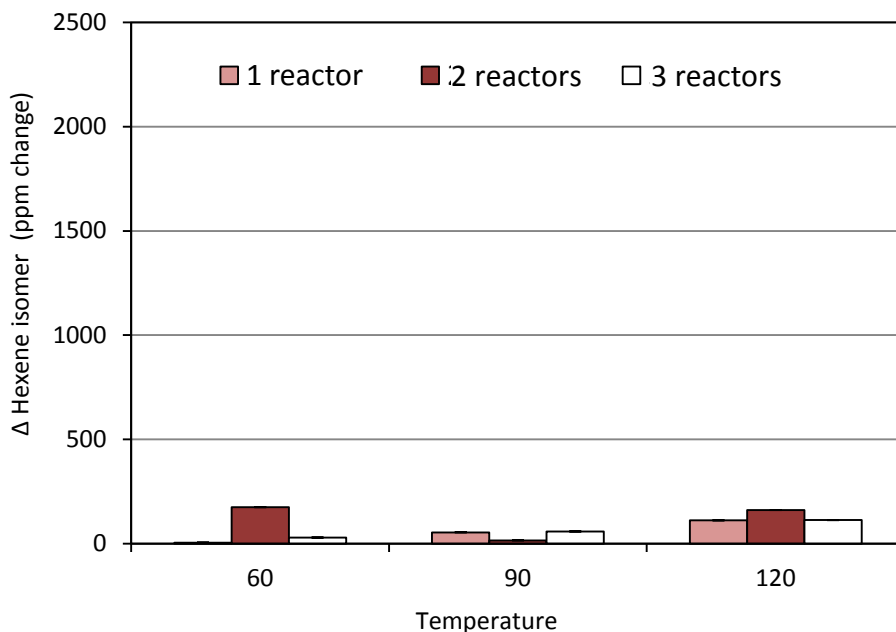


Figure 6.27: Hexene isomer net change for 1, 2 and 3 reactors at 60, 90 and 120°C  
(Feed 2, WHSV = 3hr<sup>-1</sup>, H<sub>2</sub>/impurity ratio = 1, P = 30 bar)

## 6.5. Degree of hydrogen dissolution

A further experiment was conducted employing a smaller hydrogen dissolving vessel, with a volume of approximately 5 times less than that of the original, in which full dissolution of hydrogen in the olefin is unlikely to have been achieved (based on earlier dissolution experiments of *Ramasary, 2008*). The aim of the test was to ascertain whether hydrogen dissolution in the olefin feedstock was important for either conversion and/or selectivity. It was furthermore aimed to resolve whether low hydrogen/impurity ratio, or rather the absence of gaseous hydrogen in the feed mixture, was the cause of the high catalyst performance observed.

The equivalent available contacting volume of the smaller hydrogen dissolving vessel was approximately 2 cm<sup>3</sup> as compared to the original vessel volume of 11 cm<sup>3</sup>. Operating conditions were identical to those of run 1; single reactor, feed 3, WHSV = 11hr<sup>-1</sup>, H<sub>2</sub>/impurity ratio = 1.

The results are illustrated in figure 6.28, which compares the alkyne conversions to those observed for run 1 with the original dissolver (dissolver 1). The 1-hexyne conversions observed using the smaller dissolver are significantly suppressed, by a factor of between 5 and 10, compared to those observed using the original equipment.

Figure 6.29 compares the 1-hexene gains observed using the different size dissolvers; the 1-hexene gain was notably suppressed (less than 1000 ppm) in the test employing the smaller dissolver.

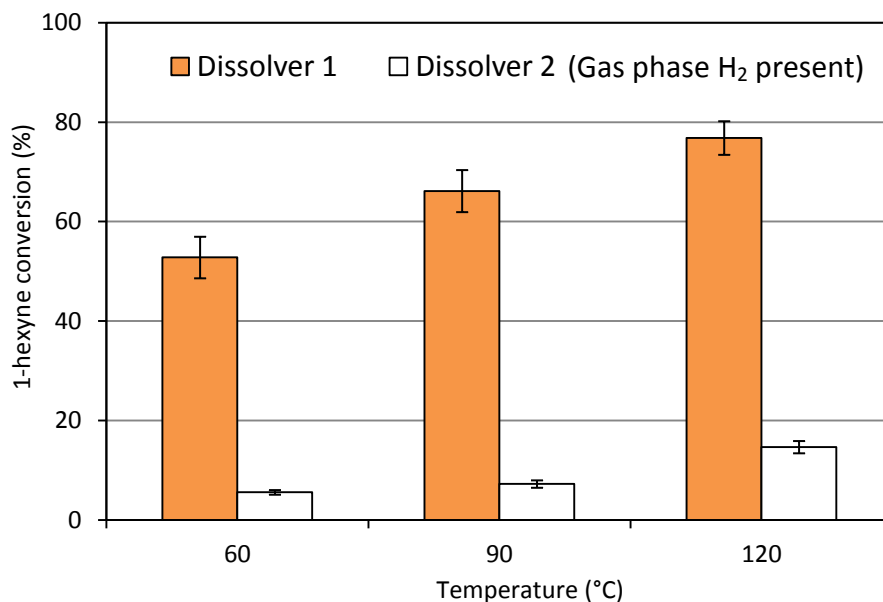


Figure 6.28: 1-hexyne conversion for dissolver 1 and dissolver 2 at 60, 90 and 120°C  
(Single reactor, Feed 3, WHSV = 11hr<sup>-1</sup>, H<sub>2</sub>/impurity ratio = 1; Dissolver 1 = ~11 cm<sup>3</sup>, Dissolver 2 = ~2 cm<sup>3</sup>)

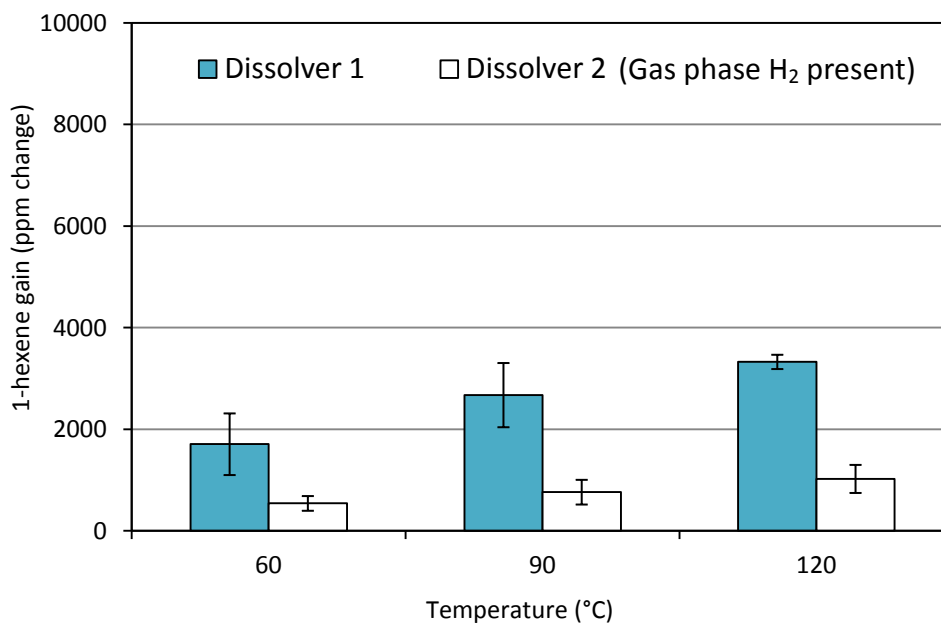


Figure 6.29: 1-hexene gain for dissolver 1 and dissolver 2 at 60, 90 and 120°C  
(Single reactor, Feed 3, WHSV = 11hr<sup>-1</sup>, H<sub>2</sub>/impurity ratio = 1; Dissolver 1 = ~11 cm<sup>3</sup>, Dissolver 2 = ~2 cm<sup>3</sup>)

## 7. Discussion

---

### 7.1. Preliminary findings

The results of the preliminary studies established the following:

- The experimental test unit and the catalyst diluent (SiC) are inert with regard to isomerisation and hydrogenation, and as such all observed activity can be attributed to the catalyst (see section 6.2.1).
- Previous results using the old equipment (*Julius, 2008*) were reproducible using the newly designed and constructed test unit (see section 6.2.2, figures 6.1 - 6.4). As such it could be concluded that the operation of the new unit was satisfactory. Using the old test unit, relatively large fluctuations in 1-hexyne conversion had been observed due to valve switching during sampling, as well as due to the emptying of the waste vessel during operation. This problem has been largely eliminated in the design of the new test unit.
- For the new test unit, results are reproducible within an acceptable range of scatter (see section 6.2.3 and Figure 6.5).
- The same mass of catalyst was used in reproducing experiments and this therefore confirms that the catalyst pellets have largely consistent metal loadings.
- Catalyst activity is stable with time on stream (see section 6.2.4 and figure 6.6). In experimental work (see table 5.1) individual catalyst charges were on stream for periods of up to 4 weeks without deactivation, and thus all data was obtained under non-deactivating conditions.

## 7.2. Overall findings

### 7.2.1. Impurity conversion

A key objective of the project was to investigate the removal of a variety of impurities at industrially relevant levels; from feed levels of ~ 2000 ppm to final levels of less than 100 ppm. Overall, it was observed that the removal of 1-hexyne is readily achieved even at these low feed levels given a  $H_2$ /impurity ratio of 2 (figure 7.1). Removal of the diene impurities was also observed but to a lesser extent (figures 7.2 and 7.3); it is believed that this can be improved through operation at lower space velocity and careful modification of the available gold surface area by decreasing gold particle size.

Operation under excess hydrogen resulted in a significant increase in individual impurity conversions from those observed for the overall  $H_2$ /impurity ratio of 1. Clearly an excess of hydrogen is advantageous to facilitate the high conversion of the alkyne for all reactor configurations as observed in figure 7.1.

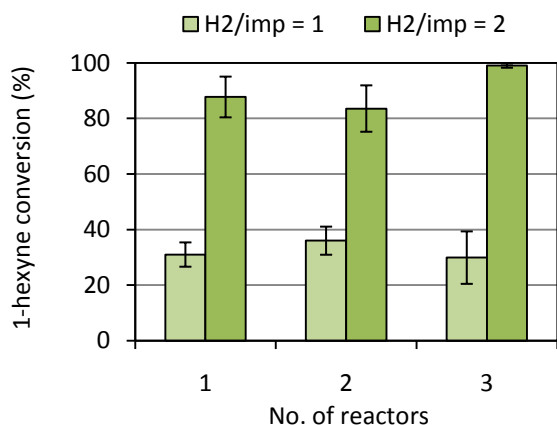


Figure 7.1: 1-hexyne conversion at 120°C for 1, 2 and 3 reactors under overall  $H_2$ /impurity of 1 and 2

(■ Run 4, ■ Run 5: Feed 1, WHSV = 3hr<sup>-1</sup>, P = 30 bar)

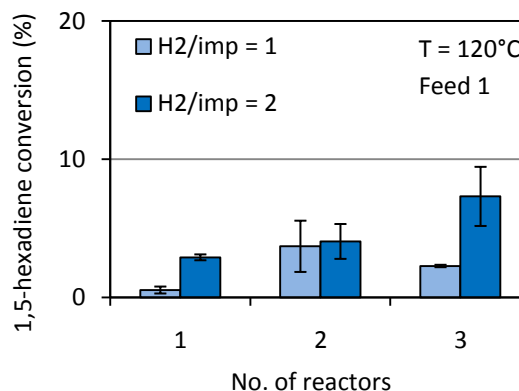


Figure 7.2: 1,5-hexadiene conversion at 120°C for 1, 2 and 3 reactors under overall  $H_2$ /impurity of 1 and 2

(■ Run 4, ■ Run 5: Feed 1, WHSV = 3hr<sup>-1</sup>, P = 30 bar)

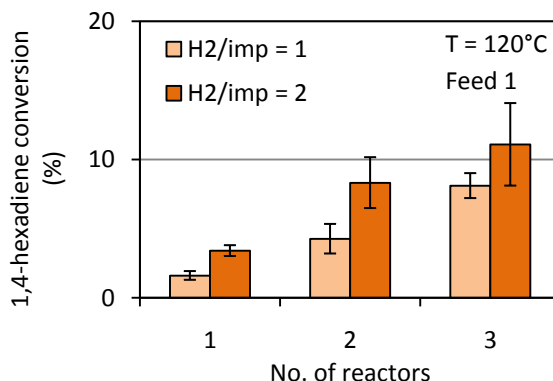


Figure 7.3: 1,4-hexadiene conversion at 120°C for 1, 2 and 3 reactors under overall  $H_2$ /impurity of 1 and 2

(■ Run 4, ■ Run 5: Feed 1, WHSV = 3hr<sup>-1</sup>, P = 30 bar)



However, operation under excess hydrogen also increases the undesired loss of 1-hexene, particularly in the multiple reactor configurations, as illustrated in figure 7.4. However, in the case of a single reactor a small gain was observed at 120°C. This indicates that operation with a H<sub>2</sub>/impurity ratio of 2 is feasible as long as all hydrogen is supplied upfront and no hydrogen replenishment takes place. Even for operation with 3 reactors where an increased 1-hexene loss is observed, the loss is relatively small at approximately 6000 ppm. In terms of the key objectives, this demonstrates that high 1-hexyne specificity is achieved even at low impurity feed and effluent levels.

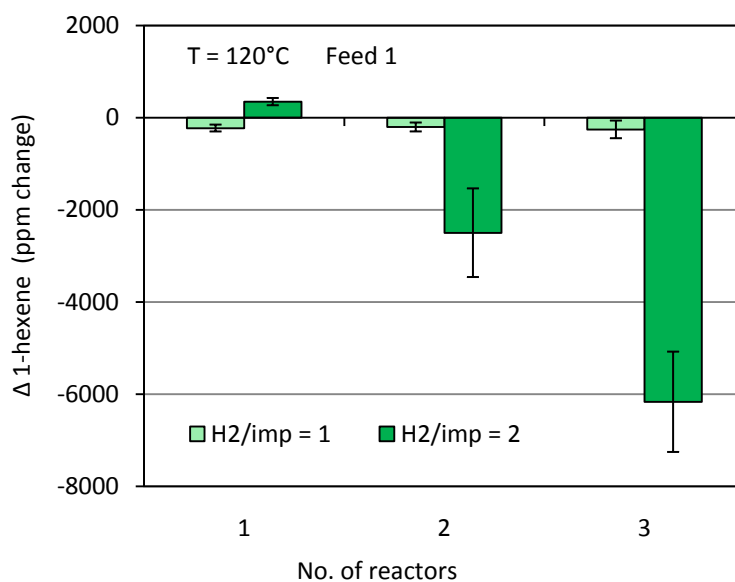


Figure 7.4: 1-hexene gain/loss at 120°C for 1, 2 and 3 reactors under H<sub>2</sub>/impurity of 1 and 2

(■ Run 4, ■ Run 5: Feed 1, WHSV = 3hr<sup>-1</sup>, P = 30 bar)

### 7.3. Effect of reactor configuration and limited hydrogen availability

#### 7.3.1. Alkyne conversion

Figure 7.5 illustrates the 1-hexyne conversion comparing 1, 2 and 3 reactor configurations. At 60°C the highest conversion was observed for the single reactor, while at 90°C and 120°C similar alkyne conversions, within the range of error, were observed regardless of reactor configuration. This suggests that at the higher temperatures the limited availability of hydrogen provided by the multiple reactor configurations does not affect the hydrogenation of the 1-hexyne. Possibly at the low reaction temperature of 60°C the reduced hydrogen coverage of active sites provided in the multiple reactor configurations results in a depressed conversion.

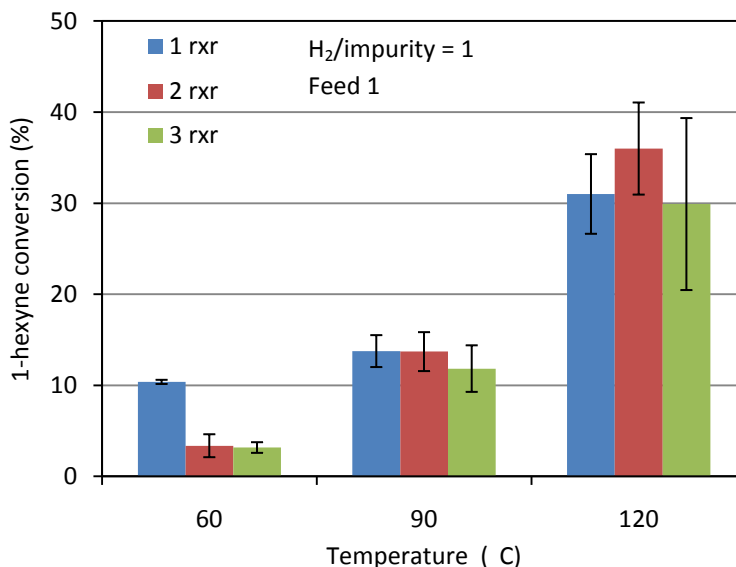


Figure 7.5: Comparing 1-hexyne conversion for different reactor configurations at 60, 90 and 120°C

(Run 4: Feed 1, WHSV = 3 hr<sup>-1</sup>, H<sub>2</sub>/impurity = 1, P = 30 bar)

### 7.3.2. Diene conversion

Figures 7.6 and 7.7 compare the 1,5- and 1,4-hexadiene conversions respectively. Little or no conversion of 1,5-hexadiene was observed for the single reactor configuration; this increased slightly as multiple reactors were used, but conversion remained less than 5% of the 2000 ppm present under test conditions. 1,4-hexadiene exhibited a similar trend, with conversion generally increasing as the number of reactors was increased, approaching 10% conversion of the 2000 ppm 1,4-hexadiene present.

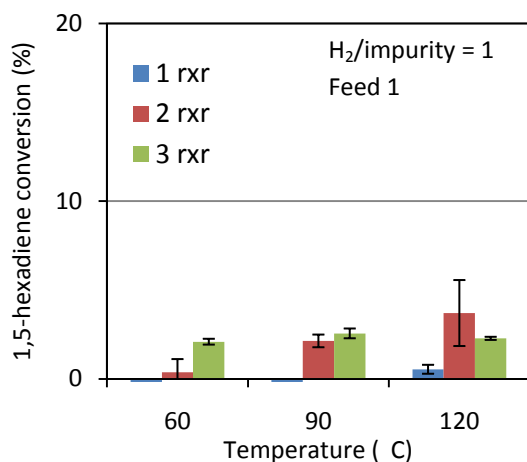


Figure 7.6: Comparing 1,5-hexadiene conversion for different reactor configurations at 60, 90 and 120°C

(Run 4: Feed 1, WHSV = 3 hr<sup>-1</sup>, H<sub>2</sub>/impurity = 1, P = 30 bar)

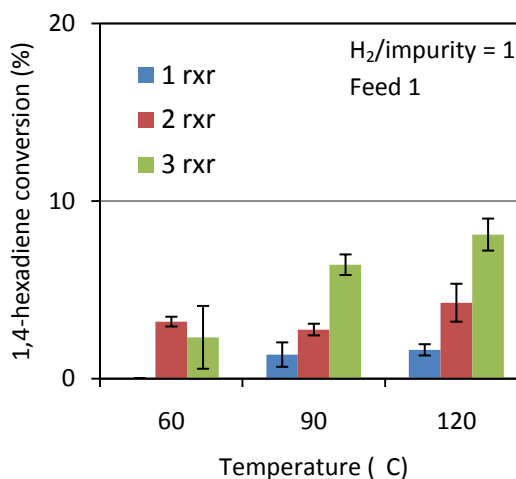


Figure 7.7: Comparing 1,4-hexadiene conversion for different reactor configurations at 60, 90 and 120°C

(Run 4: Feed 1, WHSV = 3 hr<sup>-1</sup>, H<sub>2</sub>/impurity = 1, P = 30 bar)

These observations suggest that the limited hydrogen availability in the multiple reactor configurations allows for improved diene removal. However, this is contradictory to the results observed for the alkyne (figure 7.5) where reduced hydrogen coverage resulted in a depressed conversion at 60°C.

The increased diene removal may be potentially explained by the results for total impurity conversion by hydrogenation (figure 7.8); where the total impurity conversion by hydrogenation for the different reactor configurations are very similar at each temperature, despite the increased diene conversions observed for the 2 and 3 reactor configurations. Since the diene conversion only takes into account the change in that specific species, this could indicate that the change is a result of an isomerisation to another diene, and is therefore not reflected in the total impurity conversion, which takes into account only the conversion that

occurred via hydrogenation. Further investigation into the exact behaviour of diene impurities must be considered in future work.

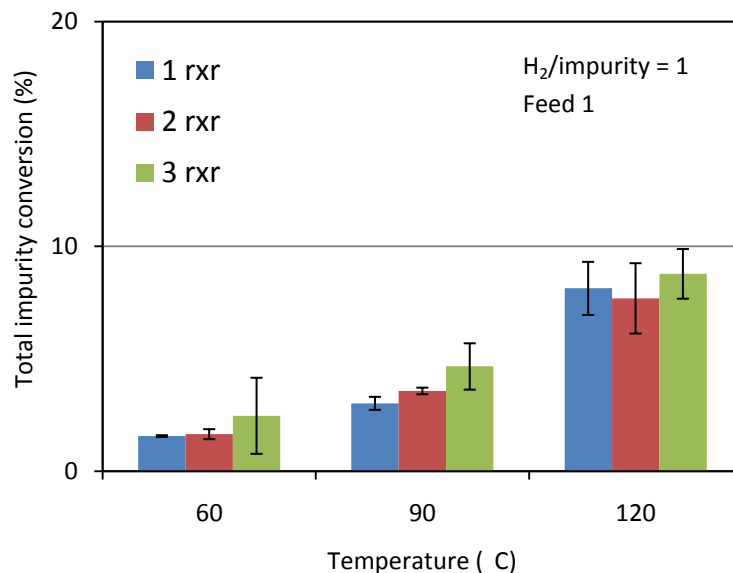


Figure 7.8: Total impurity conversion by hydrogenation for different reactor configurations at 60, 90 and 120°C (Run 4: Feed 1, WHSV = 3 hr<sup>-1</sup>, H<sub>2</sub>/impurity = 1, P = 30 bar)

### 7.3.3. 1-hexene loss, n-hexane and hexene isomer ppm changes

Overall the changes in 1-hexene content under stoichiometric hydrogen (as illustrated in section 7.1, figure 7.4) are too small to be considered particularly significant, however, the observed loss for all reactor configurations at 120°C does indicate that at this temperature some loss of 1-hexene is unavoidable, even at low hydrogen levels.

Figure 6.19 illustrates that under excess hydrogen ( $H_2/\text{impurity} = 2$ ), a 1-hexene gain was observed for the single reactor case at 60, 90 and 120°C. This indicates that for a single reactor some of the converted 1-hexyne did not undergo total hydrogenation to n-hexane but rather was partially hydrogenated, resulting in the observed 1-hexene gain – a result that is somewhat surprising for operation under excess hydrogen.

Figure 7.4 compares the 1-hexene gain/loss for different reactor configurations at 120°C with the most noticeable trend being that, under excess hydrogen, increasing the number of reactors results in an increased loss of 1-hexene. This indicates that the reduced availability of hydrogen provided by the multiple reactor configurations does not curb the loss of 1-hexene and that this setup seemingly promotes 1-hexene

loss. The single reactor setup appears to be the most promising in terms of minimising the undesired loss of 1-hexene, and maximising the potential gain in 1-hexene.

The ppm changes in n-hexane under stoichiometric hydrogen (figure 6.15) were small overall. Under excess hydrogen at 120°C (figure 7.9) it was observed that the n-hexane content increased as the number of reactors was increased, reaching a maximum net change of ~5000 ppm.

Similarly, in terms of hexene isomer content (figure 7.10), the ppm amount of hexene isomers increased as more reactors were used. Comparing the n-hexane and hexene isomer ppm changes, it is apparent that even under excess hydrogen the majority of lost 1-hexene is as a result of hydrogenation to n-hexane (comparing figures 7.9 and 7.10). There is no clear explanation as to why the use of multiple reactors results in an increase in the hydrogenation of 1-hexene to n-hexane, as reduced hydrogen coverage of sites is expected to limit hydrogenation. The increased linear velocity for multiple reactors and possible mass transfer limitations may play a role in these findings and these possibilities should be further investigated.

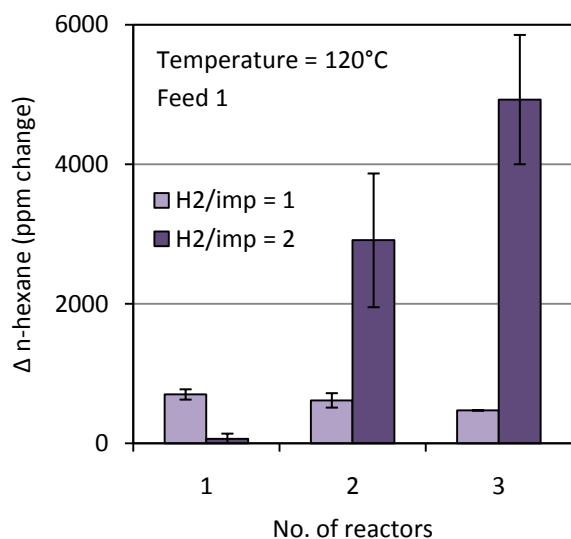


Figure 7.9:  $\Delta$  n-hexane at 120°C for 1, 2 and 3 reactors under H<sub>2</sub>/impurity of 1 and 2

(■ Run 4, ■ Run 5: Feed 1, WHSV = 3hr<sup>-1</sup>, P = 30 bar)

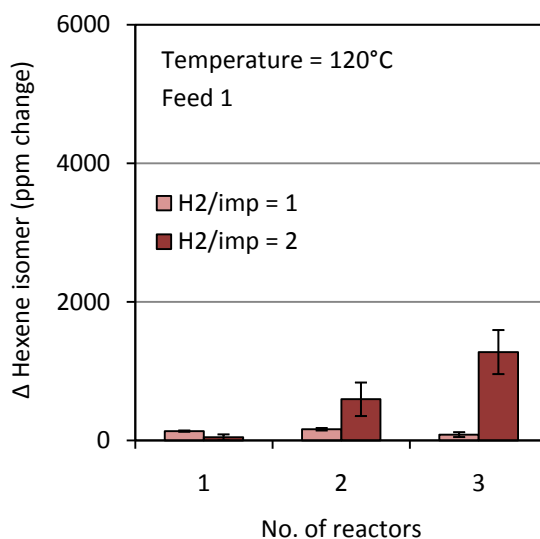


Figure 7.10:  $\Delta$  Hexene isomer at 120°C for 1, 2 and 3 reactors under H<sub>2</sub>/impurity of 1 and 2

(■ Run 4, ■ Run 5: Feed 1, WHSV = 3hr<sup>-1</sup>, P = 30 bar)

#### 7.4. Relative reactivity of impurities

In all of the experimental work conducted it was apparent that, as expected, 1-hexyne is the most reactive of the impurities. The conversion of the hexadiene impurities did occur but at significantly depressed levels (typically 5-10 times lower).

Tests employing a feed excluding 1-hexyne as an impurity (Feed 2 in table 5.3) were carried out to clarify the reactivity of diene and cyclic impurities in the absence of the alkyne (figures 6.22 - 6.24). Of the 3 model impurities present in this feed (1,5-HD, 1,4-HD and MCP), 1,4-HD was the most reactive throughout, however, these conversions were generally still less than 10%. Low conversions of 1,5-HD did occur, but only at 120°C. The cyclic impurity, MCP, showed no measurable conversion irrespective of the test conditions applied in this study. This finding may signify that no (or only very limited) removal of cyclic impurities by hydrogenation is practical under conditions of low 1-hexene loss, whereas diene removal is possible but will prove much more difficult than the removal of the alkyne. The relative reactivity of the impurities included in this study can be described by the series:

1-hexyne >> 1,4-hexadiene > 1,5 hexadiene > 1-hexene >> 1-methyl-cyclopentene

## 8. Conclusions

---

This study has assessed the performance and feasibility of gold on titania as a catalyst for the selective hydrogenation of low levels of impurities in a 1-hexene stream. The single gold catalyst employed in this study was prepared via wet impregnation, with the specific aim of preparing large gold crystallites. The preparation yielded large particles containing average particle sizes well in excess of 75 nm.

Selective hydrogenation using gold catalysts has been previously investigated at the University of Cape Town and has exhibited potential for the removal of alkyne impurities from a 1-hexene stream. The main focus of this study was to investigate a more realistic impurity regime in terms of the specific impurities present and their respective concentrations in the olefin stream. As such, feeds included low (~ 2000 ppm) levels of C<sub>6</sub> alkadiene and cyclic impurities. Aims were to investigate the effects of H<sub>2</sub>/impurity ratio and the use of multiple reactor setups, with interstage hydrogen addition, to achieve better control of the hydrogen levels within the system.

The study has conclusively illustrated that 1-hexyne conversions of greater than 90% can be achieved at low impurity feed levels (~2000 ppm), without significant loss of valuable 1-hexene (less than 4000 ppm loss). However, the removal of diene and cyclic impurities proved much more difficult. The conversion of hexadiene impurities did occur, albeit at low levels of generally less than 10%, whilst no measurable conversion of cyclic impurities was observed. The relative reactivity of the impurities studied can be described by the series:

1-hexyne >> 1,4-hexadiene > 1,5 hexadiene > 1-hexene >> cyclics

Overall, the best conditions for the conversion of the alkyne were achieved using a single reactor, with no hydrogen replenishment, utilising a H<sub>2</sub>/impurity ratio of two. This attains greater than 90% conversion of the alkyne at 120°C, whilst achieving a small desirable 1-hexene gain. For this setup diene conversion is low (~5%), although this can be improved by the use of multiple reactors – albeit at increasing loss of valuable 1-hexene.

Contrary to expectations, operation with multiple reactors, where the hydrogen levels are kept low and replenished stepwise, did not minimise the loss of 1-hexene but rather resulted in an increased 1-hexene loss. This was mainly a result of 1-hexene hydrogenation to n-hexane.

It is clear from results comparing different size hydrogen dissolution vessels that the dissolution of hydrogen in the liquid feed is critical not only for the hydrogenation of 1-hexyne, but is also a requirement for achieving desirable high/negative specificity. The necessary contacting volume between the hydrogen gas and liquid feed must be available for complete dissolution to occur. It is therefore very important in experimental work of this nature to ensure that the dissolver unit is of sufficient size to allow complete dissolution to take place.

In terms of declaring the process industrially viable there is still significant work required in terms of the increasing the removal of diene impurities. This may be improved through operating at a lower WHSV and increasing the available gold surface area by using a catalyst containing smaller gold particles. There still exists a need for a deeper understanding of the observed phenomena, particularly the conversion of the diene impurities and the increased loss of 1-hexene observed for operation with multiple reactors.



**Literature references**

**Ardiaca, N.O., Bressa, S.P., Alves, J.A., Mart'inez, O.M., Barreto, G.F.**, 'Experimental procedure for kinetic studies on egg-shell catalysts: The case of liquid-phase hydrogenation of 1,3-butadiene and n-butenes on commercial Pd catalysts', *Catalysis Today* 64, 2001, p.205–215

**Arnold, H., Dobert, F. and Gaube, J.**, 'Hydrogenation Reactions', *Handbook of Heterogenous Catalysis*, 5, 1997, p. 2165-2168.

**Böhringer, W.**, *Class notes CHE5040 – Chemicals from oil*, Centre for Catalysis Research, Department of Chemical Engineering University of Cape Town, 2008

**Bond, G.C. and Sermon, P.A.** , "Gold Catalysts for Olefin Hydrogenation," *Gold Bulletin* , (1973) 102 - 105.

**Bond, G. C. and Rawle, A. F.**, 'Catalytic hydrogenation in the liquid phase. Part 1: Hydrogenation of isoprene catalysed by palladium, palladium-gold and palladium-silver catalysts', *Journal of Molecular Catalysis A: Chemical* 109, 1996, 261-271.

**Brown, T.**, 'Selective Hydrogenation for Industrial 1-Hexene Purification', M.Sc. thesis, Catalysis Research Unit, Department of Chemical Engineering University of Cape Town, 2004.

**Chemical Marketing Reporter**, 'Sasol tie for alpha-olefins', Vol. 247 Issue 17, 24/4/95, p. 34.

**Chemical Marketing Reporter**, 'Alpha-Olefins', Vol. 261 Issue 4, 1/28/2002.

**Debuisschert, Q., Conso, I. and Fritz, A.**, 'Commercial Applications of Pyrolysis Gasoline Upgrading', 2nd Russian Petrochemical Technology Conference, Moscow, 2003.

**Deganello, G., Parmaliana, A., Frusteri, F. and Duca, D.**, 'Selective Hydrogenation of acetylene in ethylene feedstocks on Pd catalysts', *Applied Catalysis A: General* 146, 1996, p. 269-284.

**Guczi, L., Schay, Z., Stefler, G., Liotta, L.F., Deganello, G., and Venezi, A. M.** 'Pumice-Supported Cu–Pd Catalysts: Influence of Copper on the Activity and Selectivity of Palladium in the Hydrogenation of Phenylacetylene and But-1-ene', *Journal of Catalysis* 182, 1999, p. 456–462.

**Himelfarb, P. B. and Bolinger, C. M.** US Patent 6 388 162 B1, 2002.

**Hugon, A., Delannoy, L. and Louis, C.,** 'Gold based catalysts performances in selective hydrogenation of butadiene in an excess of propene', Abstract from the 20<sup>th</sup> North American Catalysis Society Meeting, 2007.

**Hutchings, G. J. and Haruta, M.,** 'A golden age of catalysis: a perspective', *Applied Catalysis A: General*, 291, 2005, p. 2–5.

**Jia, J., Haraki, K., Kondo, J., Domen, K. and Tamaru, K.,** 'Selective Hydrogenation of acetylene over Au/Al<sub>2</sub>O<sub>3</sub> catalyst', *Journal of Physical Chemistry B* 104, 2000, p. 11153-11156.

**Julius, M.,** 'Selective hydrogenation of the impurities in a 1-hexene stream using Pd- and Au-based catalysts supported on TiO<sub>2</sub>', M.Sc. thesis, Catalysis Research Unit, Department of Chemical Engineering, University of Cape Town, 2008.

**Le Page, J.-F., Cosyns, J., Courty, P., Freund, E., Franck, J.-P., Jacquin, Y., Juguin B.; Marcilly, Marcilly, C., Martino, G., Miquel, J., Montarnal, R., Sugier, A. and Van Landeghem, H.,** *Applied Heterogenous Catalysis*, Technip: Paris, 1987, p. 329-355.

**Lopez-Sanchez, J. and Lennon, D.,** 'The use of titania- and iron oxide-supported gold catalysts for the hydrogenation of propyne', *Applied Catalysis A: General* 291, 2005, p. 230-237.

**McPherson, J.S. and Fletcher, J.C.Q.,** 'Olefin Purification via catalytic hydrogenation', University of Cape Town, unpublished research report (Octene work), 2000.

**McPherson, J.S.**, '*1-Hexene purification via selective catalytic hydrogenation*', M.Sc. thesis, Catalysis Research Unit, Department of Chemical Engineering University of Cape Town, 2003.

**Molnár, A., Sárkány, A. and Varga, M.**, '*Hydrogenation of carbon-carbon multiple bonds: chemo-, region- and stereo-selectivity*', J. of Molecular Catalysis A: Chemical, Vol. 173, Issues 1-2, 2001, p. 185-221.

**Nierlich, F. and Obenhaus, F.**, Erdöl, Kohle-Erdgas-Petrochem. 39, 1986, p. 73–78.

**Nijhuis, T.A., van Koten, G. and Moulijn, J.A.**, '*Optimised palladium catalyst systems for the selective liquid-phase hydrogenation of functionalized alkynes*', Applied Catalysis A: General 238, 2003, p. 259-271.

**Ponec, V. and Bond, G.C.**, '*Catalysis by Metals and Alloys*', Elsevier Science B.V, 1995.

**Ramasary, A.**, '*Purification of 1-hexene via selective catalytic hydrogenation*', M.Sc. thesis, Catalysis Research Unit, Department of Chemical Engineering University of Cape Town, 2008.

**Rase, H.**, '*Handbook of commercial catalysts*', Edition no.1, 2000.

**Sales, E., Mendes, M. and Bozon-Verduraz, F.**, '*Liquid-Phase Selective Hydrogenation of Hexa-1,5-diene and Hexa-1,3-diene on Palladium Catalysts. Effect of Tin and Silver Addition*', Journal of Catalysis 195, 2000a, p. 96-105. a)

**Sales, E., Jove, J., Mendes, M. and Bozon-Verduraz, F.**, '*Palladium, Palladium-Tin, and Palladium-Silver catalysts in the selective hydrogenation of hexadienes: TPR, Mössbauer, and infrared studies of adsorbed CO*', Journal of Catalysis 195, 2000b, p. 88-95.

**Segura, Y., Lopez, N. and Perez-Ramirez, J.**, '*Origin of the superior hydrogenation selectivity of gold nanoparticles in alkyne + alkene mixtures: Triple- versus double-bond activation*', Journal of Catalysis 247, 2007, p. 383-386.

Zanella, R., Louis, C., Giorgio, S. and Touroude, R., 'Crotonaldehyde hydrogenation by gold supported on  $TiO_2$ : structure sensitivity and mechanism', *Journal of Catalysis* 223, 2004, p. 328-339.

Zhang, Q., Li, J., Liu, X. and Zhua, Q., 'Synergetic effect of Pd and Ag dispersed on  $Al_2O_3$  in the selective hydrogenation of acetylene', *Applied Catalysis A: General* 197, 2000, p. 221–228.

### **Electronic references**

[nexant.ecnext.com](http://nexant.ecnext.com), 'Market overview: Alpha-olefins', 2004, [Accessed 03.2008]

[www.colin-houston.com](http://www.colin-houston.com), 'Proposed study: ALPHA-OLEFINS - WORLD MARKETS, 2005-2015', 2006, [Accessed 03.2008]

[www.cpchem.com](http://www.cpchem.com), 'Proprietary Selective 1-Hexene Process Yields Top Honors for Chevron Phillips Chemical', 2005, [Accessed 03.2008]

[www.engineeringnews.co.za](http://www.engineeringnews.co.za), Hill, L., 'State-of-the-art technology for new Sasol plant' 2006, [Accessed 04.2008]

[www.innovene.com](http://www.innovene.com), 'Linear alpha olefins overview: 1-hexene' 2006, [Accessed 04.2008]

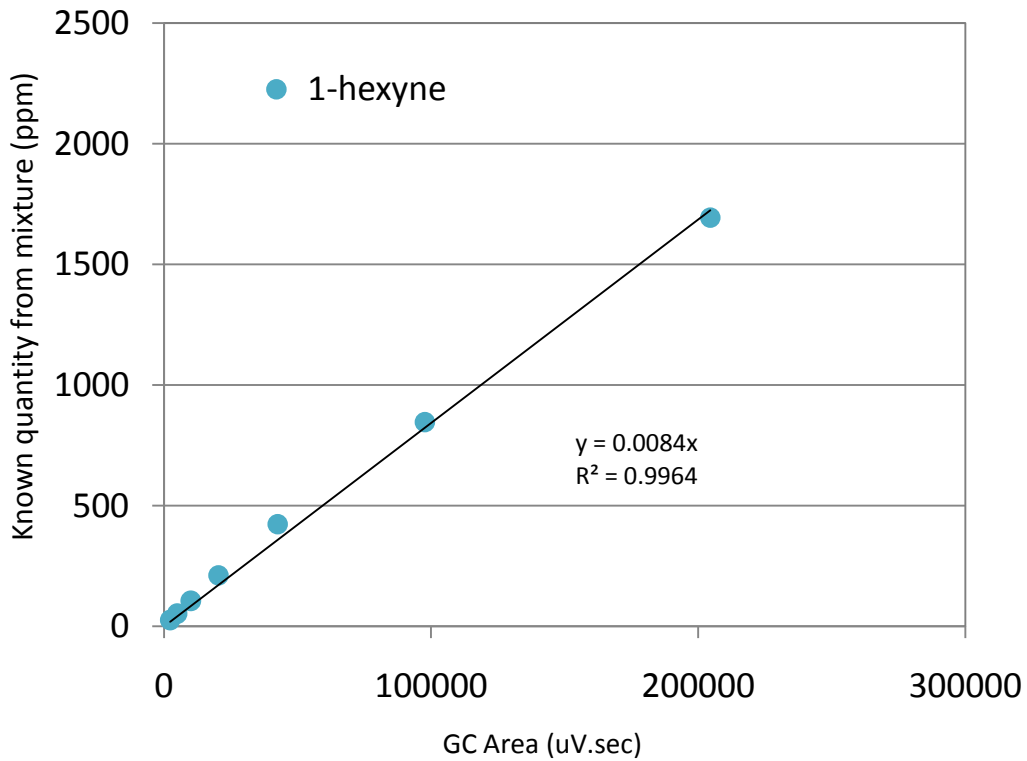
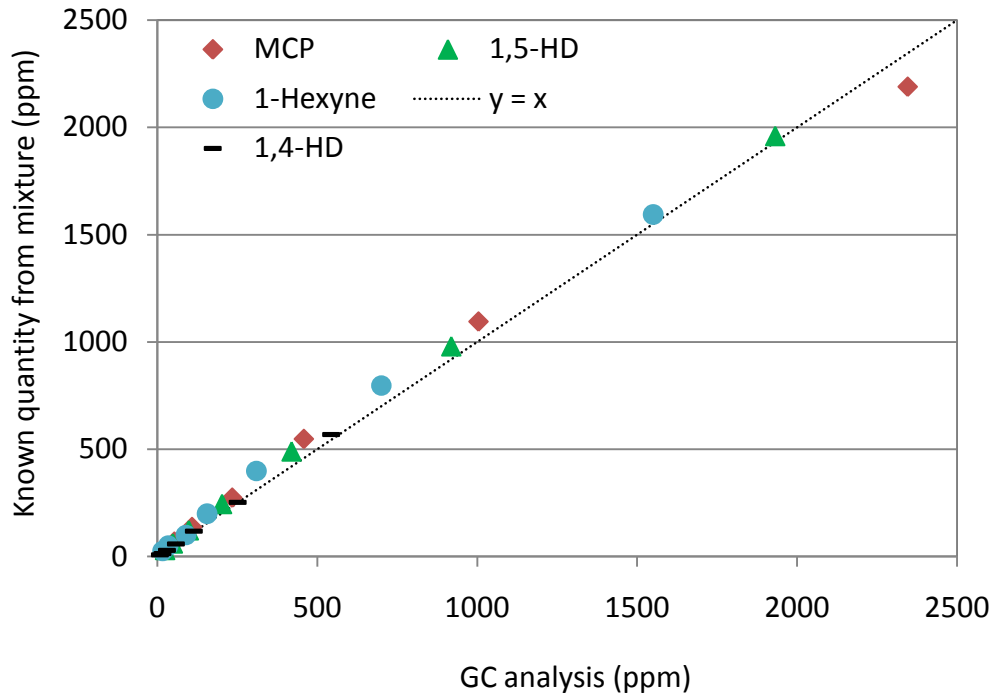
[www.jmcatalysts.com](http://www.jmcatalysts.com), 'Catalysts and absorbents for steam cracker application', 2008, [Accessed 05.2008]

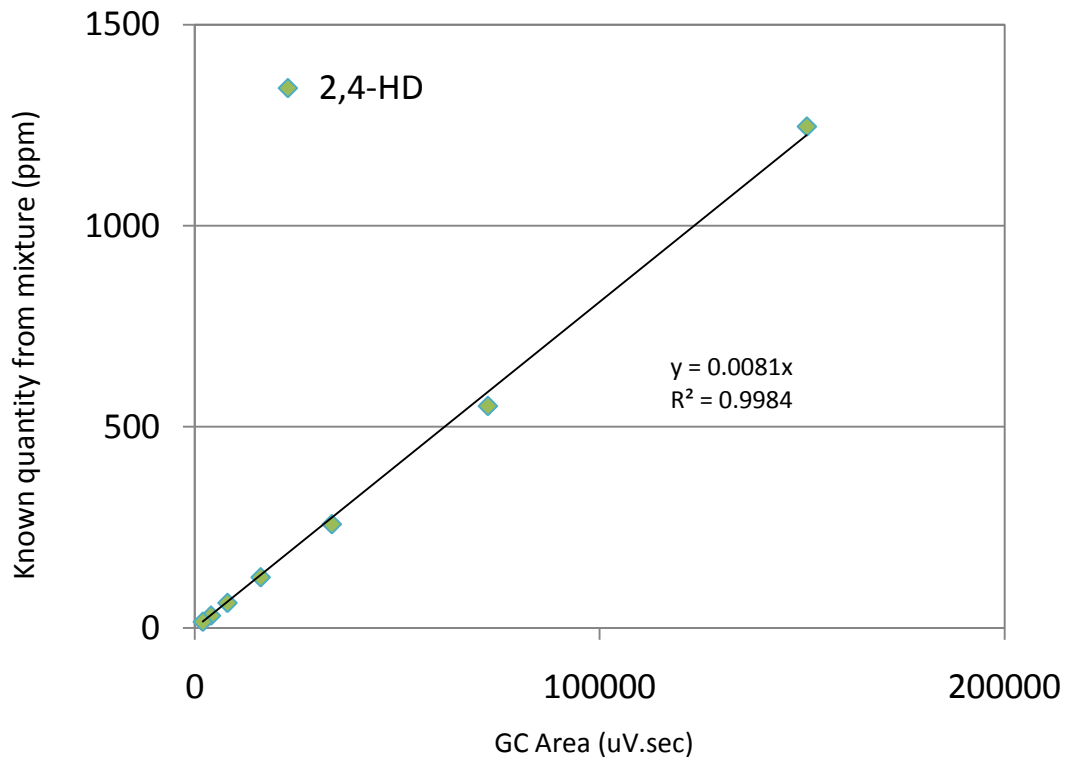
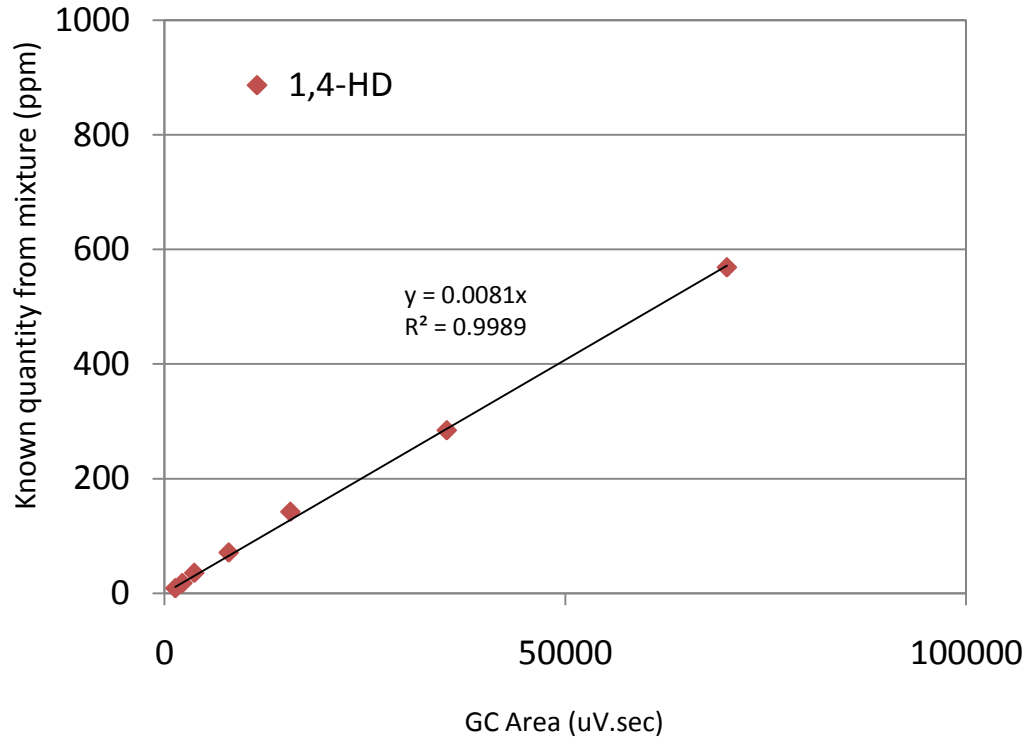
[www.the-innovation-group.com](http://www.the-innovation-group.com), 'Chemical profile: Alpha Olefins (Linear)', 2002, [Accessed 03.2008]

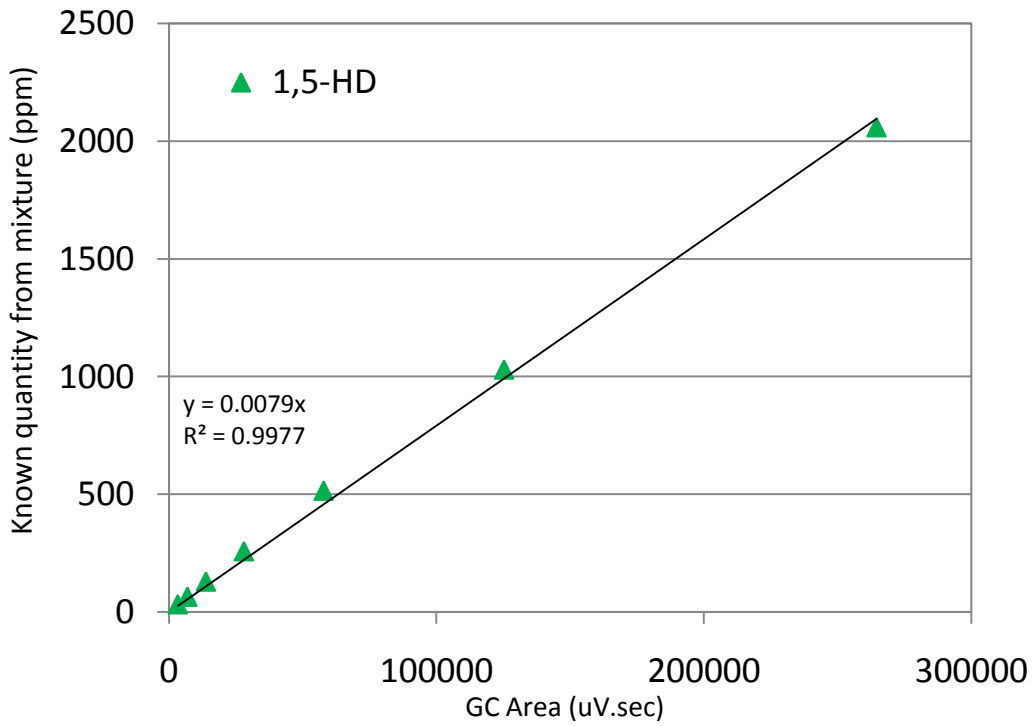
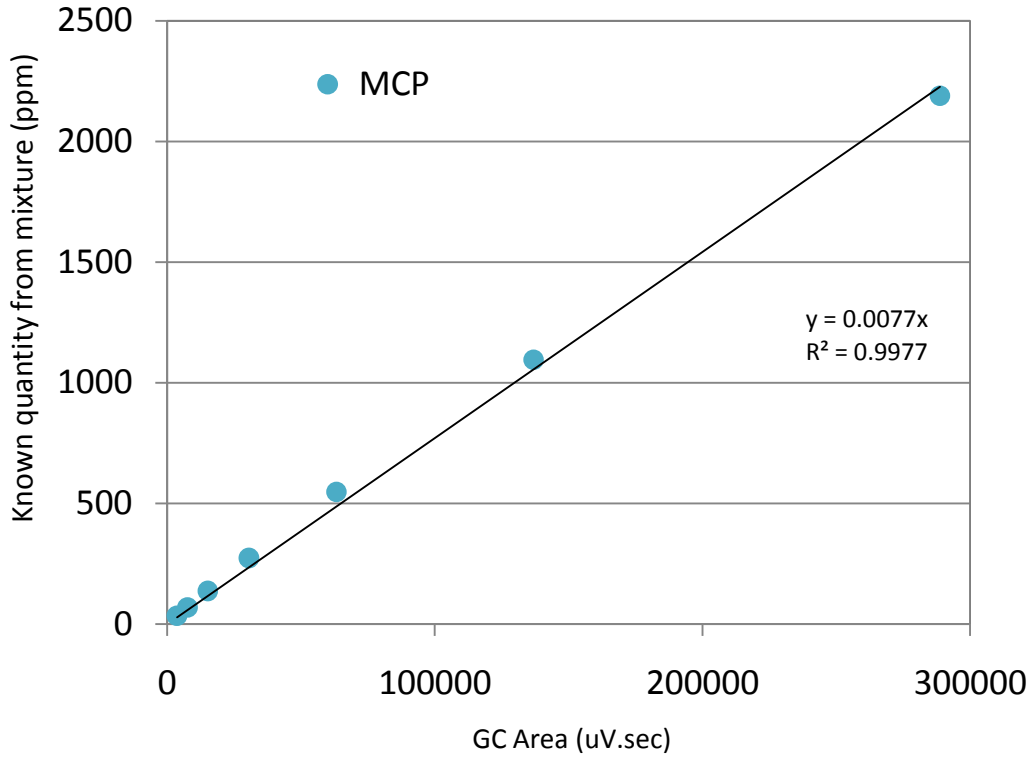


### Appendix I – Calibration curves

- Model impurities

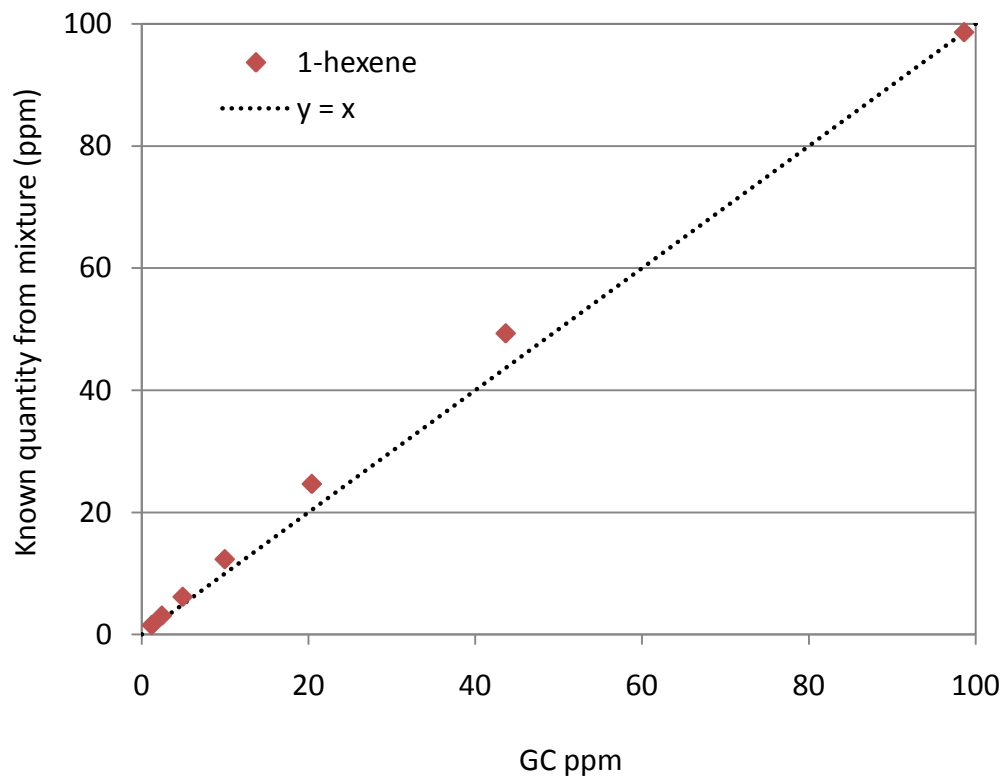
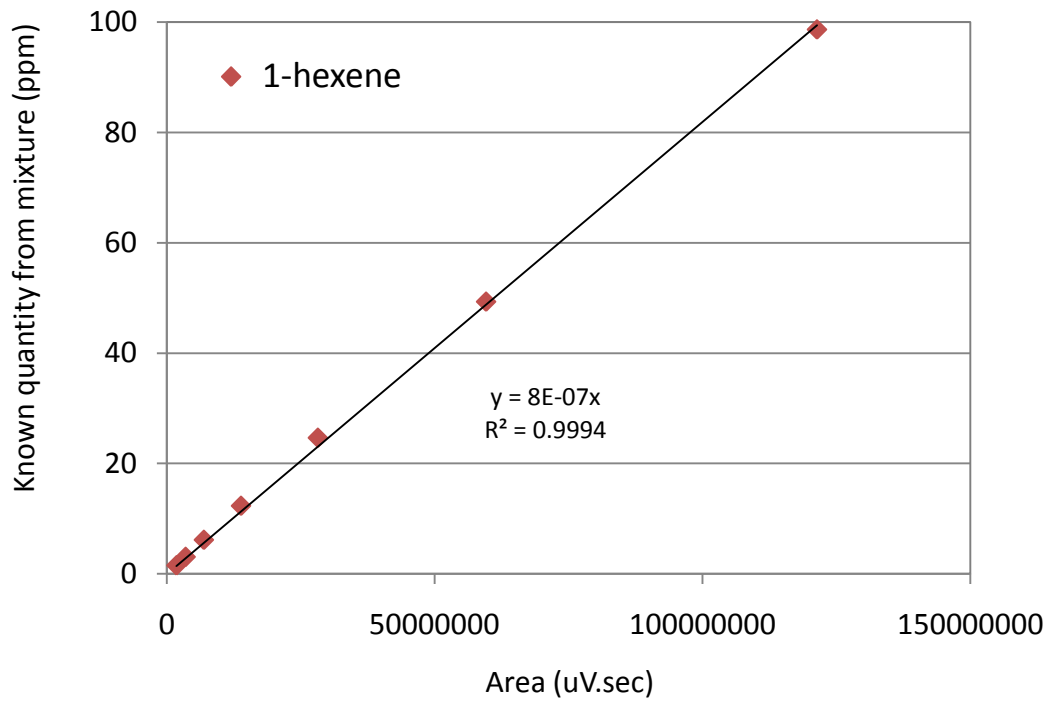








- 1-hexene



## Appendix II - Preparation of feed mixture by mass

	1-hexene	1-hexyne	1,5-hexadiene	2,4-hexadiene	1,4-hexadiene	1-methyl-cyclopentene
<b>Molar mass</b> (g/mol)	84.16	82.15	82.15	82.15	82.15	82.15
<b>ρ</b> (g/l)	673	715	694	720	710	778

### Feed 1:

Impurity concentration required is 0.2 mol % of each of the 5 impurities. Impurity compounds were added based on a known mass of 1-hexene already weighed out. The calculation of the mass of each impurity compound required was calculated using equation A1.

$$\text{Mass}_{\text{Impurity required}} = \text{Molar mass}_{\text{Impurity}} \times \frac{0.2}{99} \times \frac{\text{Mass}_{1\text{hexene weighed}}}{\text{Molar mass}_{1\text{hexene}}} \quad (\text{A1})$$

The mass of each of the compounds was measured out accordingly. The actual number of moles of the respective constituent was then determined by equation A2.

$$\text{No Moles}_{\text{Impurity1}} = \frac{\text{Mass}_{\text{Impurity1 weighed}}}{\text{Molar mass}_{\text{Impurity1}}} \quad (\text{A2})$$

Using the determined numbers of moles of all the feed constituents, their accurate actual mole fractions were calculated.

**Feed 2:**

Impurity concentration required is 0.2 mol % of each of the 3 impurities. As for feed 1, impurity compounds were added based on a known mass of 1-hexene already weighed out. The calculation of the mass of each impurity compound required was calculated using equation A3.

$$\text{Mass}_{\text{Impurity required}} = \text{Molar mass}_{\text{Impurity}} \times \frac{0.2}{99.4} \times \frac{\text{Mass}_{1\text{hexene weighed}}}{\text{Molar mass}_{1\text{hexene}}} \quad (\text{A3})$$

The mass of each of the compounds was measured out accordingly. The actual number of moles of the respective constituent was then determined as for feed 1, by equation A2.

Using the determined numbers of moles of all the feed constituents, their accurate actual mole fractions were calculated.

**Feed 3:**

For feed 3 the impurity concentration required is 1 mol % of only 1-hexyne. The mass of 1-hexyne required was calculated based on a known mass of 1-hexene weighed out, using equation A4.

$$\text{Mass}_{1\text{-hexyne required}} = \text{Molar mass}_{1\text{hexyne}} \times \frac{1}{99} \times \frac{\text{Mass}_{1\text{hexene weighed}}}{\text{Molar mass}_{1\text{hexene}}} \quad (\text{A4})$$

The mass of 1-hexyne was measured out accordingly. The actual number of moles was then determined as for feed 1, by equation A2.

Using the determined numbers of moles of all the feed constituents, their accurate actual mole fractions were calculated.

## Appendix III – Tabulated hydrogenation data

Hydrogenation data calculated according to the equations as described in the data work-up section (section 5.6.3)

Note:

- The data obtained for each experiment is shown in the following tables. The feed mixture used for each experiment is described in the table heading (table 6.2 further details the contents of each feed mixture). Testing was performed at 60, 90 and 120°C for each experiment and thereafter returned to 60°C to determine whether catalyst deactivation had been taking place. No catalyst deactivation was observed for all catalysts.
- The impurity conversions are listed, 2,4-hexadiene and 1-methyl-cyclopentene are excluded where no change was seen. Also tabulated are the changes (net gain / loss) in % composition of 1-hexene, hexene isomers and n-hexane. For 1-hexene net gain / loss a positive value describes a gain, while a negative value illustrates an overall loss.

Run 1	FEED3	H <sub>2</sub> /impurity = 1				1 reactor		
Time	Temp	X 1-hxy	X 1,5-HD	X 1,4-HD	X mcp	Gain 1-hxe	Gain hxe isomers	Gain hxa
hour	C	%	%	%	%	abs %	abs %	abs %
29.0	60	59.3	-	-	-	0.26	0.04	0.06
29.0	60	58.9	-	-	-	0.26	0.04	0.06
32.0	60	49.1	-	-	-	0.16	0.05	0.06
32.0	60	49.6	-	-	-	0.16	0.05	0.06
34.5	60	51.6	-	-	-	0.10	0.10	0.06
34.5	60	48.4	-	-	-	0.08	0.09	0.06
		-	-	-	-			
51.0	90	55.0	-	-	-	0.16	0.09	0.06
51.0	90	56.2	-	-	-	0.16	0.08	0.06
53.5	90	62.6	-	-	-	0.26	0.03	0.04
53.5	90	61.6	-	-	-	0.27	0.03	0.03
55.5	90	66.8	-	-	-	0.26	0.06	0.04
55.5	90	63.6	-	-	-	0.18	0.07	0.05
58.0	90	78.6	-	-	-	0.37	0.07	0.04
58.0	90	77.6	-	-	-	0.36	0.07	0.04
59.0	90	70.4	-	-	-	0.34	0.05	0.03
59.0	90	69.2	-	-	-	0.31	0.06	0.04
		-	-	-	-			
78.3	120	81.6	-	-	-	0.38	0.08	0.06
78.3	120	81.0	-	-	-	0.31	0.09	0.06
81	120	72.6	-	-	-	0.32	0.03	0.09
81	120	72.1	-	-	-	0.32	0.03	0.09

Run 2a		FEED 1		H <sub>2</sub> /impurity = 1						
Time	Temp	RXR	X 1-hxy	X 1,5-HD	X 1,4-HD	X total	Gain 1-hxe	Gain hxa	Gain hxe isomers	
hour	C		%	%	%	%	abs %	abs %	abs %	
26	120	1	46.4	2.5	5.0	8.8	-0.20	0.04	0.22	
26	120	1	46.0	2.3	4.4	9.5	-0.20	0.04	0.22	
27	120	1	32.5	1.3	3.0	6.3	-0.14	0.03	0.15	
27	120	1	32.5	1.4	2.9	6.1	-0.14	0.03	0.15	
27	120	1	32.4	1.3	2.4	6.3	-0.14	0.03	0.15	
29	120	1	30.9	1.2	2.3	6.9	-0.11	0.02	0.13	
29	120	1	30.9	1.1	2.3	6.4	-0.11	0.02	0.13	
29	120	1	31.1	1.2	2.4	6.9	-0.11	0.02	0.13	
30	120	1	48.9	0.9	2.0	11.5	-0.02	0.02	0.08	
30	120	1	48.8	0.6	1.7	11.7	-0.01	0.02	0.08	
30	120	1	49.0	0.8	2.0	11.4	-0.02	0.02	0.08	

51.5	90	1	11.6	2.0	2.9	3.1	0.01	0.01	0.02
51.5	90		11.2	1.8	5.1	3.6	0.00	0.01	0.02
52.5	90		12.8	1.6	3.5	5.1	-0.01	0.00	0.00
52.5	90		12.7	1.4	3.5	5.3	-0.01	0.00	0.00
54	90		12.9	2.5	3.4	3.3	-0.01	0.00	0.00
54	90		12.6	2.7	3.1	3.0	-0.01	0.00	0.00
56	90		12.4	2.5	3.1	3.4	-0.01	0.00	0.00
56	90		12.7	2.1	3.3	2.6	-0.01	0.00	0.00

74.5	60	1	1.7	1.9	6.0	2.2	-0.03	0.00	0.00
74.5	60		0.8	1.6	4.8	3.1	-0.02	0.00	0.00
75.5	60		-0.2	1.9	4.7	1.9	-0.03	0.00	0.00
75.5	60		-0.1	1.7	4.8	2.2	-0.03	0.00	0.00
77	60		3.5	1.9	1.4	1.2	-0.03	0.00	0.00
77	60		2.7	2.0	3.8	1.5	-0.04	0.00	0.00

---

Run 2b			FEED 1	H <sub>2</sub> /impurity = 1					
Time	Temp	Rxr	X 1-hxy	X 1,5-HD	X 1,4-HD	X total	Gain 1-hxe	Gain hxa	Gain hxe isomers
hour	C		%	%	%	%	abs %	abs %	abs %
28	60	1	10.3	-0.1	0.0	1.4	0.00	0.01	0.01
28	60		10.1	-0.2	0.0	1.6	0.00	0.01	0.01
29.5	60		11.0	-0.2	-0.1	1.6	0.00	0.00	0.01
29.5	60		10.5	0.0	0.1	1.7	0.00	0.00	0.01
31	60		10.3	-0.1	0.0	1.5	0.00	0.00	0.00
31	60		10.2	-0.1	0.1	1.6	0.00	0.00	0.00
49	90		1	13.3	-0.1	2.7	3.4	-0.01	0.01
51	90	16.0		-0.3	1.8	3.0	-0.03	0.02	0.03
51	90	15.8		-0.3	0.8	3.5	-0.02	0.01	0.03
52	90	14.6		-0.4	0.7	2.8	-0.02	0.01	0.03
52	90	14.8		-0.4	0.6	2.9	-0.02	0.01	0.03
53	90	14.0		-0.1	1.0	2.3	-0.03	0.01	0.03
53	90	14.2		-0.2	0.4	2.8	-0.03	0.01	0.03
73.5	120	1		22.3	0.4	5.6	5.9	-0.03	0.01
75	120		35.6	1.0	6.0	9.6	-0.02	0.11	0.08
75	120		35.5	1.1	3.7	10.3	-0.03	0.11	0.09
76.5	120		33.4	0.5	-0.1	8.3	-0.01	0.11	0.07
76.5	120		33.8	0.4	3.5	9.1	-0.02	0.11	0.07
80	120		32.8	0.1	-0.5	8.1	-0.01	0.11	0.06
80	120		32.4	0.4	-0.1	7.9	-0.01	0.11	0.06
82	120		34.5	0.4	1.2	8.6	-0.01	0.11	0.06
82	120		34.0	0.2	0.5	8.9	-0.01	0.11	0.06

Run 3		FEED 1	H <sub>2</sub> /impurity = 1						
Time	Temp	No. RXR	X 1-hxy	X 1,5-HD	X 1,4-HD	X total	Gain 1-hxe	Gain hxa	Gain hxe isomers
hour	C		%	%	%	%	abs %	abs %	abs %

27.0	60	1	10.5	-0.4	0.0	1.4	0.00	0.00	0.00
27.0	60	1	10.2	-0.5	0.1	1.6	0.00	0.00	0.00
29.0	60	1	10.2	-0.1	0.0	1.4	0.00	0.01	0.01
29.0	60	1	10.1	-0.2	0.0	1.7	0.00	0.01	0.00
31.5	60	1	10.7	-0.2	0.1	1.6	0.00	0.00	0.01
31.5	60	1	10.4	-0.3	0.1	1.8	0.00	0.01	0.01

48.0	90	1	14.7	-0.3	0.9	2.7	-0.02	0.01	0.03
48.0	90	1	16.1	-0.3	1.9	2.9	-0.03	0.02	0.03
49.0	90	1	15.7	-0.3	0.8	3.3	-0.02	0.01	0.03
49.0	90	1	14.7	-0.2	0.6	2.9	-0.02	0.01	0.03
51.0	90	1	14.2	-0.2	1.1	2.5	-0.03	0.01	0.03
51.0	90	1	14.3	-0.2	0.4	2.6	-0.03	0.01	0.03

73.0	120	1	34.4	1.1	-0.1	7.9	-0.01	0.11	0.08
73.0	120	1	34.2	0.3	1.2	8.9	-0.02	0.10	0.08
74.0	120	1	35.4	0.2	0.5	9.6	-0.02	0.11	0.07
74.0	120	1	33.4	0.9	6.0	9.0	-0.01	0.11	0.07
76.0	120	1	33.6	0.5	3.3	8.3	-0.01	0.11	0.06
76.0	120	1	32.8	0.4	-0.2	8.3	-0.02	0.11	0.07
77.0	120	1	22.6	0.1	5.6	6.0	-0.03	0.07	0.09
77.0	120	1	35.8	0.4	3.7	10.3	-0.01	0.11	0.06
77.0	120	1	32.2	0.4	-0.1	8.6	-0.01	0.11	0.07

98.0	60	1	10.0	-0.2	0.0	1.6	0.00	0.00	0.01
98.0	60	1	11.0	-0.2	-0.1	1.6	0.00	0.00	0.01
100.0	60	1	10.1	-0.1	0.1	1.5	0.00	0.00	0.00
100.0	60	1	10.4	-0.1	0.0	1.4	0.00	0.01	0.01

121.0	60	2	1.5	1.0	4.9	1.8	0.01	0.00	0.00
121.0	60	2	3.6	-0.5	3.3	1.9	-0.03	0.00	0.00
122.5	60	2	5.0	-0.1	0.0	1.8	-0.01	0.00	0.00
122.5	60	2	3.3	1.0	1.9	1.4	-0.01	0.00	0.00
124.0	60	2	4.6	0.2	4.1	2.2	0.02	0.00	0.00



146.0	90	2	13.5	3.7	5.8	3.8	0.01	0.00	0.01
147.5	90	2	14.3	3.9	6.2	3.3	0.01	0.00	0.01
147.5	90	2	16.0	4.1	4.7	3.6	0.00	0.00	0.02
150.0	90	2	17.4	4.2	6.3	4.0	0.01	0.00	0.02
150.0	90	2	10.5	4.8	6.4	3.3	0.00	0.01	0.01

171.0	120	2	41.5	2.9	2.9	5.3	-0.05	0.01	0.08
171.0	120	2	42.2	3.0	2.9	5.6	-0.05	0.01	0.08
173.0	120	2	36.0	1.9	5.8	10.4	0.00	0.02	0.07
173.0	120	2	36.2	2.5	5.4	10.2	-0.01	0.02	0.07
174.5	120	2	33.9	7.1	2.8	6.98	-0.02	0.02	0.06
174.5	120	2	34.6	6.2	4.3	7.69	-0.02	0.02	0.06

194.0	60	3	2.3	2.4	0.6	0.4	-0.02	0.00	0.00
194.0	60	3	3.6	2.0	3.9	2.5	0.01	0.00	0.00
196.0	60	3	3.8	2.1	4.3	1.1	0.01	0.01	0.00
197.0	60	3	3.3	1.9	0.5	5.8	0.01	0.01	0.04

219.0	90	3	6.7	3.0	5.5	3.9	0.02	0.00	0.00
220.0	90	3	4.9	2.7	6.1	0.7	0.01	0.00	0.00
221.0	90	3	5.3	2.3	6.8	5.6	0.01	0.00	0.00
221.0	90	3	5.7	2.3	7.2	5.8	0.02	0.00	0.00

243.0	120	3	15.7	2.4	9.0	7.2	0.03	0.00	0.01
244.0	120	3	39.8	2.3	7.2	10.4	-0.01	0.01	0.06
245.5	120	3	34.2	2.1	8.6	8.7	-0.04	0.01	0.08

270.0	60	1	10.9	-0.2	0.1	1.4	0.00	0.00	0.01
271.0	60	1	10.3	-0.6	0.1	1.6	0.00	0.00	0.00

Run 4		FEED 1		H <sub>2</sub> /impurity = 2					
Time	Temp	RXR	X 1-hxy	X 1,5-HD	X 1,4-HD	X total	Gain 1-hxe	Gain hxa	Gain hxe isomers
hour	C		%	%	%	%	abs %	abs %	abs %

26	60	1	16.6	2.6	3.2	4.6	0.03	0.01	-0.01
26	60	1	15.8	2.6	3.2	4.5	0.03	0.01	-0.01
28	60	1	14.4	2.6	2.7	4.2	0.03	0.01	-0.01
28	60	1	14.5	2.6	2.7	4.4	0.03	0.01	-0.01
29	60	1	14.6	2.3	2.8	4.1	0.03	0.00	-0.01
29	60	1	14.5	2.3	2.8	4.1	0.03	0.00	-0.01
31	60	1	17.7	2.4	2.7	4.6	0.04	0.00	-0.01
31	60	1	17.6	2.3	2.8	4.7	0.04	0.00	-0.01

59	90	1	19.9	2.0	3.0	5.1	0.04	0.01	-0.01
59	90	1	21.4	2.5	2.9	4.8	0.04	0.01	-0.01
60	90	1	25.0	2.4	3.2	5.3	0.03	0.01	-0.01
60	90	1	24.3	2.6	3.0	5.0	0.04	0.01	-0.01
61.5	90	1	25.0	2.8	3.1	5.3	0.04	0.01	-0.01
61.5	90	1	24.9	2.8	3.1	5.3	0.04	0.01	-0.01
62.5	90	1	20.8	2.6	1.4	5.0	0.04	0.01	-0.01
62.5	90	1	24.9	2.1	3.5	5.2	0.02	0.01	-0.01

86	120	1	86.8	2.9	3.0	5.1	0.04	0.00	-0.01
86	120	1	82.7	2.9	3.4	5.0	0.04	0.00	-0.02
88	120	1	95.9	2.9	2.8	9.5	0.03	0.00	-0.01
88	120	1	93.9	2.5	4.0	8.4	0.03	0.00	-0.01

109	60	2	9.3	1.4	1.1	2.2	0.01	0.00	0.00
109	60	2	10.2	1.4	0.9	2.0	0.02	0.00	0.00
109	60	2	8.4	1.1	0.9	2.3	0.02	0.00	0.00
111	60	2	11.2	1.3	0.4	2.3	0.02	0.00	0.00
111	60	2	12.6	1.6	0.6	2.4	0.02	0.00	0.00
111	60	2	11.9	1.6	0.5	2.6	0.01	0.00	0.00
112.5	60	2	14.5	1.6	0.6	2.8	0.02	0.00	0.00

112.5	60	2	13.3	1.4	0.7	2.8	0.02	0.00	0.00
112.5	60	2	13.9	1.7	0.7	2.5	0.02	0.00	0.00

134	90	2	27.8	1.5	3.6	6.2	0.03	0.00	0.02
134	90	2	27.2	1.0	3.0	6.3	0.02	0.00	0.02
134	90	2	27.6	1.4	3.5	5.9	0.03	0.00	0.02
135.5	90	2	37.4	1.9	3.7	7.7	0.02	0.01	0.03
135.5	90	2	38.0	1.9	3.8	7.7	0.02	0.01	0.03
135.5	90	2	37.6	1.8	3.7	7.6	0.02	0.01	0.04
136.5	90	2	34.1	1.4	3.6	7.3	0.03	0.01	0.03
136.5	90	2	34.6	1.4	3.6	7.3	0.04	0.01	0.02
136.5	90	2	34.8	1.6	3.5	7.5	0.03	0.01	0.02

157.5	120	2	78.0	5.2	10.1	10.4	-0.39	0.09	0.39
157.5	120	2	78.1	5.2	10.6	9.0	-0.39	0.09	0.39
157.5	120	2	78.0	5.4	8.5	9.7	-0.40	0.09	0.39
159	120	2	96.1	4.7	9.9	13.0	-0.31	0.07	0.35
159	120	2	96.0	4.7	9.3	13.1	-0.31	0.07	0.35
159	120	2	96.1	4.7	9.8	12.7	-0.31	0.07	0.36
161	120	2	99.5	2.2	5.5	12.8	-0.05	0.02	0.13
161	120	2	99.5	2.1	5.9	12.7	-0.04	0.02	0.13
161	120	2	99.5	2.2	5.3	13.7	-0.04	0.02	0.13

182	60	3	8.0	0.4	1.2	2.7	-0.01	0.01	0.02
182	60	3	8.1	0.3	1.3	2.2	-0.01	0.01	0.02
182	60	3	8.0	0.2	0.5	2.3	-0.01	0.01	0.02
183	60	3	8.2	0.4	0.0	2.6	0.00	0.00	0.01
183	60	3	8.2	0.5	0.0	3.0	0.00	0.00	0.01
183	60	3	8.7	0.6	1.1	1.9	0.00	0.00	0.01
185	60	3	9.5	0.2	-0.1	3.2	0.01	0.00	0.00
185	60	3	10.2	0.3	0.2	2.9	0.01	0.00	0.00
185	60	3	9.6	0.3	0.2	2.3	0.02	0.00	0.00

207	90	3	13.3	0.3	0.4	3.3	-0.01	0.01	0.02
207	90	3	13.2	0.3	0.2	3.0	-0.01	0.01	0.02
207	90	3	13.0	0.2	0.0	2.6	-0.01	0.01	0.02
209	90	3	11.9	0.2	0.6	3.3	0.00	0.01	0.02
209	90	3	11.5	0.1	0.5	2.8	0.00	0.01	0.02

209	90	3	11.9	0.2	0.0	2.8	-0.01	0.01	0.02
210.5	90	3	7.7	0.2	0.1	2.2	0.00	0.00	0.01
210.5	90	3	7.8	0.0	-0.1	2.0	0.00	0.00	0.01
210.5	90	3	7.7	0.0	-0.2	1.3	0.00	0.00	0.01

232	120	3	70.1	4.0	6.7	11.7	-0.40	0.08	0.41
232	120	3	70.0	4.2	6.7	11.3	-0.40	0.08	0.40
232	120	3	70.3	4.1	6.5	11.4	-0.40	0.08	0.40
234	120	3	98.7	9.6	14.2	10.2	-1.00	0.17	0.89
234	120	3	98.6	9.5	14.2	7.7	-1.00	0.17	0.89
234	120	3	98.7	9.5	14.1	8.0	-1.00	0.17	0.89
235.5	120	3	98.6	8.2	12.7	11.2	-0.84	0.14	0.78
235.5	120	3	98.7	8.5	12.2	10.8	-0.84	0.14	0.78
235.5	120	3	98.7	8.5	12.5	8.6	-0.84	0.14	0.78

Run 5		FEED 2	H <sub>2</sub> /impurity = 1						
Time	Temp	RXR	X mcp	X 1,5-HD	X 1,4-HD	X total	Gain 1-hxe	Gain hxa	Gain hxe isomers
hour	C		%	%	%	%	abs %	abs %	abs %

24.0	60	1	-0.1	0.0	2.3	1.3	0.00	0.00	0.00
24.0	60	1	-0.1	1.0	2.4	0.8	0.00	0.00	0.00
25.5	60	1	0.1	-0.3	4.1	1.9	0.00	0.00	0.00
25.5	60	1	0.0	-0.3	4.9	1.3	0.00	0.00	0.00
26.0	60	1	0.0	0.2	3.3	1.2	0.00	0.00	0.00
26.0	60	1	0.0	0.1	3.4	1.3	0.00	0.00	0.00

49.00	90.00	1	-0.3	0.0	7.3	1.7	0.00	0.01	0.01
49.00	90.00	1	0.0	-0.2	7.4	1.8	0.00	0.01	0.01
50.00	90.00	1	0.0	0.0	7.1	1.9	0.00	0.01	0.01
50.00	90.00	1	-0.1	0.0	8.8	2.3	0.00	0.01	0.01
51.50	90.00	1	-0.1	0.1	7.7	1.9	0.00	0.01	0.01
51.50	90.00	1	0.0	0.0	7.6	2.0	0.00	0.01	0.01

72	120	1	0.1	0.8	10.2	2.8	-0.04	0.01	0.05
72.00	120	1	0.5	0.7	10.3	3.2	-0.05	0.01	0.07
73.50	120	1	0.5	2.3	10.9	2.5	-0.08	0.01	0.08
73.50	120	1	0.1	2.2	9.6	2.3	-0.08	0.01	0.08
74.00	120	1	0.0	0.5	12.1	2.4	-0.08	0.01	0.07
74.00	120	1	0.0	0.6	12.3	2.5	-0.08	0.01	0.07

98.00	60.00	2	-0.1	0.7	4.1	1.2	0.04	0.01	0.01
98.00	60.00	2	0.2	1.1	6.4	1.5	0.00	0.02	0.01
99.50	60.00	2	0.1	0.3	5.4	1.4	-0.04	0.02	0.02
99.50	60.00	2	0.0	1.0	4.3	1.3	0.00	0.01	0.01
101.00	60.00	2	0.0	0.8	3.4	1.2	0.00	0.02	0.01

121.0	90	2	0.1	0.2	5.4	1.5	-0.01	0.00	0.01
121.0	90	2	-0.1	0.0	5.0	2.6	-0.02	0.00	0.01
122.0	90	2	0.0	0.0	5.1	0.9	-0.02	0.00	0.01
122.0	90	2	-0.1	0.1	6.9	1.7	-0.01	0.00	0.01
123.5	90	2	0.1	0.1	7.3	1.6	-0.02	0.00	0.01
123.5	90	2	0.0	0.1	6.4	2.2	-0.02	0.00	0.01

144.0	120	2	0.1	1.0	9.7	2.5	-0.06	0.01	0.04
-------	-----	---	-----	-----	-----	-----	-------	------	------

144.0	120	2	-0.1	1.7	8.3	2.1	0.01	0.02	0.10
144.5	120	2	-0.2	1.8	10.9	2.4	-0.09	0.02	0.10
144.5	120	2	0.0	1.7	9.6	2.3	-0.06	0.02	0.08
146.0	120	2	0.0	1.5	8.9	2.1	-0.05	0.02	0.10
146.0	120	2	0.2	1.4	10.4	2.6	-0.05	0.01	0.08

169.0	60	3	0.3	-0.1	2.1	1.1	-0.02	0.00	0.03
169.0	60	3	0.4	0.0	2.2	1.1	-0.02	0.00	0.03
171.0	60	3	0.9	0.1	4.9	1.9	0.00	0.00	0.01
171.0	60	3	0.9	0.0	4.8	1.8	0.00	0.00	0.01

195	90	3	0	2	7	1	-0.12	0.01	0.10
195	90	3	0	2	7	1	-0.11	0.00	0.09
196	90	3	0	0	6	1	-0.04	0.00	0.03
196	90	3	0	0	6	1	-0.04	0.00	0.04

216.0	120	3	-0.1	1.0	8.3	1.8	-0.11	0.01	0.09
216.0	120	3	-0.1	1.0	8.4	1.8	-0.11	0.01	0.10
217.5	120	3	-0.2	2.2	6.9	1.9	-0.21	0.01	0.17
217.5	120	3	-0.1	2.3	6.8	1.9	-0.20	0.01	0.16
218.0	120	3	0.1	3.4	10.1	1.8	-0.16	0.02	0.24
218.0	120	3	0.1	3.3	10.0	1.9	-0.17	0.02	0.25

Appendix IV – Fold out reference table

Table 6.1: Summarised list of experimental runs

<i>Run</i>	<i>Number of reactors</i>	<i>Reactor packing</i>	<i>Feed</i>	<i>WHSV</i> ( $g_{feed}/g_{cat}\cdot hr$ )	<i>H<sub>2</sub>/impurity ratios</i> (mol/mol)	<i>Temperatures</i> (°C)
0 (blank)	1	SiC	Feed 1	3	1	60, 90, 120
1	1	Au/TiO <sub>2</sub>	Feed 3	11	1	60, 90, 120
2a, 2b	1	Au/TiO <sub>2</sub>	Feed 1	3	1	60, 90, 120
3	1, 2, 3	Au/TiO <sub>2</sub>	Feed 1	3	1	60, 90, 120
4	1, 2, 3	Au/TiO <sub>2</sub>	Feed 1	3	2	60, 90, 120
5	1, 2, 3	Au/TiO <sub>2</sub>	Feed 2	3	1	60, 90, 120

Table 6.2: Approximate feed compositions

<i>Feed 1:</i>		<i>Feed 2:</i>		<i>Feed 3:</i>	
1-hexene	98.7%	1-hexene	99.1%	1-hexene	98.7%
1-hexyne	0.2%			1-hexyne	1%
1,5-hexadiene	0.2%	1,5-hexadiene	0.2%		
1,4-hexadiene	0.2%	1,4-hexadiene	0.2%		
1-methyl-1-cyclopentene	0.2%	1-methyl-1-cyclopentene	0.2%		
2,4-hexadiene	0.2%				
Other*	0.3%	Other*	0.3%	Other*	0.3%

\*Other refers to n-hexane and branched C<sub>6</sub> alkanes that were introduced with the 1-hexen

